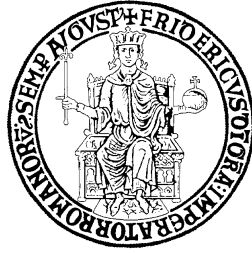


UNIVERSITY OF NAPLES "FEDERICO II"



Doctorate School in Molecular Medicine

Doctorate Program in Neuroscience

Coordinator: Prof Lucio Annunziato

XXVIII Cycle

“Critical role of $K_v3.4$ Potassium Channel in $A\beta$ oligomers effects on neuron excitability, astrocytes activation and cognitive functions in Alzheimer’s Disease”

TUTOR:

Prof Anna Pannaccione

PhD STUDENT:

Dr Roselia Ciccone

ACCADEMIC YEAR 2015-2016

INDEX

SUMMARY	Pag. 3
INTRODUCTION	Pag. 5
CHAPTER 1: Alzheimer's disease	Pag. 6
1.1. Epidemiology	Pag. 6
1.2. Clinical features of Alzheimer's disease	Pag. 8
1.3. Diagnosis of Alzheimer's disease	Pag. 9
1.4. Neuropathological alterations in Alzheimer's Disease	Pag. 10
1.4.1. Amyloid pathology	Pag. 12
1.4.2. Neurofibrillary tangles	Pag. 16
1.5 Braak staging	Pag. 17
1.6 Hypothesis of Alzheimer's Disease pathogenesis	Pag. 19
1.6.1 Amyloid cascade hypothesis	Pag. 19
1.6.2 Tau hypothesis	Pag. 21
1.7 Changes in ionic homeostasis in Alzheimer's Disease	Pag. 22
1.7.1 Calcium dysregulation and excitotoxicity	Pag. 22
1.8 Mitochondrial dysfunction	Pag. 23
1.9 Synaptic degeneration in Alzheimer's Disease	Pag. 24
1.10 Oxidative Stress	Pag. 26
1.11 Inflammation	Pag. 27
1.11.1 Astrogliosis in Alzheimer's Disease	Pag. 27
1.11.2 Astrocytes and potassium homeostasis	Pag. 29

1.12 Animal models of Alzheimer's Disease	Pag. 30
1.12.1 APP transgenic mice	Pag. 31
1.12.2 PS transgenic mice	Pag. 32
1.12.3 Tau transgenic mice	Pag. 33
1.12.4 Multiple-transgenic models: Triple-Transgenic	Pag. 33
1.12.5 Tg2576 mouse model	Pag. 34
CHAPTER 2: Potassium channels	Pag. 35
2.1 Ion channels	Pag. 35
2.2 Potassium channels	Pag. 36
2.3 Voltage gated potassium channels	Pag. 39
2.3.1 The pore domain and the voltage sensor	Pag. 39
2.3.2 The gating	Pag. 40
2.4 Traffic of K _v channels	Pag. 41
2.5 Regulatory subunits	Pag. 41
2.5.1 KCNE family	Pag. 42
2.6 K _v 3 channels	Pag. 43
2.7 Regulation of K _v 3 channels	Pag. 45
2.8 Pharmacology of K _v 3 channels	Pag. 46
2.9 Contributions of K _v 3 channels to neuronal excitability	Pag. 46
CHAPTER 3: Pathological implications of K_v3 potassium channels	Pag. 49
3.1 Potassium dysregulation in Alzheimer's Disease	Pag. 49
3.1.1 K _v 3.4 and Alzheimer's Disease	Pag. 50

3.2	Critical role of potassium homeostasis in apoptosis	Pag. 51
3.2.1	K _v 3.4 and apoptosis	Pag. 52
3.3	Critical role of potassium homeostasis in memory and learning	Pag. 53
CHAPTER 4: Aims and Design of the Present Study		Pag. 55
4.1	Rationale and aims of the present study	Pag. 56
CHAPTER 5: Materials And Methods		Pag. 57
5.1	Drugs and chemicals	Pag. 58
5.2	Mice	Pag. 59
5.2.2	Genotyping: PCR analysis	Pag. 59
5.2.3	Behavioural tests	Pag. 61
5.2.3.1	Open Field	Pag. 61
5.2.3.2	T maze spontaneous alternation	Pag. 62
5.3	Cell Cultures	Pag. 62
5.3.1	PC-12 Cells	Pag. 62
5.3.2	Chinese Hamster Ovary Cells (CHO)	Pag. 63
5.3.3	Mouse Hippocampal Neurons	Pag. 64
5.3.4	Primary Astrocytes Cultures	Pag. 65
5.4	Solubilization of A β peptide and cellular treatments	Pag. 66
5.4.1	A β ₁₋₄₂ Oligomers conditions	Pag. 66
5.5	Electrophysiological recordings	Pag. 67
5.6	Western Blot	Pag. 69
5.7	Immunoprecipitation	Pag. 70

5.8	Assessment of nuclear morphology	Pag. 72
5.9	Immunocytochemistry	Pag. 72
5.10	Rna Interfering	Pag. 73
5.11	Statistical Analysis	Pag. 74
CHAPTER 6: Results		Pag. 76
6.1	A β ₁₋₄₂ peptide aggregates to form low molecular weight oligomers (dimers and trimers) in Tg2576 mice at the early stages of Alzheimer's Disease	Pag. 76
6.2	A β ₁₋₄₂ trimers deposition in young Tg2576 mice correlates with the overexpression of K _v 3.4 Channel Subunits and its accessory subunit MiRP2	Pag. 77
6.3	Changes in K _v 3.4 and in its accessory subunit MiRP2 protein expression are related to disease stage	Pag. 80
6.4	K _v 3.4 activity increases in hippocampal neurons obtained from Tg2576 mice	Pag. 83
6.5	K _v 3.4 over expression induces caspase-3 activation culminating in neuronal death	Pag. 86
6.6	K _v 3.4 selective knockdown effect on K _v 3.4 protein expression in rat hippocampal neurons and mouse hippocampal neurons	Pag. 88
6.7	K _v 3.4 selective knockdown prevents caspase-3 activation and apoptotic events in Tg2576 mice	Pag. 90
6.8	K _v 3.4 selective knockdown reduces A β production and trimers deposition in Tg2576 mice, improving memory performance	Pag. 93
6.9	BDS 1-8 fragment, obtained from full BDS-I toxin, could	Pag. 96

be an innovative pharmacological strategy to block $K_v3.4$ in Tg2576 mice

- 6.10** $A\beta_{1-42}$ exposure increases $K_v3.4$ expression and induces the astrocytes activation Pag. 99
- 6.11** $A\beta_{1-42}$ exposure increases $K_v3.4$ activity in primary astrocytes, whereas the $K_v3.4$ silencing prevents $A\beta_{1-42}$ -effect Pag. 102
- 6.12** Silencing of $K_v3.4$ significantly reduced astrocytes activation in Tg2576 mice in the early stages of Alzheimer's Disease Pag. 104
- CHAPTER 7: Discussion** Pag. 105
- REFERENCES** Pag. 116

ABBREVIATIONS

AD	Alzheimer's Disease
NFTs	Neurofibrillary tangles
EOAD	Early onset Alzheimer's Disease
LOAD	Late onset Alzheimer's Disease
FAD	Familial Alzheimer's disease
APP	Amyloid Precursor Protein
PS-1	Presenilin-1
PS-2	Presenilin-2
apoE	Apolipoprotein E
MCI	Mild Cognitive Impairment
CSF	Cerebrospinal fluid
PET	Positron-emission tomography
p-tau	Phosphorylated-tau
MRI	Magnetic Resonance Imaging
SPECT	Single-Photon Emission Computed Tomography
GFAP	Glial Fibrillary Acidic Protein
APPsβ	Ectodomain of APP
βCTF or C99	APP Carboxy-Terminal Fragment
BACE	β -site APP cleaving enzyme
αCTF or C83	APP Carboxy-Terminal Fragment
AICD	APP Intracellular Domain
LTP	Long Term Potentiation
MAPT	Microtubule-Associated Protein Tau
CNS	Central Nervous System
PNS	Peripheral Nervous System
PHF	Paired Helical Filaments
MTL	Medial Temporal Lobe
NMDA	N-methyl-D-aspartate
AMPA	2-amino-3-(3-hydroxy-5-methylisoxazol-4-yl) propanoic acid
ROS	Reactive Oxygen Species
GFAP	Glial Fibrillary Acidic Protein
IL-1β	Interleukin-1 β
TNF-α	Tumor Necrosis Factor- α
IFN-γ	Interferon- γ
Ca²⁺	Calcium

ER	Endoplasmic Reticulum
ATP	Adenosine triphosphate
mPTP	Mitochondrial Permeability Transition Pore
CytC	CytochromeC
PDGF	Platelet-Derived Growth Factor
PrP	Prion Protein
FTDP-17	Frontotemporal Dementia And Parkinsonism Linked To Chromosome 17
K_v	Voltage Gated Potassium Channels
ER	Endoplasmic Reticulum
KChip	K ⁺ Channel Interacting Proteins
KChAP	K ⁺ Channel Associated Protein
DPPLs	Dipeptidyl Aminopeptidase Like Proteins
MinK	Minimal K ⁺ currents
MiRPs	MinK-related peptides
PC-12	Pheochromocytoma Cells
TEA	Tetraethylammonium
4-AP	4-aminopyridine
BDS-I	Blood Depressing Substance I
BDS-II	Blood Depressing Substance II
[K⁺]_i	Intracellular Potassium Concentrations
HPLC	High Performance Liquid Chromatography
HFIP	1,1,1,3,3,3-Hexafluoro-2-Propanol
IP	Immunoprecipitation

SUMMARY

Voltage gated potassium channels (K_V) play a pathogenetic role in many neurodegenerative disorders, including Alzheimer's Disease (AD). Recently, it has been demonstrated that hippocampal neurons and NGF-differentiated PC-12 cells exposed to $A\beta_{1-42}$ display a selective over-expression and increased activity of $K_V3.4$ potassium channels. The goal of this study has been to further investigate the role of $K_V3.4$ channels in a transgenic mouse model of AD, Tg2576. Firstly, we observed an over-expression of $K_V3.4$ and its accessory subunit MiRP2 in the hippocampus of young Tg2576 mice (3 months old), whereas no significant modification was observed in elderly Tg2576 mice (14-18 months old). Moreover, Tg2576 hippocampal neurons showed an early increase in $K_V3.4$ channel activity. These data suggested that $K_V3.4$ up-regulation play a critical role in the early stages of AD, since it contributes to neuronal hyperexcitability induced by the accumulation of $A\beta_{1-42}$ dimers and trimers occurring in these stages. The immunocytochemical analysis showed that the early increase in $K_V3.4$ expression was accompanied by an altered subcellular distribution of this protein in Tg2576 hippocampal neurons, in particular we observed a more intense $K_V3.4$ immunosignal localized to the soma plasma membrane. Intriguingly, the over-expression and increase activity of $K_V3.4$ in young Tg2576 mice were accompanied by the activation of caspase-3. Moreover, the $K_V3.4$ silencing *in vivo* by intracerebroventricular injection, not only strongly reduced $K_V3.4$ expression but also prevented caspase-3 activation. Interestingly, si $K_V3.4$ reduced the $A\beta_{1-42}$ trimers levels in the same young Tg2576 mice suggesting the possible indirect link between $K_V3.4$ over-expression, caspases activation and $A\beta_{1-42}$ trimers deposition.

Several studies showed that $A\beta_{1-42}$ trimers are closely related to memory impairment occurring in the early stages of AD. Our studies performed by T-maze spontaneous alternation test indicated that Tg2576 mice (3 months old) exhibited the impairment of exploration ability, spatial learning and memory abilities. Interestingly, Tg2576 mice in the presence of siK_v3.4 displayed the amelioration in exploration ability and memory performance. Furthermore, the Open Field test showed that Tg2576 mice (3 months old) were hyperactive since they travelled a greater average distance compared to Wild Type mice. Attractively, Tg2576 in the presence of siK_v3.4 displayed a reduction in the distance traveled compared to Tg2576 mice in the absence of siK_v3.4. Collectively, these data proposed that the inhibition of K_v3.4, ameliorating memory performance and non-cognitive symptoms, could become a new pharmacological target in the care of AD. To this aim we tested a new synthetic compound, BDS1-8, containing the first eight aminoacids from full length BDS-I, a well known K_v3.4 inhibitor. BDS1-8 was able to prevent both increased K_v3.4 activity and caspase-3 activation induced by $A\beta_{1-42}$ oligomers. At last, we observed an up-regulation of K_v3.4 and GFAP protein expression in primary astrocytes exposed to $A\beta_{1-42}$ peptide. Interestingly, coexpression and co-immunoprecipitation studies revealed a large overlap and a direct binding of K_v3.4 with GFAP. Moreover, the *in vivo* siK_v3.4 significantly down-regulated GFAP in Tg2576 mice (3 months old) confirmig the closely link between GFAP and K_v3.4. These data suggested that GFAP might promote channel trafficking in precise membrane domains facilitating the accumulation of K_v3.4 channel, in order to modulate cellular mechanisms mediated by K⁺ ions. Collectively, our data suggest a critical role of K_v3.4 in $A\beta$ oligomers effects on neuron excitability, astrocytes activation and cognitive functions in AD.

INTRODUCTION

Chapter 1: Alzheimer's Disease

1.1 Epidemiology

AD is the most common neurodegenerative disorder in the aging population. It is characterized by cognitive impairment, progressive degeneration of neuronal populations and formation of amyloid plaques composed of amyloid β (A β) deposits and neurofibrillary tangles (NFTs) (Selkoe, 2001). AD is named by Alois Alzheimer, a Bavarian psychiatrist, who in 1907 first reported the case of a middle aged woman who developed memory deficits and cognitive impairments (Alzheimer, 1907). After the Alzheimer's description, for a long time, little progress has been achieved in defining AD pathogenesis. This situation began changing in the 1960s, when the advent of electron microscopy allowed to describe the ultrastructural changes underlying the two classical lesions which Alzheimer had linked: senile plaques and NFTs (Selkoe, 2001). Parallel to these neuropathological modifications, various neurotransmitter systems are altered in the brain tissues of subjects with AD (Quirion, 1993). In the mid-1970s was observed a reduction in neurons synthesizing and releasing acetylcholine. In particular, was found a reduction in the amounts and activities of two specific enzymes: choline acetyltransferase and acetylcholinesterase (Selkoe, 2001). After the pioneering work of Davies and Maloney (1976), various groups (Perry *et al.*, 1977; Coyle *et al.*, 1983; Etienne *et al.*, 1986; Perry *et al.*, 1986) reported about the alteration of cortical and hippocampal cholinergic projections in AD. In the late 1970s, were identified deficits of other neurotransmitter systems in AD brain tissue (Greenwald, 1983; Davies P, 1983). It became progressively more clear that AD did not involve degeneration of a single transmitter class of

neurons but was highly heterogeneous (Nordberg, 1993). In 2006 the worldwide prevalence of dementia is as high as 26 million, and it was predicted that the percentage of cases will grow fourfold to 106.8 million by the year 2050 (Reitz and Mayeux, 2014). Approximately, 4.6 million new cases were recognized every year (Ferri *et al.*, 2005), about 70% of these cases were attributed to AD. The incidence of dementia increases exponentially with age, the most prominent increase occurs during the 7th and 8th decades of life. Based on its age of onset, AD is classified into early onset AD (EOAD, onset < 65 years) around for 1–5% of all cases, and late-onset AD (LOAD, onset ≥ 65 years) around for >95% of affected. EOAD have a definite genetic element, they are inherited in an autosomal dominant manner (McDowell, 2001). Genetic linkage analyses have led to the identification of three genes associated with familial AD (FAD): Amyloid β -Protein Precursor (APP) on chromosome 21 (Goate *et al.*, 1991), presenilin-1 (PS-1) on chromosome 14 (Sherrington *et al.*, 1995), and presenilin-2 (PS-2) on chromosome 1 (Rogaev *et al.*, 1995). The vast majority of AD cases occur in sporadic form after 65 years of age, lacking alterations in the known set of genetic markers, which suggests either environmental causes or a combination of environmental and genetic factors. Nevertheless, the sporadic late-onset cases of AD also have a genetic component as the apolipoprotein E (apoE) gene in chromosome 19 (Strittmatter *et al.*, 1993). Previous evidence of the involvement of chromosome 19 has been confirmed by the finding of an association between AD and the apoE on chromosome 19. apoE has three alleles: apoE- ϵ 2, apoE- ϵ 3, and apoE- ϵ 4. A total of 80% of familial and 64% of sporadic AD late onset cases have at least one apoE- ϵ 4 compared to 31% of control subjects. This

finding implicates apoE- ϵ 4 as an important factor in the etiology of AD (Corder *et al.*, 1993).

1.2 Clinical features of Alzheimer's disease

The disease often begins as a syndrome termed mild cognitive impairment (MCI), which is usually characterized by a memory complaint and impairments on formal testing, intact general cognition, preserved daily activities and absence of explicit dementia. MCI is considered as a transitional stage between normal aging and early AD. The clinical manifestations of symptomatic AD include increasing difficulties with memory and with other cognitive functions (executive functions, language, attention, judgment, etc). In the late stages of AD, mental functions and activities of daily living are increasingly impaired and patients become profoundly demented (Basic Neurochemistry, George J. Siegel, 2005). People with AD, at the beginning of the disorder, do not seem to have any difficulty remembering distant events but may, for example, forget having done something five minutes ago. The earliest cognitive deficit seems to be the impairment of episodic memory (the ability to recall events that are specific to a time and place). In addition to the changes that occur in memory and cognitive abilities, people with AD have additional symptoms that impair vision (agnosia), speech (aphasia) and motor function (apraxia). **Agnosia** is the inability to interpret vision accurately and to process sensory information. Agnosia is also described as loss or diminution of the ability to recognize objects, sounds, smells, tastes, or other sensory stimuli. **Aphasia** is the inability to use and interpret language appropriately; it impairs the production or comprehension of speech and the ability to read or write. **Apraxia** is the inability to perform familiar movements on command; it is

a disorder of motor planning. Impairment of other cognitive functions becomes increasingly prominent during the course of the disease. As the pathology spreads to involve cortical association areas, this gives rise to a dementia syndrome that is characterized by deficits in attentional and executive functions (a cluster of high-order capacities, which include selective attention, behavioral planning and the manipulation of information in problem-solving tasks), in semantic memory (word, face and object knowledge), in language, praxis, and in constructional and visuospatial abilities (Nestor *et al.*, 2004). The loss of procedural memory induces difficulties in routine activities such as dressing, washing and cooking. In AD patients are evident emotional problems, such as anxiety, paranoia, frustration or irritability, hallucinations, anger, aggression or hostility.

1.3 Diagnosis of Alzheimer's disease

Criteria for the clinical diagnosis of AD were established in 1984. The criteria are proposed as a guide for the diagnosis of probable, possible, and definite AD (McKhann *et al.*, 1984). AD dementia is characterized by progressive impairment of memory and other cognitive functions. Neuropsychological tests provide positive evidence of the diagnosis of dementia and help to assess the course and response to therapy. The doctor will interview the person being tested and others close to him or her to collect information about recent and past mental and physical illnesses. The doctor will assess mental status, memory, the ability to solve simple problems and other thinking skills. Moreover all cognitive tests are sensitive to differences in age, education and cultural variation among individuals (Albert *et al.*, 2011). Recently, criteria for the clinical diagnosis of AD established in 1984 have been improved through

the integration of biomarkers to evaluate disease state. Biomarkers are parameters (physiological, biochemical, anatomic) that can be measured and that reflect specific features of disease related to pathophysiological processes (Clifford *et al.*, 2011). Some biomarkers directly reproduce the pathology of AD. Evidence suggests that both A β deposition and elevated tau/phosphorylated tau are biomarkers of AD. The biomarkers of A β accumulation include both cerebrospinal fluid (CSF) measures of lower A β ₁₋₄₂ levels and positron-emission tomography (PET) evidence of A β deposition, using a variety of specific ligands. The biomarkers of tau accumulation include CSF measures of increased total tau or phosphorylated-tau (p-tau). Therefore, the two biomarkers in combination are really clarifying. Moreover, for an accurate diagnosis of AD it is also necessary to evaluate neuronal injury, through a number of structural and functional measures, including brain atrophy, and hypometabolism or hypoperfusion obtained with magnetic resonance imaging (MRI), PET, and single-photon emission computed tomography (SPECT) imaging.

1.4 Neuropathological alterations in Alzheimer 's Disease

The typical lesions of AD are the extracellular deposits of A β in parenchymal plaques, vascular amyloid and the intraneuronal NFTs (**Fig 1B**) (Serrano-Pozo *et al.*, 2011). Those classical lesions are accompanied by astrogliosis (Verkhratsky *et al.*, 2010) and microglial cell activation that can cause or aggravate neuron damage (Li *et al.*, 2014). Generalized astrogliosis, manifested by cellular hypertrophy and by an increase in expression of glial fibrillary acidic protein (GFAP) and astroglial S100B protein, was routinely observed in postmortem tissues from AD patients (Nagele *et al.*, 2004). The

activated astrocytes are closely involved in the neuroinflammatory component of AD through the release of cytokines, proinflammatory factors, and nitric oxide/reactive oxygen species neurotoxicity (Heneka *et al.*, 2010). Furthermore it is known the correlation between the degree of astrogliosis and cognitive decline.

Fig.1 Alzheimer's Disease Pathology

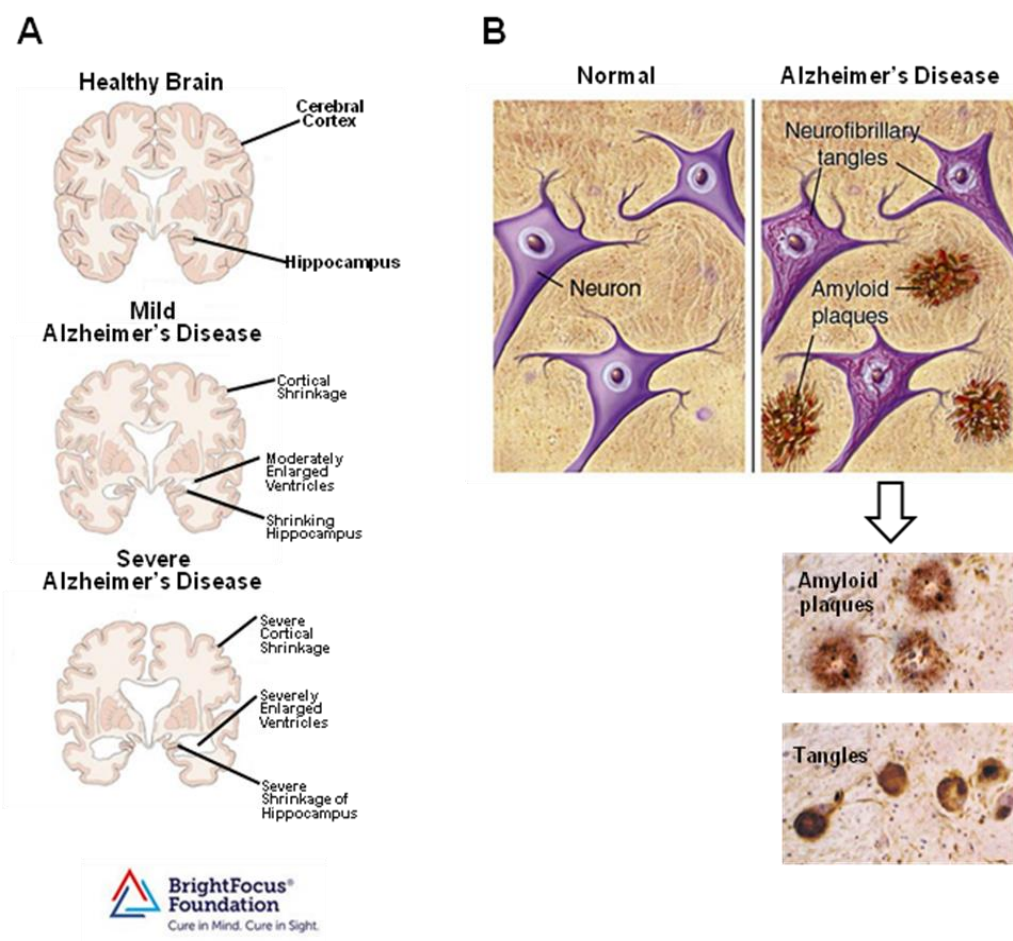


Fig.1 Alzheimer's disease pathology. (A) Healthy brain versus Alzheimer's disease brain. **(B)** Neuropathological hallmarks of Alzheimer's disease: Amyloid Plaques and Neurofibrillary Tangles (NFTs).

1.4.1 Amyloid pathology

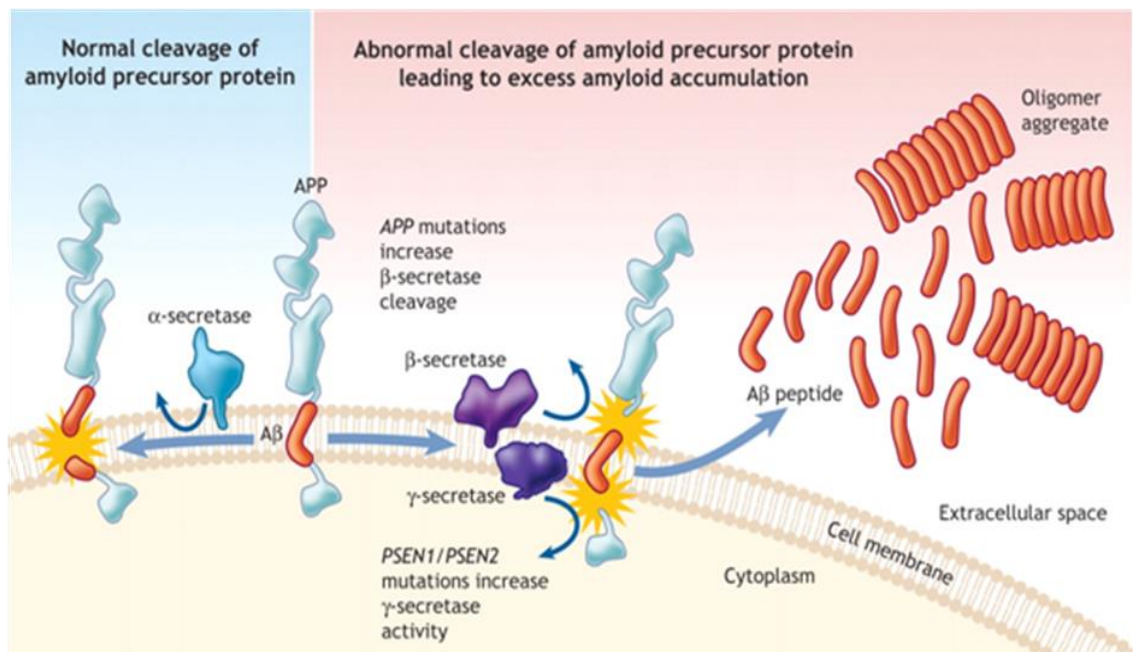
Neuritic plaques, one of the two brain lesions observed in Alzheimer's original patient, are microscopic foci of extracellular amyloid deposition. Much of the fibrillar A β found in the neuritic plaques is the species ending at aminoacid 42 (A β_{42}), the slightly longer, more hydrophobic form that is particularly prone to aggregation. A β deposits are also observed in normal aging individuals, but at a lower density (Perry *et al*, 1978). The "*amyloid hypothesis*" suggests that the accumulation of A β fragments 1–40 and 1–42 is primarily responsible for AD pathology, and the imbalance of A β production and A β clearance induces the cognitive impairments associated to AD (Jacobsen *et al.*, 2006). According to the amyloid hypothesis of AD, the overproduction of A β is a consequence of the disruption of the process that regulate the proteolytic cleavage of the APP (De-Paula *et al.*, 2012). Biologic studies have shown that AD-causing mutations in APP and in presenilin-1 (PS1) or PS2 enhance the production of the A β_{42} peptide. The improved production of the A β_{42} peptide results in an increase in A β_{42} levels, or in an increase in the A β_{42} /A β_{40} ratio. A β_{42} peptide with its C-terminal alanine and isoleucine residues is more hydrophobic and aggregates more rapidly than A β_{40} peptide (Haas and Selkoe, 2007). Moreover the neurotoxic potential of the A β peptide results from its biochemical properties that promote aggregation into insoluble oligomers and protofibrils. These fibrillary A β species accumulate into senile and neuritic plaques. These processes, accompanied to reduction of A β clearance from the brain, leads to the extracellular accumulation of A β , and the consequent activation of neurotoxic cascades that ultimately lead to cytoskeletal changes, neuronal dysfunction and cellular death. A β peptide is derived by sequential proteolytic processing from a large type I trans-membrane protein, the APP

that is present in several cell types, including neurons and astrocytes. The function of the APP remains not fully understood, although several studies have demonstrated a number of its putative physiological roles. The APP extracellular domain could function as a cell surface receptor; could have a role in cell-substratum adhesion and in neurite outgrowth and synaptogenesis (Zheng *et al.*, 2006). Furthermore the APP intracellular domain could be involved in cell migration, synapse remodeling and cell signaling (Zheng *et al.*, 2006). The proteolytic enzymes involved in APP processing are named secretases: α , β , and γ (Haass *et al.*, 2004). The name “secretases” refers to the secretion of the proteolytically cleaved substrates. There are two different pathways to process APP: the amyloidogenic pathway, which leads to A β generation; and the non-amyloidogenic pathway, which prevents A β generation. In the amyloidogenic pathway the cleavage of APP is mediated from the consecutive action of β - and γ -secretase producing A β peptide (Haass *et al.*, 2004). The β -secretase cuts a large part of the ectodomain of APP (APPs β), generating an APP carboxy-terminal fragment (β CTF or C99), which is then cleaved by γ -secretase. β -secretase, also known as β -site APP cleaving enzyme (BACE1 and 2), is considered the enzyme that controls the A β production, and BACE-directed therapy is currently one of the aims of several researches (Yan and Vassar, 2014). At the end of the amyloidogenic pathway, A β is released and then found in extracellular fluids such as plasma or cerebrospinal fluid. In the non-amyloidogenic pathway, APP is cleaved in the middle of the A β region by the α -secretase activity. This processing generates a truncated APP CTF (α CTF or C83). The successive intramembrane cut by γ -secretase liberates a truncated A β peptide called p3. Furthermore γ -Secretase not only liberates A β (from C99) and p3 (from C83)

but also generates the APP intracellular domain (AICD) which is released into the cytosol (**Fig. 2**). A β is produced as a monomer, but quickly aggregates to form multimeric complexes, from low molecular weight dimers and trimers to higher molecular weight protofibrils and fibrils (LaFerla *et al.*, 2007). Protofibrils are transient structures which appear earlier to the formation of mature amyloid fibrils and can be named prefibrillar aggregates. The oligomeric species of A β exert a pathological role compromising cognition, learning and memory, synaptic function and long term potentiation (LTP) (Walsh *et al.*, 2002). The A β peptide was first identified as a component of extracellular amyloid plaques; but in the last years a large number of studies have demonstrated the presence of intracellular A β , that also plays a pathophysiological role in the progression of AD. In the first study reporting the presence of intraneuronal A β , an antibody against residues 17–24 of A β was used, and A β -immunoreactive material was observed in neurons from the brain and spinal cord of individuals with or without AD (Grundke-Iqbal *et al.* 1989). Several studies, in various transgenic models of AD, indicated that A β may accumulate intracellularly and that memory impairments precede the accumulation of extracellular plaques (Oddo *et al.*, 2006). The accumulation of intraneuronal A β is an early event in the AD progression, preceding the formation of extracellular A β deposits. Indeed, it has been demonstrated that intraneuronal A β levels decrease as extracellular plaques accumulate (Mori *et al.* 2002). Evidence suggests that intracellular A β may contribute to pathology by facilitating tau hyperphosphorylation, disrupting proteasome and mitochondria function, and triggering calcium and synaptic dysfunction (LaFerla *et al.*, 2007). Three clinical phases of AD may be defined: **1**) pre-symptomatic (or pre-clinical) AD, which may last for several years or decades

in which the overproduction and accumulation of A β in the brain reaches a critical level that triggers the amyloid cascade; **2)** pre-dementia phase of AD (compatible with the phase of MCI), in which early-stage pathology is present; **3)** clinically defined dementia phase of AD, in which cognitive and functional impairment is severe: at this stage there is significant accumulation of neuritic plaques and neurofibrillary tangles (De-Paula *et al.*, 2012).

Fig.2 APP proteolytic cleavage



Christopher Patterson MD et al. CMAJ 2008;178:548-556

Fig.2 APP proteolytic cleavage. The amyloid precursor protein (APP) is a transmembrane protein that can undergo a series of proteolytic cleavages by secretase enzymes. When it is cleaved by α -secretase and γ -secretase enzymes, the cleavage is not amyloidogenic. Instead, when APP is cleaved by β - and γ -secretase enzymes, neurotoxic A β peptides are released and accumulate into oligomers aggregate.

1.4.2 Neurofibrillary tangles

Tau (tubulin-associated unit) is a low molecular weight protein, which displayed the ability to promote microtubule assembly and stability (Weingarten *et al.*, 1975); it is found in both neuronal and non-neuronal cells, but predominating in neurons (Rossi *et al.*, 2008). In addition to the functions already known, tau is involved in the maintenance of axonal transport of vesicles and organelles and in providing linkage for signal transduction (Buee *et al.*, 2000). Tau is a product of the microtubule-associated protein (MAPT) gene, located on chromosome 17 (Neve *et al.*, 1986). The tau gene, through complex post-transcriptional processing, produces three transcripts: a less abundant 2kb tau transcript which encodes for a tau principally targeted to the nucleus; 6kb transcript which encodes for tau predominantly directed to the soma/axons in the central nervous system (CNS); 8/9 kb transcript producing a tau specially expressed in the retina and peripheral nervous system (PNS). The tau molecule is subdivided into four regions: N-terminal acidic region, Proline-rich region/domain, repeat domain region and C-terminal region (Maina *et al.*, 2016). The adult brain expresses six isoforms of tau, which derive from alternative mRNA splicing and differ by the presence of three or four tubulin binding domains (repeats) of 31 or 33 aminoacids in the C-terminal portion, and none, one or two inserts in the N-terminal region. Tau, mostly in a dephosphorylated state, has been localized in the plasma membrane of different cells; its N-terminal domain mediates the interaction with the plasma membrane (Buee *et al.*, 2000). Interestingly, this tau-membrane interaction is highly dynamic and depends on phosphorylation. Hyperphosphorylation of tau, its aggregation in paired helical filaments (PHF) and NFTs in vulnerable neurons are one of the hallmark of AD (Martin *et al.*,

2011). Tau pathology, is also seen in several other human neurodegenerative disorders, called tauopathies. In everyone of these disorders the accumulation of the abnormally hyperphosphorylated tau is associated with neurofibrillary degeneration and dementia. The abnormal hyperphosphorylation of tau precedes its accumulation in the affected neurons in AD. The abnormally hyperphosphorylated tau was discovered not only in neurofibrillary tangles but also in cytosol from AD brains. Quantitative immunocytochemical studies have revealed deposits of only abnormally phosphorylated tau, but not normal tau, in neurons without tangles. These results suggest that the abnormal hyperphosphorylation of tau precedes its accumulation into neurofibrillary tangles (Baner et al., 1989). The abnormally hyperphosphorylated tau is found in AD brain in two different pools: as polymerized into neurofibrillary tangles and as non-fibrillized form in the cytosol. Since the abnormal filaments are highly insoluble, NFTs remain in the extracellular space following the complete degeneration of the affected neuron and become extracellular “ghost” tangles. The abnormally hyperphosphorylated tau not only is unable to stimulate microtubule assembly and to bind microtubules, but also sequesters normal tau, inhibits the assembly and disrupts the microtubules. The impairment of the microtubule network in the affected neurons compromises axonal transport, leading to retrograde degeneration which, in turn, results in dementia (Iqbal et al., 2004).

1.5 Braak staging

The deposition of A β ₁₋₄₂ peptide and the development of neurofibrillary tangles are important histopathological hallmarks of AD. In the Braak staging, the medial temporal lobe (MTL) serves as a model to evaluate the changes in the

anatomical distribution of different types of A β -deposits occurring in the course of AD, as well as to assess the relationship between the development of A β -deposition and neurofibrillary pathology (Thal *et al.*, 2000). In the first of 4 phases of β -amyloidosis there are diffuse non-neuritic plaques in the basal temporal neocortex, while the hippocampus is lacking of A β . The same A β deposits type appears in the second phase within the external entorhinal layers, in the internal entorhinal layers and in the hippocampal sector CA1. In addition to the regions involved in phase 2, in the third phase, A β -deposits appear in the molecular layer of the fascia dentata, in the molecular layer of both the entorhinal region and the temporal neocortex. In addition, A β -deposits appear in the parvopyramidal layer of the presubicular region of the cortex. In hippocampal sector CA1 the number of plaques has increased predominantly in the superficial pyramidal layer. The fourth phase is characterized by diffuse plaques in the hippocampal sector CA4 (Braak and Braak, 1991). Furthermore, NFTs exhibit a characteristic distribution pattern permitting the differentiation of six stages. A hierarchical staging system for the neuropathological changes in AD has been elaborated following the distribution of NFTs (Braak and Braak, 1994). In stages I and II (the transentorhinal stages), NFTs are restricted to the entorhinal cortex and the CA fields of hippocampus. Stages III and IV (the limbic stages) are characterized by moderate numbers of NFTs in the hippocampus, basolateral amygdala, and limbic nuclei of the thalamus. In stages V and VI (the isocortical stages) all hippocampal subfields and isocortical association areas are severely affected.

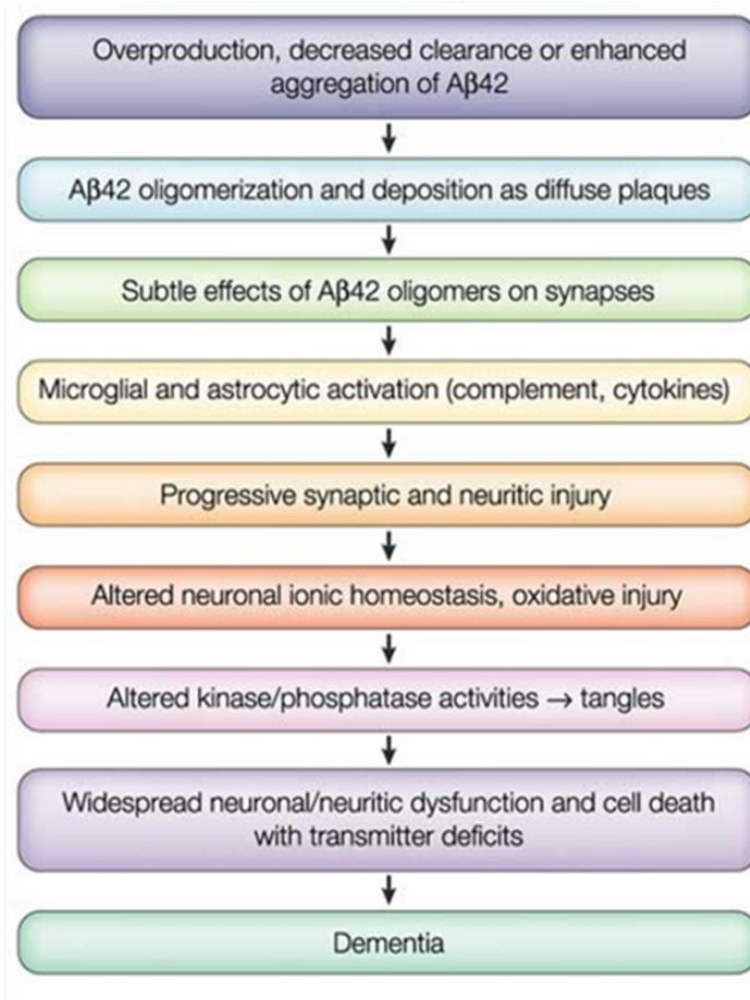
1.6 Hypothesis of Alzheimer's Disease pathogenesis

During the past decades various hypotheses have been suggested to explain the molecular pathogenesis of AD, of which the principal are the “amyloid cascade hypothesis” and the “tau and tangle hypothesis”.

1.6.1 Amyloid cascade hypothesis

The amyloid cascade hypothesis postulates that the deposition of A β peptide in the brain parenchyma starts a sequence of events that culminate with AD dementia (**Fig. 3**). A β levels can be elevated by enhanced production and/or reduced clearance. In particular, the A β_{42} /A β_{40} ratio can be increased by mutations in three different genes (*APP*, *PS1* and *PS2*) that cause familial forms of AD. This increase of A β_{42} enhances oligomers formation, which causes severe and permanent changes of synaptic function. Furthermore, the deposition of A β_{42} in the brain parenchyma induces local inflammatory responses (microgliosis and astrocytosis), synaptic spine loss and neuritic dystrophy. Collectively, these events result in oxidative stress, altered ionic homeostasis and additional biochemical changes. Moreover, NFTs are induced by altered kinase and phosphatase activities and contribute to additional defects, including some in axonal transport. The cascade culminates in synaptic/neuronal dysfunction and cell death, leading to progressive dementia (Haass and Selkoe, 2007; Karran *et al.*, 2011).

Fig.3 Amyloid Cascade Hypothesis



Citron M. Nat Reviews Neuroscience, 2004

Fig.3 Amyloid Cascade hypothesis. The deposition of Aβ peptide in the brain is a central event in AD pathology triggering a sequence of events that culminate with AD dementia.

1.6.2 Tau hypothesis

The tau hypothesis of AD pathogenesis proposes that dysregulation of tau phosphorylation, misfolding, subsequent aggregation of tau and tau fibrillization may play a significant role in synaptic and neuronal loss. Aggregation of altered tau produces different effects at various stages of AD. Interestingly, in early stages of AD, the loss of normal tau function may pilot neurodegeneration. Therefore, in the progression of the disease, toxic effects of tau aggregates may accelerate the neurodegeneration. Misfolded, truncated tau protein promotes activation of microglia and leukocyte infiltration in the transgenic model of tauopathy. Tau-mediated neurodegeneration may occur through neuroinflammatory processes, impaired axonal transport, oxidative stress, or a combination of these processes. As support for the central role of tau aggregation, tauists assert that the cognitive decline in late stages of AD has a strong correlation with tangle formation, whereas it weakly correlates with A β burden. However, since in non-AD tauopathies tau proteins aggregation occurs in the absence of A β deposition, it is likely that tangles are not sufficient to induce amyloid plaques in AD. In fact, although A β aggregates and NFTs are the hallmarks of AD, they don't develop temporally in parallel in human brain and NFTs arise only after A β accumulation. A transgenic mouse model overexpressing both mutant APP and mutant tau has both plaques and tangles (Lewis *et al*, 2001). Interestingly, the double mutant has more tangles than tau-mutant mice alone and tangles appear in brain areas that are unaffected in single mutant-tau transgenic mice. In a parallel experiment another group showed that injection of amyloid into the cerebrum of mutant tau transgenic mice exacerbated tangle pathology (Gotz *et al*, 2001). These

models together demonstrate that tangles and plaques are linked pathogenetically.

1.7 Changes in ionic homeostasis in Alzheimer's Disease

Sodium (Na^+) and potassium (K^+) ions are critical for "nerve impulses" or "spikes", membrane transport, and other cellular processes. In neurons, action potentials play a central role in cell-to-cell communication and are generated by transmembrane voltage-gated ion channels. At the beginning of the action potential, the opening of Na^+ channels allow an inward flow of Na^+ ions, which changes the electrochemical gradient, causing depolarization. Repolarization occurs with the opening of K^+ channels; there is an outward current of K^+ ions, that induce the return of the electrochemical gradient to the resting state. Changes in brain Na^+ and K^+ ion homeostasis in AD are a recent finding. Vitvitsky *et al.*, measured Na^+ and K^+ concentrations in postmortem brain samples of AD individuals and age-matched controls. In AD samples they found Na^+ increase of 20-25 %, and K^+ increase of 15% (Vitivitsky *et al.*, 2012; Graham *et al.*, 2015).

1.7.1 Calcium dysregulation and excitotoxicity

Calcium (Ca^{2+}) is one of the most important intracellular messengers in the brain, it is essential for neuronal development, synaptic transmission and plasticity, and for the regulation of various metabolic pathways. The regulation of Ca^{2+} concentration in neuronal cells is very complex, involving proteins localized on the plasma membrane, cytosol, mitochondria, and endoplasmic reticulum (ER). Several evidence suggested that calcium also plays a prominent role in the pathogenesis of AD (Mattson and Chan, 2001) and that

A β peptide can induce an increase of intracellular calcium levels causing excitotoxicity (Mattson and Chan, 2003). The Ca²⁺ hypothesis of AD suggests that the deleterious effects of A β peptide depend on the dysregulation of Ca²⁺ signaling (LaFerla 2002). The general notion is that abnormal amyloid metabolism induces an upregulation of neuronal Ca²⁺ signaling that is responsible for the initial decline in memory and subsequent apoptosis. Therefore, Ca²⁺ plays important roles in synaptic plasticity by its actions at both pre- and postsynaptic terminals. In addition, there is increasing evidence that A β peptide also acts on microglial cells and astrocytes (Saijo & Glass, 2011) to induce local inflammatory response that contributes to Ca²⁺ signaling deregulation. A β peptide can promote Ca²⁺ influx by forming calcium-selective channels in membranes or by activating cell surface receptors coupled to calcium influx (Mattson and Chan, 2003). In addition, A β peptide impairs membrane calcium pumps and enhances calcium influx through voltage-dependent channels and ionotropic glutamate receptors. Thus, it's necessary to find a new therapeutic approach in order to stabilize intracellular Ca²⁺ homeostasis.

1.8 Mitochondrial dysfunction

Mitochondria, the major organelles in neurons, produce energy as adenosine triphosphate (ATP). Other functions of mitochondria are: the regulation of calcium homeostasis and apoptotic mechanisms, the generation of free radicals. More evidence have indicated that mitochondrial dysfunction involves alterations of mitochondrial respiratory chain enzymes, generation of ROS, opening of mitochondrial permeability transition pore (mPTP), structural abnormalities of mitochondria, oxidative stress and apoptosis (Hauptmann *et*

al., 2006). These mitochondrial abnormalities are identified early in AD, before A β deposition, and are related to A β or tau pathology (Swerdlow *et al.*, 2010). In 2004, Swerdlow and colleagues have proposed the paradigm of "mitochondrial cascade hypothesis" (Swerdlow *et al.*, 2004). This hypothesis supposed that FAD and sporadic AD are not etiologically same (Swerdlow *et al.*, 2014). In FAD, excessive A β accumulation slowly impairs mitochondrial functions which further initiate other AD related pathologies such as oxidative stress or neuroinflammation. In sporadic AD, age related occurrence of mitochondrial dysfunctions causes a variety of pathologies including oxidative stress and apoptosis. A β peptide accumulation in mitochondria causes: the inhibition of mitochondrial respiratory enzyme complex-II and IV; a decrease in ATP production; an increase in ROS production (Swerdlow *et al.*, 2010). Further, A β peptide overproduction leads to dysfunctioning of mitochondrial Ca²⁺ channels and enhancement of cytochromeC (CytC) release (Caspersen *et al.* 2005). It has also been reported that A β peptide accumulation causes abnormal expression of mitochondrial proteins which are involved in mitochondrial fission and fusion machinery, causing abnormal mitochondrial morphology and mitochondria degradation (Manczak *et al.*, 2011). In conclusion, alteration in mitochondrial bioenergetics, mitochondrial dynamics, mitochondrial trafficking and oxidative stress play a key role in AD. Thus, therapeutic strategies in AD are wanted to target mitochondrial dysfunction, to enhance mitochondrial bioenergetics or to reverse oxidative stress.

1.9 Synaptic Degeneration in Alzheimer's Disease

Studies performed in human brains and *in vivo* and *in vitro* models support the concept of the synapse failure during AD. Synaptic dysfunction occurs early,

followed by pre-synaptic and spine loss, axonal dystrophy and neuronal loss (Overk and Masliah, 2014). Therefore, patients with MCI display loss of pre-synaptic proteins such as synaptophysin, VAMP2, and SNAP25 and post-synaptic markers such as PSD95 and Shank1 (Pham *et al.*, 2010). The memory impairment in AD patients correlates with synaptic loss in the neocortex and limbic system (DeKosky *et al.*, 1990). In contrast, cognitive impairment does not correlate with A β plaques in the brain. In AD the loss of synapses is higher than the neuronal loss, suggesting that synaptic damage precedes the loss of neuronal cell. Recent studies have highlighted that A β oligomers might be responsible for the synaptic damage and memory deficits (Lacor *et al.*, 2007). Furthermore, A β oligomers once bound to synapses, can dysregulate the activity and reduce the surface expression of both N-methyl-D-aspartate (NMDA) and 2-amino-3-(3-hydroxy-5-methylisoxazol-4-yl)-propanoic acid (AMPA) types of glutamate receptors, impairing signaling pathways involved in synaptic plasticity (Paula-Lima *et al.*, 2013). Recent studies suggest an emerging role for Tau in the synaptic damage. It was been demonstrated that mice over-expressing human Tau display significant synaptic degeneration, suggesting that soluble Tau is synaptotoxic (Pooler *et al.*, 2014). Interestingly, the Tau reduction with immunotherapy ameliorates behavioral deficits, synaptic dysfunction and network degeneration. The molecular mechanisms of synaptotoxicity of A β oligomers implicate: disruption of neuronal calcium homeostasis (De Felice *et al.*, 2007; Paula-Lima *et al.*, 2011), oxidative damage to neurons (De Felice *et al.*, 2007; Decker *et al.*, 2010), inflammatory processes (Bomfim *et al.*, 2012; Ledo *et al.*, 2012), mitochondrial fragmentation and dysfunction (Saraiva *et al.*, 2010; Paula-Lima

et al., 2011), and disruption of fast axonal transport leading to synaptic dysfunction, synapse elimination and cell death (De Felice *et al.* 2007).

1.10 Oxidative Stress

Reactive oxygen species (ROS) are cytotoxic products of normal mitochondrial metabolism. Imbalance between mitochondrial ROS production and the intracellular levels of antioxidant leads to oxidative stress, a condition associated with apoptosis, inflammation, ischemia-reperfusion injury, and neurodegenerative diseases. The production of ROS plays a role in synaptic signaling, with ROS acting as messenger molecules in the process of LTP, a model for synaptic plasticity and learning. By contrast, abnormally elevated ROS levels have been implicated in the age-related impairment of LTP. Thus, elevated ROS levels in neurons can be detrimental as well as degenerative. Indeed exaggerated ROS levels are implicated in the molecular etiology of AD. *In vitro* studies indicate that cell exposure to A β oligomers leads to toxicity due to calcium influx, and to oxidative free radical damage. In fact A β oligomers stimulate a prominent increase in ROS formation through the activation of NMDA receptors, leading to a rapid increase in neuronal calcium levels. The dysregulation of ROS levels by A β oligomers may contribute to the early memory impairment in AD. These results provide a mechanistic link between activation of NMDA receptors, calcium influx, and ROS formation induced by A β oligomers.

1.11 Inflammation

In AD brain, damaged neurons and neurites, insoluble amyloid β peptide deposits and NFTs provide evident stimuli for inflammation. Biochemical and neuropathological studies underlined an important relationship between inflammation and AD progression (Steardo *et al.*, 2015). Indeed gliosis is a neuropathological feature in AD brains.

1.11.1 Astrogliosis in Alzheimer's Disease

In brain of AD patients, A β plaques are surrounded by reactive astrocytes and activated microglia. Nevertheless, the role of these activated glial cells remains still unknown. In AD conditions these cells undergo important morphological and functional changes and are considered to be involved in the onset and progression of the disease. Astrocytes are the most abundant and heterogeneous type of glial cells in the CNS. They are essential in the control of cerebral homeostasis (Verkhratsky and Butt, 2013), the main provider of glutamine to neurons and crucial players in the regulation of extracellular potassium (Halassa and Haydon, 2010). Moreover, astrocytes have an essential role in neuronal excitability (Halassa and Haydon, 2010) and synaptic function (Perea *et al.*, 2014). In particular, they perceive neuronal and synaptic activity through activation of ion channels, neurotransmitter transporters and receptors (Perea *et al.*, 2014). Astrocytes can regulate the activity of neurons and synapses by the uptake of neurotransmitters or by the release of gliotransmitters, contributing to neuronal network function (Perea *et al.*, 2009). Astrocytes and neurons are in very close contact and they can communicate bidirectionally. To define the signaling between astrocytes and

neurons and to highlight the direct involvement of astrocytes in synaptic function, it has been developed a novel concepts of “*tripartite synapse*” (Araque *et al.*, 1999). Interestingly, astrocytes play a protective role at tripartite synapse; they release antioxidants that protect neurons from oxidative stress and essential nutrients when demand is increased; they also take up excess of glutamate preventing glutamate toxicity. In AD, astrocytes undergo morphological and functional changes called astrogliosis. Astrogliosis is highlighted by increased glial fibrillary acidic protein (GFAP) expression. Interestingly, A β deposition is able to modify astrocytes physiological function. Thus, astrocytes may exhibit a “reactive” or “activated” phenotype (Verkhratsky *et al.*, 2014). Activation of these cells is a protective response aimed at removing detrimental stimuli. In fact, the “reactive” state starts with the intention to control and remove the brain damage, however it has deleterious consequences. Indeed, reactive gliosis is a self-perpetuating process which, at the end, exacerbates the injury. Astrocytes, together with microglia, are the cellular component of the innate immunity in the CNS. They act as critical players of the neuroinflammatory response (Ransohoff and Brown, 2012). Several studies demonstrated that astrocytes possess tools to internalize and metabolize A β in vivo; they possess a complex apparatus able to take up A β (Wyss-Coray *et al.*, 2003). Other studies reported that astrocytes could synthesize A β *de novo* (Zhao *et al.*, 2011). In fact, astrocytes possess the necessary machinery to synthesize A β . APP and BACE1 overexpression in astrocytes supports the notion that A β accumulation could be secondary to its production by activated astrocytes. Neuroinflammation usually involves the release from activated glia of neurotoxic molecules, including ROS, nitric oxide (NO), and pro-inflammatory chemokines and

cytokines such as interleukin-1 β (IL-1 β), tumor necrosis factor- α (TNF- α), and interferon- γ (IFN- γ). Excessive levels of these mediators are able to induce neuronal damage through a variety of mechanisms in AD. A limited number of studies investigated the effects of pro-inflammatory cytokine and A β stimulation on BACE1 and APP levels and β -secretase processing of APP in astrocytes. The effects of TNF- α and IFN- γ on A β production have been demonstrated in cultured cells including astrocytes (Blasko *et al.*, 2000). By contrast, other studies have shown that A β itself is able to stimulate astrocytes to secrete pro-inflammatory molecules *in vitro* and *in vivo* (Zhong *et al.*, 2007). In summary, astrocytes normally maintain and support the function of neurons; under inflammatory conditions they can contribute to the production of A β in the brain. Anti-inflammatory drugs that inhibit astrocytes activation and cytokine production (Combs *et al.*, 2000) may also suppress the APP amyloidogenic pathway.

1.11.2 Astrocytes and potassium homeostasis

Astrocytes membranes have a high potassium conductance due to their abundant expression of potassium channels. Glial cells have the ability to maintain extracellular potassium concentration ($[K^+]_e$) at a constant level. This function has been called “K⁺-spatial buffering”, originally proposed by Orkand *et al.*, 1966. They proposed the hypothesis that glia have a function to aspirate K⁺ ions at the sites where $[K^+]_e$ is high to transport them within the cell, and to extrude the ions at the sites where $[K^+]_e$ is low. Two conditions are necessary for optimal K⁺-spatial buffering: 1) the glial cells should form a syncytium in which K⁺ currents can cross relatively long distances; and 2) these cells should be highly and selectively permeable to K⁺. This mechanism minimizes

the deleterious effects of prolonged increases of $[K^+]_e$ resulting from neuronal activity. Thus, astrocytes modulate neuronal excitability and contribute to functions that depend on the transmembrane potassium gradient. To prevent undesirable neural excitation, glial cells aspirate excess extracellular K^+ ions.

1.12 Animal models of Alzheimer's Disease

Animal models of AD must mimic the disease both pathologically and behaviorally. Janus *et al* proposed 5 expectations for a credible rodent model of AD: **1)** mice should exhibit progressive neuropathology culminating in one or more of pathologic hallmarks of AD (plaques, NFTs); **2)** mice should exhibit cognitive deficits evident in different behavioral paradigms targeting the same memory system; **3)** in the case of experiments employing FAD mutations, phenotypic changes documented in 2 and 3 should be correlated with the presence of the FAD mutations; **4)** key facets of the phenotype as for 1 and 3 should be confirmed in independent transgenic lines harboring the same construct, to exclude the contribution of insertional mutations; **5)** key facets of the phenotype as for 1 and 3 should have been confirmed in several laboratories. Several strains of transgenic mice overexpressing FAD-related mutated genes have been created. These animals show a variety of phenotypes that are similar to AD but none of them represent a full scene of AD.

1.12.1 APP transgenic mice

Transgenic mice are created by expressing variants of APP, PS-1, PS-2, apoE, or tau genes. Mice that overexpress mutated forms of APP gene were the first transgenic models of AD. These mice develop a large variety of behavioral, biochemical, pathological, and physiological characters simulating AD, although not all characters have been represented within an individual mouse line. One of these models, the Tg2576 line, is used in the current study and its features will be discussed in detail in a separate section. The earliest transgenic models of AD overexpressed full-length (Lamb *et al*, 1993; Pearson *et al*, 1993) or C-terminal fragments (Kammesheidt *et al*, 1992) of wild-type APP (Mucke *et al*, 2000). Three different promoters (PDGF, PrP and Thy-1) and at least three mutations [V717I (Moechars *et al*, 1999), V717F (the PDAPP line, Games *et al*, 1995) and K670N/M671L (Hsiao *et al*, 1996)] produce age-dependent increases in A β concentration and deposition into amyloid plaques. However, none of these models share all the pathological changes seen in human AD. NFTs are absent in all these models, although hyperphosphorylated forms of tau are detectable. The severe loss of neurons and synapses, described in human AD, is not prominent in APP transgenic mice. In contrast, synaptic degeneration and dysfunction has been reported in all the models studied. Structural changes include reduced synaptophysin immunoreactivity, altered neurite path, dendritic spine loss and retreating of dendrites. Among the behavioural phenotype, hippocampal dysfunction is the earliest and most prominent feature of AD. Thus, behavioural testing of mouse AD models has focused on spatial learning and memory. APP transgenic mice model have been shown to develop deficits in spatial learning and memory in a variety of behavioural test (Hsiao *et al*, 1996; Jacobsen *et al*, 2006).

Interestingly, the severity of some behavioural deficits coincides with onset of amyloid deposition (Walsh *et al*, 2002).

1.12.2 PS transgenic mice

Mutations in PS-1 and PS-2 cause FAD. More than 170 mutations in PS-1 and 14 mutations in PS-2 have been linked to FAD. Both PS-1 and PS-2 FAD mutant transgenic lines have been generated by pronuclear injection using a variety of heterologous promoter (Elder *et al.*, 2010). These models only show increased production of A β 42 without formation of neuritic plaques or neuronal loss. When crossed with plaque forming APP FAD mutant lines, the PS-1 FAD mutants cause earlier and more extensive plaque deposition. Although single transgenic PS-1 or PS-2 mice do not form plaques, they exhibit a number of pathological features including age-related neuronal and synaptic loss as well as vascular pathology. They also exhibit increased susceptibility to excitotoxicity injury most likely on the basis of exaggerated calcium release from the endoplasmic reticulum. Several studies have addressed the effects of PS-1 FAD mutants on electrophysiological parameters in hippocampal slice cultures. These studies revealed that PS-1 FAD mutants cause the enhancement of LTP in the hippocampus, but this effect appears to be age-dependent and lost with aging. Some studies have evaluated whether PS FAD mutant transgenic mice display behavioral abnormalities using standard series of tests. PS FAD mutant mice have performed normally or the deficits have been inconsistent. Due to the lack of plaques, PS FAD mutant mice have been less studied than APP or APP/PS FAD mutant mice.

1.12.3 Tau transgenic mice

The first tau transgenic models used expression of wild type four-repeat (Götz *et al.*, 1995) and three-repeat (Brion *et al.*, 1999) of human tau. These mice reproduced aspects of human pathology, such as hyperphosphorylation of tau protein. Although tau solubility decreases in age-dependent manner, these mice did not form NFTs, unless the mice reached a very old age (Ishihara *et al.*, 2001). Later, many groups discovered pathogenic tau mutations for producing animal models. Following the identification of pathogenic mutations in Tau in frontotemporal dementia and parkinsonism linked to chromosome 17 (FTDP-17), several groups described the formation of NFTs in neurons and glial cells in mice transgenic for mutant human tau. The first published NFT-forming model expressed human P301L tau (Lewis *et al.*, 2000). The P301L mouse model presents NFTs in brain and in spinal cord, also showed abnormal tau filaments. Moreover, the progression of neurofibrillary pathology and neuronal loss is also correlated with the progression of deficits in spatial memory, indicating a detrimental effect of NFTs on memory (Santa-cruz *et al.*, 2005). To reproduce the A β plaque and NFT pathologies in a single mouse model, double-transgenic strain was developed crossing Tg2576 mice that produce A β with JNPL3 tau mice (P301L mutation). This double transgenic mouse, called TAPP, showed amyloid pathology, that greatly enhanced NFT formation (Lewis *et al.*, 2001).

1.12.4 Multiple-transgenic models: Triple-Transgenic

The 3xTg-AD mice, harboring mutations of APP (Swedish), PS-1 (M146V), and tau (P301L), has been developed by Oddo *et al.* (2003b) to study the

interaction between A β and tau and their effect on synaptic function. 3xTg-AD mice gradually develop plaques and tangles. This is the first transgenic model to develop an age-related and neuropathological phenotype that includes both plaque and tangle pathology in AD relevant brain region. Synaptic dysfunction, including LTP deficits, appears in an age-related manner. Therefore, deficits in long-term synaptic plasticity correlate with the accumulation of intraneuronal A β (Oddo *et al.*, 2003b). Interestingly, as is the case of human AD, it's find that A β deposits precede tau alterations in the 3xTg-AD mice. In subsequent studies, treatment of 3xTg mice with anti-A β antibodies, or antibodies specific for oligomeric forms of A β , led to the rapid clearance of accumulated A β deposition and early tau lesions in the cell body (Oddo *et al.*, 2004; Oddo *et al.*, 2005).

1.12.5 Tg2576 mouse model

The APPSWE mouse was developed in the laboratory of Karen Hsiao at the University of Minnesota, in association with the Mayo Clinic. This model was created by microinjecting the human *APP*₆₉₅ gene containing the double “Swedish” mutation (Lys670→Asn, Met671→Leu) K670N, M671L into B6SJLF2 zygotes (Hsiao *et al.*, 1996). The mutant gene induced the overexpression of APP695 in the brains of mice over 2 months of age, and thus, elevated brain levels of A β (Hsiao *et al.*, 1996). In addition to amyloid pathology, Tg2576 mice also show activated microglia, reactive astrocytes and neuritic dystrophy, which mimic what is observed in AD. Learning and memory abilities of these mice have also been measured using a large number of behavioural tests.

Chapter 2: Potassium channels

2.1 Ion channels

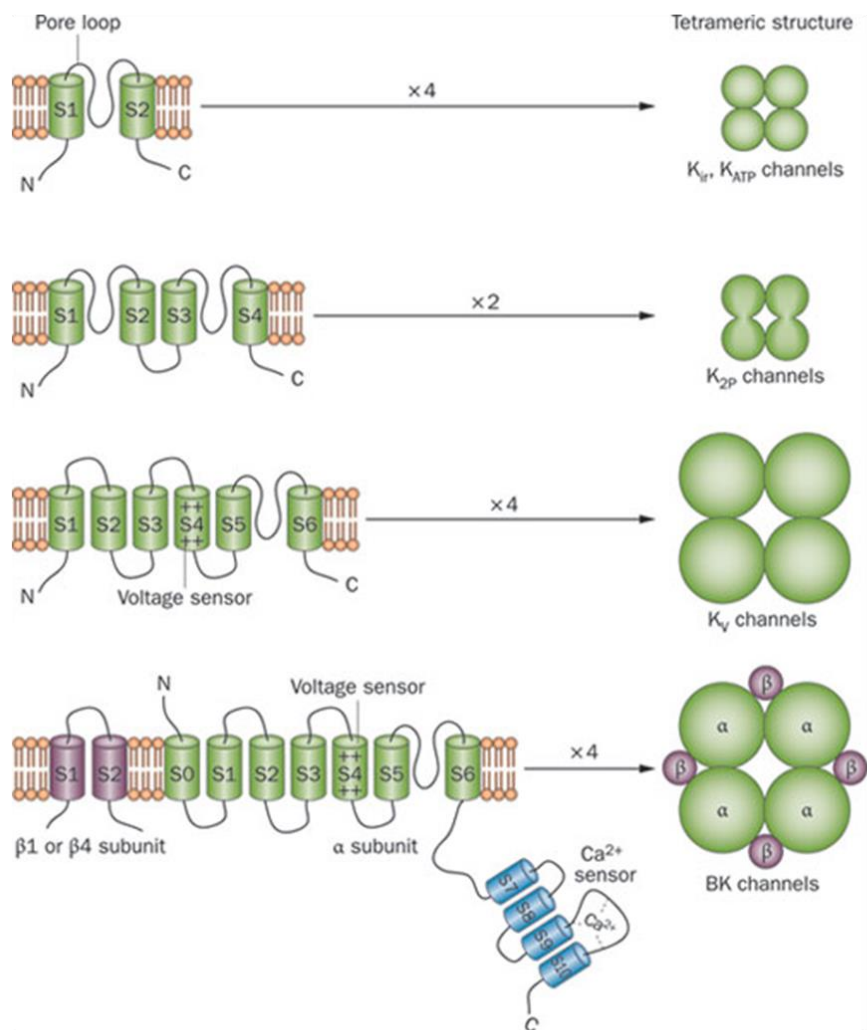
Ion channels are transmembrane proteins, inserted in the phospholipid bilayer of the plasma membrane (or organellar membranes) of cells, which passively consent the flow of ions in and out of the cell down their electrochemical gradient. Ion channels regulate ion flux in response to specific signalling stimuli that trigger the channels to switch between an “open” (in presence of the gating stimulus) and “closed” (in absence of the gating stimulus) conformational states. Ion channels can be divided into three classes that include slowly modulated channels, ligand-gated ion channels and voltage-gated ion channels. Voltage-gated ion channels are essential for the production of action potentials which permit rapid transmission of signals between distant organs on a millisecond. These channels include sodium, calcium and potassium channels, as well as channels with mixed sodium-potassium conductances and hyperpolarization-activated, cyclic-nucleotide gated, cation non-selective (HCN) channels. Sodium and calcium channels are composed of four concatemerized transmembrane domains each containing six transmembrane helices or segments, S1-S6. Instead, potassium channels exist as four separate subunits that are assembled together as tetramers (Xu *et al.*, 1995). The three fundamental voltage-gated channel families work together to produce neuronal and myocyte action potentials. In addition to their physiological roles in maintaining cellular ion homeostasis and controlling the bioelectrical properties of the cell membrane, it has been shown that dysregulation of ion channel function has a role in many pathological diseases (channelopathies) (Kass *et al.*, 2005).

2.2 Potassium channels

Potassium (K^+) channels include a large family of homologous membrane proteins. In excitable tissues, they regulate cardiac pacemaking, action potentials, and neurotransmitter release; in non-excitabile cells, they play important roles in hormone secretion, cell proliferation, cell volume regulation, and lymphocyte activation, migration, differentiation, proliferation and apoptosis (Dubois *et al.*, 1993; O'Grady *et al.*, 2005). Potassium channels can be subdivided in different families, depending on the architecture of their conducting subunits (α subunit): two transmembrane domains and one pore channels (2TM/1P) (Yang *et al.* 1995); four transmembrane domains and two pore channels (4TM/2P) ; six transmembrane domains and one pore channels (6TM/1P) (**Fig. 4**). The 2TM channels are the phylogenetically oldest potassium channels; each subunit is composed of one pore region surrounded by two TM domains. Initially termed “anomalous” rectifiers, these channels conduct an inward potassium current and little outward current during depolarization. The 4TM channels, or tandem pore domain channels, are a class of potassium channels where each alpha subunit contains two pore-forming sequences (Kim, 2005). Often termed leak or background channels, these channels are generally voltage-independent and can contribute to setting the resting membrane potential and regulating cellular excitability. Members of the 4TM channel group can be regulated endogenously by a variety of stimuli including pH, second messengers, temperature and also exogenously by general anesthetics. The 6TM channels are the largest class of potassium channels and are divided into two subclasses, the calcium-activated and the voltage-gated channels. These channels are tetramers of 6TM alpha subunits containing one pore domain each (Jenkinson, 2006).

Changes in voltage or intracellular calcium cause these channels to open and conduct an outward flow of potassium. Calcium-activated potassium channels include large (big), intermediate and small conductance channels (BK, IK and SK, respectively). The function of IK channels, expressed in erythrocytes and endothelium, includes the regulation of cell volume and blood pressure. SK channels are predominantly expressed in the nervous system and contribute to the after hyperpolarization that regulates action potential firing rates (Stocker, 2004). BK channels are highly expressed in smooth muscle and neurons and are involved in processes such as vasodilation and neurotransmitter release.

Fig.4 K⁺ channels architecture



Petkov GV. Nature Reviews, 2011

Fig.4 K⁺ channels architecture. **2TM/P** channels consist of two transmembrane (TM) helices with a P loop between them and one pore region. **4TM/2P** consist of two repeats of 2TM/P channels. **6TM/1P** channels consist of six transmembrane helices and one pore region. **8TM/2P** channels are hybrids of 6TM/P and 2TM/P. S4 is marked with plus signs to indicate its role in voltage sensing in the voltage-gated K⁺ channels.

2.3 Voltage gated potassium channels

Potassium channels activated by voltage are named voltage-gated potassium channels; nomenclature for these channels is “K_V”, which represents the specificity for the potassium ion (K) and the mode of activation, voltage (v). According to the International Union of Pharmacology (IUPHAR) they are divided into twelve families, K_V1-12. Phylogenetic trees of the K_V channels divided these channels into three groups: **a)** K_V1–K_V6 and K_V8–K_V9 families; **b)** the K_V7 family; **c)** the K_V10–K_V12 families (Gutman *et al.*, 2003). The typical voltage-gated K⁺ channel assembles in four identical (or similar) transmembrane subunits surrounding a central pore. Each subunit has six transmembrane segments (S1–S6), with both N- and C- termini on the intracellular side of the membrane. Assembly into a tetramer forms two domains: a voltage sensing domain (S1-S4) and pore domain (S5-S6).

2.3.1 The pore domain and the voltage sensor

The pore domain contains two regulatory modules: the selectivity filter and the intracellular channel gate (Long *et al.* 2007). K_V channels are selectively permeable to potassium, this selectivity is reached through a sequence of aminoacids near the extracellular side of the ion conducting pathway (Thr-Val-Gly-Tyr-Gly) (Doyle *et al.*, 1998). This sequence is crucial for the selectivity filter of the channel; in fact mutations in this sequence lead to a lack of K⁺ ion selectivity (Heginbotham *et al.*, 1994). The access of ion conducting pore is controlled by intracellular gate comprised of the S6 C-terminal end, which form a bundle crossing that obstructs the pore when the channel is closed. The voltage sensing domain is comprised of the S1-S4 helices of the α-subunits

and is responsible for detecting changes in membrane potential. S4 playing a major role, contains a positive charged aminoacids (Lys o Arg) repetitively 4 to 8 times. This creates a positively charged surface along the S4 which senses the membrane potential. S1-S3 segments, plenty of negative charges, complete the voltage sensing domain and help to stabilize the positively charged S4 segment in the lipid bilayer (Long *et al.*, 2005). Upon membrane depolarization, the positively charged S4 helices move out toward the cell exterior, resulting in a widening of the ion conduction entrance. Membrane repolarization causes the S4 helices to move back into the membrane, forcing the shift of the linker helix between the S4 and S5. This movement near the intracellular side of the cell compresses the gate and prevents the flux of ions.

2.3.2 The gating

There are three established mechanisms by which the voltage-gated K⁺ channels can close: two of them involve a conformational constriction of the permeation pathway, and one involves conditional plugging of the pore by an auto-inhibitory part of the channel protein (Yellen, 2002).

1) *Sliding helix model*: the channel can close by pinching shut at the intracellular entrance. This intracellular or S6 gate obstructs entrance from the cytoplasmic surface to the water-filled 'cavity' in the centre of the channel protein (Durell *et al.*, 1998).

2) *Transporter-like model*: a second mechanism for closing the pore uses the S6 gate to regulate the binding of an auto-inhibitory peptide that is part of the channel. The N terminus of K⁺ channels can act as a channel blocker, probably by binding directly to the cavity (Chanda *et al.*, 2005).

3) *Paddle model* in which a voltage sensor paddle comprised by S4 and the C-terminal half of S3 form a rigid structure that moves through the membrane in a close proximity to S1 and S2 (Ruta *et al.*, 2005).

2.4 Traffic of K_V channels

K_V channels are synthesized and assembled as tetrameric complexes in endoplasmic reticulum (ER) (Lu *et al.*, 2001). The perfect folding of K_V may require the intervention of chaperons such as Heat Shock Protein (Hsp) or calnexin. From the ER, K_V channels complexes continue their journey to the plasma membrane, passing through cis-medial- and trans-Golgi elements. Along this trafficking to Golgi apparatus, K_V channels undergo modification, such as N-linked glycosylation, tyrosine, serine or threonine's phosphorylation. Interestingly, phosphorylation modify channel's activity, surface membrane targeting and recycling (Misonou *et al.*, 2004). Ubiquitination also regulates K_V 's membrane levels.

2.5 Regulatory subunits

Accessory subunits influence a wide range of K_V channel properties, such as gating, post-translational modifications, traffic, subcellular localization and pharmacology. Different regulatory subunits have been described, some of them are cytoplasmic [$K_V\beta$ subunits, KChip (K^+ Channel Interacting Proteins)] and KChAP (K^+ Channel Associated Protein) and others are transmembrane proteins [(KCNEs and DPPLs (dipeptidyl aminopeptidase like proteins)] (Li *et al.*, 2006). $K_V\beta$ are cytoplasmic regulatory subunits which interact with K_V channels. There are three subfamilies of $K_V\beta$: $K_V\beta1$, $K_V\beta2$ and $K_V\beta3$.

Stoichiometry association with K_V channels is 1:1 (Long *et al.*, 2005). $K_V\beta 1$ interacts with all the member of K_V1 members; $K_V\beta 2$ interacts with K_V1 and K_V4 members; $K_V\beta 3$ interacts with $K_V1.2$, $K_V1.3$, $K_V1.4$ and $K_V1.5$. **KChips** interact specifically with K_V4 members, especially with $K_V4.2$ and $K_V4.3$. KChips slow the inactivation, regulate traffic and localization, modulate membrane mobility and endocytosis of K_V4 . Stoichiometry association with K_V channels is 1:1. **KChAP** accessory subunits improve the current amplitude of K_V channels and have a role as chaperone leading to an increase in the surface expression of the channel (Pourrier *et al.*, 2003; Li *et al.*, 2006). They can associate to $K_V1.1-1.5$ and $K_V2.1-2.2$. **DPPLs** interact with K_V4 channels and lead to an increase in surface expression and a significant acceleration of the inactivation time of channels (Strop *et al.*, 2004). **KCNEs** are small transmembrane proteins which interact with a wide range of K_V channels. The family is composed of five members (KCNE1-5) and has an ubiquitous expression (McCrossan and Abbott, 2004).

2.5.1 KCNE family

KCNE genes encode a family of single transmembrane domain proteins called MinK-related peptides (MiRPs) that function as ancillary or β subunits of K_V channels. MiRPs cannot form functional ion channels alone, however when co-expressed with pore forming K_V α subunits, they form stable complexes and serve to modulate important biophysical properties of the channel. When co-expressed in heterologous systems, MiRPs confer changes in K_V channel conductance, gating kinetics and pharmacology, and are fundamental to the properties of some native currents. The **KCNE1** gene encoding MinK (Minimal K^+ currents) was originally cloned from rat kidney in 1988 (Takumi *et al.*,

1988). The name MinK reflects early thinking that this protein was the minimal size needed to form K^+ channels. MinK is a 130-amino-acid protein with a molecular weight of 15 kDa. Two splicing isoforms have been described: KCNE1a, which is more ubiquitously; KCNE1b which is a heart specific isoform. The **KCNE2** gene encoding minK-related peptide 1 (MiRP1), whereas **KCNE3** and **KCNE4** gene encoding MiRP2 and MiRP3 respectively. Human MinK and related peptides are integral membrane proteins, 103–177 residues in length, their single transmembrane domain flanked by an extracellular N-terminal and cytosolic C-terminal. MiRPs cannot form functional ion channels alone, however they form stable complexes with pore forming $K_V\alpha$ subunits. MiRP subunits may modulate the gating of a particular α subunit type. MinK/MiRPs are widely expressed in mammalian tissues, in particular into heart, smooth muscle and epithelia, skeletal muscle, and brain (Abbott *et al.*, 2001; McCrossan *et al.*, 2003; McCrossan and Abbott, 2004).

2.6 K_V3 channels

The family of mammalian K_V3 genes, related to the *Drosophila Shaw* gene, consisting of four subfamilies, encodes the subunits of tetrameric voltage-gated K^+ channels. There is convincing evidence that subunits of the same subfamily, but not of different subfamilies, form heteromultimeric channels. There are four K_V3 genes known both in rodents and humans, that generate multiple products by alternative splicing. The analysis of cDNAs predicts the existence of twelve different K_V3 proteins in mammals. The four K_V3 subunits are designated $K_V3.1-4$ and encoded by the genes *Kcnc1-4* in rodents or KCNC1-4 in humans. *Kcnc1* has at least two known variants that change the C terminus of the protein designated $K_V3.1a$ and $K_V3.1b$. *Kcnc2* has three

variants and *Kcnc4* has four known variants. *Kcnc3* has three published and more unpublished variants affecting the 3'UTR (Rudy *et al.*, 1992; Rudy *et al.*, 1999). In rodents, three of the four K_V3 genes ($K_V3.1$ – $K_V3.3$) are expressed mainly in brain. $K_V3.4$ is lowly expressed in brain, but strongly in skeletal muscle. Low levels of $K_V3.1$ are also seen in skeletal muscle, while low levels of $K_V3.3$ mRNAs are found in kidney and lung. $K_V3.1$, $K_V3.3$, and $K_V3.4$ products have also been identified in pheochromocytoma cells (PC12). Three of four K_V3 genes ($K_V3.1$, $K_V3.2$, and $K_V3.3$) are expressed largely in the CNS; whereas $K_V3.4$ transcripts are also present in the CNS but are more abundant in skeletal muscle. *In situ* hybridization studies in the CNS reveal discrete and specific neuronal populations that express K_V3 mRNAs. In the cerebral cortex, hippocampus, and caudate-putamen, subsets of neurons can be distinguished by the expression of specific K_V3 . K_V3 mRNAs are distributed in a non-homogeneous fashion throughout the CNS. In fact, some neuronal types exhibit undetectable labeling, suggesting that they do not express significant amounts of any K_V3 mRNAs. Interestingly, many neuronal populations expressing $K_V3.1$ transcripts also express $K_V3.3$ mRNAs. Furthermore, $K_V3.4$ transcripts are present, although at lower levels, in several neuronal populations that also express $K_V3.1$ and/or $K_V3.3$ mRNAs, revealing a high potential for heteromultimer formation. Most neurons in the cerebral cortex, the epithalamus, and the hypothalamus, the amygdala, the substantia nigra compacta, and a few structures in the brainstem such showed undetectable labeling with K_V3 probes. Others, such as the pyramidal neurons in the hippocampus, particularly in the CA1 were only weakly labeled. K_V3 gene expression is prominent in the thalamus, cerebellum, brainstem, and spinal cord (Weiser *et al.*, 1994). In the cortex and the hippocampus some K_V3

mRNAs appear to be expressed in distinct sets of interneurons. Since $K_v3.4$ transcripts appear to be much less abundant throughout the CNS than the products of the three other K_v3 genes, and are mainly expressed in neurons also expressing $K_v3.1$ or $K_v3.3$ mRNAs, $K_v3.4$ subunits may act in CNS neurons as modulators of the inactivation properties of channels composed mainly of $K_v3.1$ and $K_v3.3$ proteins. The electrophysiological studies suggested that small amounts of $K_v3.4$ transcripts might be sufficient to impart fast inactivating properties to channels composed mainly of the other K_v3 subunits. K_v3 currents have several unusual properties that distinguish them from those of other K^+ channels known. These include their activation voltage range that is more positive than that of other voltage-gated K^+ channels. Another unusual feature of K_v3 currents is their fast rate of deactivation upon repolarization, first described for $K_v3.1$ currents expressed by Grissmer *et al.* These authors found that $K_v3.1$ currents deactivated about 10 times faster than other voltage-gated K^+ channels known at the time (Grissmer *et al.*, 1994).

2.7 Regulation of K_v3 channels

Several sites for protein-kinase phosphorylation are found in regions of K_v3 proteins that are thought to be intracellular. Some of these sites are found in proteins encoded by all of the genes, some are found only in proteins encoded by a single gene, and some are specific to alternatively-spliced isoforms. Three kinase systems, cAMP-dependent protein kinase (PKA), protein kinase C (PKC), and cGMP-dependent protein kinase (PKG) have now been shown to modulate K_v3 channels function in heterologous expression systems. $K_v3.1$ is modulated negatively by PKC (Macica *et al.*, 2003). An exception is $K_v3.3$,

the current of which is facilitated by PKC (Desai *et al.*, 2008). PKA also modulates K_v3 channels (Moreno *et al.*, 1995). The channels are in addition sensitive to oxidative stress (Rudy *et al.*, 1992). Less acute modulation also is exerted through association with auxiliary subunits (McCrossan *et al.*, 2003).

2.8 Pharmacology of K_v3 channels

The classic blocker for K_v3 channels has been tetraethylammonium (TEA), which blocks ~90% of K_v3 current at 1 mM where it has weak effects on calcium-activated potassium channels. K_v3 channels are also very sensitive to 4-aminopyridine (4-AP). A new set of peptides obtained from the venom of the sea anemone *Anemonia sulcata*, known as blood-depressing substance I and II (BDS-I and BDS-II) showed to block specifically, reversibly, and at low concentrations (IC_{50} values in the low nanomolar range) $K_v3.4$ channels. These toxins, are 43 amino-acids long and differ at only two positions. They share no sequence homologies with other K^+ channel toxins from sea anemones. Instead, it has been demonstrated that BDS-I and BDS-II have some sequence homologies with other sea anemone Na^+ channels toxins (Diochot *et al.*, 1998).

2.9 Contributions of K_v3 Channels to Neuronal Excitability

Potassium channels are crucial regulators of neuronal excitability, setting resting membrane potentials and firing thresholds, repolarizing action potentials and limiting excitability. K_v channels can be categorized based on their voltage sensitivity (low- or high-voltage activated) and inactivation tendencies [delayed rectifier (I_K) or A-type (I_A)] (Dodson and Forsythe, 2004).

Products of the $K_V3.1$ and $K_V3.2$ genes express similar delayed-rectifier type currents, while $K_V3.3$ and $K_V3.4$ proteins express A-type currents. A myelinated axon can be divided in three portions: an initial segment, where somatic inputs summate and initiate an action potential; a variable-length myelinated axon, which must reliably transmits the information as trains of action potentials; and a final segment, beyond which the synaptic terminal expands. Low-voltage-activated K^+ channels are prevalent in the initial axonal segment and terminal segment, in addition to juxtaparanodal location at nodes of Ranvier. High-voltage-activated K^+ channels are localized to somatodendritic regions, sometimes as density gradients. They are also localized on synaptic terminals and nodes of Ranvier in some CNS myelinated fibres (although not at peripheral nodes). Inactivating A-type channels are broadly expressed, contributing to activity-dependent effects on neuronal firing. They can also be localized to synaptic terminals. All K_V3 currents activate relatively fast at voltages more positive than -10 mV, and deactivate very fast. The activation voltage and fast deactivation rates are believed to help these channels to fast repolarize action potentials without affecting the threshold for action potential generation. The fast deactivating current generates a quickly recovering after hyperpolarization, thus maximizing the rate of recovery of Na^+ channel inactivation without contributing to an increase in the duration of the refractory period. These properties contribute to the ability of neurons to fire at high frequencies and to regulate the synaptic transmission. K_V3 currents have several properties that differentiate them from other K^+ channels. These include their activation voltage range that is more positive than that of other voltage-gated K^+ channels. The channels with the nearest activation voltage ($K_V2.1$ and $K_V2.2$) show significant activation at

10–20 mV more negative potentials. Although Kv3 channel opening becomes significant at high potentials (more positive than -10 mV), the probability of channel opening increases with voltage and $>80\%$ of the channels are opened between $+30$ and $+40$ mV.

Chapter 3: Pathological implications of K_v3 potassium channels

3.1 Potassium dysregulation in Alzheimer's Disease

A growing evidence demonstrated that $A\beta$ peptide increases intracellular Ca^{2+} concentrations ($[Ca^{2+}]_i$) and disrupts Ca^{2+} homeostasis by several mechanisms, including modulation of voltage-gated Ca^{2+} channels, formation of Ca^{2+} -permeable pores and inhibition of the Na^+/Ca^{2+} exchanger (Wu *et al.* 1997). Alteration of K^+ channel function in brain cells appears to be relevant to AD pathophysiology. Treatment with neurotoxic $A\beta$ fragments enhanced K_v channel activity in mouse SN-56 hybrid septal neuroblastoma cells (Colom *et al.*, 1998) and in primary rat cerebellar granule cells (Ramsden *et al.* 2001), as well as in rat cortical astrocytes (Jalonen *et al.*, 1997) and microglial cells (Chung *et al.* 2001). Interestingly, the inhibition of K^+ efflux, either by use of pharmacological tools or by increasing the extracellular K^+ concentration, fully prevented cell death induced by $A\beta$ (Colom *et al.*, 1998). Taken together, these studies, which complement earlier observations on K^+ channels expressed in fibroblasts, platelets and, possibly, neuronal tissues from patients with AD, appear to lend support the systemic K^+ -dysregulation hypothesis for AD (Etcheberrigaray and Bhagavan 1999). Pannaccione *et al.*, in 2005, showed that the neurotoxic $A\beta_{25-35}$ and $A\beta_{1-42}$ peptides caused a dose-dependent and time-dependent enhancement of total outward K^+ in NGF-differentiated PC-12 cells and primary rat hippocampal neurons. Biophysical and pharmacological dissection of the K^+ conductances underlying total outward K^+ currents in these cells showed that both fast inactivating (I_A)

and non inactivating (I_{DR}) components were enhanced by neurotoxic $A\beta$ treatment.

3.1.1 $K_V3.4$ and Alzheimer's Disease

Angulo *et al.* performed genomic analyses using cDNA arrays containing a pool of cDNAs. The authors focused the attention on genes whose expression changes in early stages of the disease, in order to find potential therapeutic targets useful in preventing the progression of the clinical symptoms. We found, for the first time, that the potassium channel $K_V3.4$ is already up-regulated in the early stages of AD. Moreover, the gene encoding $K_V3.4$ was also overexpressed in the late stages of AD. Immunoblot analysis of $K_V3.4$ in extracts from control and AD frontal cortex revealed a band at 105 kDa, corresponding to the molecular weight of the channel. The level of $K_V3.4$ channel protein in samples from AD early and samples from AD late was significantly higher than in controls. This result indicates that the increased level of expression of mRNA in AD samples correlates with higher levels of protein. $K_V3.4$ immunoreactivity increased in AD only in association with amyloid deposits in senile plaques. Increased $K_V3.4$ immunoreactivity occurred in the form of fine granular precipitates or larger granules surrounding βA deposits (Angulo *et al.*, 2004). Pannaccione *et al.*, in 2007, demonstrated that $A\beta_{1-42}$ treatment induced a selective up-regulation of $K_V3.4$ channel subunits through the activation of the transcriptional factor NF- κB . The action of $A\beta_{1-42}$ was not limited only to the α subunit of $K_V3.4$; in-fact, it also induced an over expression of MiRP2, a neuronal β -subunit co-assembling with $K_V3.4$ subunit and playing a crucial role in the control of its

biophysical properties and pharmacological profile (Abbott *et al.*, 2001). The hypothesis that $K_v3.4$ channels are involved in the $A\beta_{1-42}$ neurotoxic effect was further supported by the results showing that BDS-I, a $K_v3.4$ blocker (Diochot *et al.*, 1998), exerted a potent neuroprotective action in hippocampal neurons and NGF-differentiated PC-12 cells exposed to $A\beta_{1-42}$ peptide.

3.2 Critical role of potassium homeostasis in apoptosis

Apoptotic cells display a significant cell shrinkage, and K^+ efflux has been suggested to mediate this loss of volume. Intracellular potassium concentrations ($[K^+]_i$) play a key role in cell survival. Cytoplasmic K^+ loss has been shown to favor the activation of caspases and nucleases, which lead to apoptosis (Hughes *et al.*, 1997; Cain *et al.*, 2001). Indeed, several studies demonstrated that cellular K^+ depletion by valinomycin (K^+ ionophore) or plasma membrane K^+ channel over-expression induces apoptosis in different cell types. Moreover, high extracellular K^+ has been reported to inhibit both the extrinsic and the intrinsic apoptosis, probably by inhibiting the Cyt C release. Given that K^+ efflux has been proposed to be a pro-apoptotic factor, plasma membrane potassium channels mediating K^+ efflux out of the cell represent good candidates for apoptosis regulation. Furthermore, it has been demonstrated that serum deprivation or staurosporine induced apoptosis of cortical neurons in 24–48 hours. This event was associated with an early enhancement of I_K current and loss of cellular K^+ (Yu *et al.*, 1997). Attenuating the outward K^+ current with TEA or elevated extracellular K^+ reduced apoptosis (Yu *et al.*, 1997).

3.2.1 K_v3.4 and apoptosis

A similar I_K enhancement was verified with other apoptotic insults such as β A peptides (Yu *et al.*, 1998). Exposure to A β fragment 25-35 or 1-42 enhanced the delayed rectifier K⁺ current I_K, shifting its activation voltage relationship toward hyperpolarized levels and increasing maximal conductance. Reducing I_K by adding TEA raising extracellular K⁺ to 25 mM attenuated A β -induced neuronal death (Yu *et al.*, 1998). Furthermore, a study performed on SN56 cells, a cholinergic cell line from rat, described that treatment with A β ₁₋₄₂ increased delayed rectifier K⁺ currents and amplified cell death (Colom *et al.*, 1998). As previously described, Pannaccione *et al.* have been demonstrated that A β ₁₋₄₂ peptide induced a selective up-regulation of K_v3.4 channel subunits through the activation of the transcriptional factor NF- κ B. In addition, this transcriptional event is associated with a current increase carried by this channel. In addition, hippocampal neurons and NGF-differentiated PC-12 cells over expressing K_v3.4 showed an apoptotic nuclear process, as revealed by caspase-3 activation and by Hoechst 33258-monitored abnormal nuclear morphology, thus suggesting a possible link between the enhanced expression and function of this K⁺ channel and the neurotoxic consequences provoked by A β exposure. The hypothesis that K_v3.4 channels are involved in the A β ₁₋₄₂ neurotoxic effect was supported by the results showing that BDS-I, a K_v3.4 blocker (Diochot *et al.*, 1998), exerted a potent neuroprotective action in hippocampal neurons and NGF-differentiated PC-12 cells exposed to A β ₁₋₄₂ peptide (Pannaccione *et al.*, 2007). The relationship between K_v3.4 and apoptotic cell death is demonstrated by the fact that the blockade of this channel was able to prevent the apoptotic process triggered by A β ₁₋₄₂ fragment.

3.3 Critical role of potassium homeostasis in memory and learning

Advancing age is accompanied by deficits in learning and memory. Normal aging is associated with cellular and molecular changes which include a decrease in neuronal excitability and an alteration in synaptic plasticity. The age-related changes in neuronal function, as well as neuronal dysfunction associated with AD, may be the result of a dysregulation of the Ca^{2+} homeostasis. Many studies demonstrated the increase of intracellular Ca^{2+} in hippocampal neurons from aged animals or AD animal models. The increase in intracellular Ca^{2+} concentration has a number of functional consequences, the most relevant is a decrease in postsynaptic neuronal excitability. It's important to highlight that neuronal excitability affects plasticity and learning. This reduction in neuronal excitability could in turn lead an increase in the threshold for LTP, thus altering the ability of the hippocampus to encode information (Murphy *et al.*, 2004). Emerging evidence indicates that K_V channels are key regulators of neuronal excitability and that they have a critical role in learning and memory. (Giese *et al.* 2001; Solntseva *et al.* 2003). Primarily K_V channels have a role in the setting of the resting membrane potentials and in the repolarization during actions potentials in excitable cells. K_V channels are categorized based on their voltage sensitivity (low or high voltage-activated) and inactivation tendencies (delayed rectifier (I_K) or A-type (I_A)) (Dodson and Forsythe, 2004). Collectively, K_V channels set and stabilize resting membrane potential, repolarize action potentials (APs), and control the discharge frequency by regulating inter-spike intervals, thus they play a crucial role in the generation of neuronal electrical activity and influencing neuronal excitability. Changes of K_V channel activity could lead to neuronal dysfunction and disrupt

cognition. As the number and pattern of APs are necessary to encode information (Reike *et al.*, 1997), K_V channel dysfunction may alter information processing and therefore be an important link in memory disturbances. Experiments in several model have shown that the reduction in K^+ currents correlates with improved memory and LTP, whereas the increase in K^+ currents corresponds to learning and memory deficiencies (Ghelardini *et al.* 1998; Alkon, 1999). Importantly, increased K_V4 currents lowers LTP induction probability (Watanabe *et al.*, 2002), while decreased K_V4 currents enhances LTP (Frick *et al.*, 2004) and improves learning and memory (Lilliehook *et al.*, 2003). Moreover $K_V2.1$ channels regulate neuronal excitability during high frequency stimulation (Murakoshi and Trimmer, 1999; Du *et al.*, 2000; Pal *et al.*, 2003). Dephosphorylation of $K_V2.1$ channels shifts their activation curves to more hyperpolarized potentials and increases their open channel probability (Murakoshi *et al.*, 1997). The increased delayed rectifier current (I_K) leads to a diminished LTP, which is reversible by re-phosphorylation, demonstrating a strong link to this potassium channel activity (Misonou *et al.* 2004).

AIM OF THE STUDY

Chapter 4: Aims and Design of the Present Study

4.1 Rationale and aims of the present study

Accumulating evidence suggests that $K_v3.4$ play a role in AD pathogenesis. Thus, the goal of this study was to further the knowledge about the function played by $K_v3.4$ in a transgenic mouse model of Alzheimer's disease, Tg2576.

In particular, the specific objectives of the PhD thesis were:

1. the evaluation of $K_v3.4$ and MiRP2 protein expression in the hippocampus of Tg2576 and age-matched WT mice;
2. the assessment of $K_v3.4$ activity by patch clamp experiments in Tg2576 and WT hippocampal neurons;
3. to evaluate the implications of $K_v3.4$ in different stages of AD;
4. to assess if the pharmacological or transcriptional modulation of $K_v3.4$ could affect AD progression.

MATERIALS AND METHODS

Chapter 5: Materials And Methods

5.1 Drugs And Chemicals

Poly(D)-lysine Hydrobromide Mol Wt 30,000-70,000 (P7280), Poly(D)-lysine Hydrobromide Mol Wt >300,000 (P7405), Poly-L-lysine hydrochloride (P2658), Cytosine β -D-arabinofuranoside (Ara-C), Nimodipine, Bovine Serum Albumin (BSA), Deoxyribonuclease I from bovine pancreas (DNase), Trypsin from bovine pancreas, Proteinase K from Tritirachium album, TRI Reagent Solution, mouse monoclonal anti- α -Tubulin, rabbit polyclonal anti-GFAP, mouse monoclonal anti-A β (1-17) antibody (4G8) as well as all other materials for solution preparation, were from Sigma Aldrich (Milan, Italy). BDS-1, nerve growth factor (NGF 2.5S), Tetrodotoxin (TTX), rabbit polyclonal anti-K $_v$ 3.4, rabbit polyclonal anti-MiRP2, were from Alomone Labs (Jerusalem, Israel). Roswell Park Memorial Institute (RPMI) 1640 Medium, Dulbecco's Modified Eagle Medium (DMEM), Hanks' Balanced Salt Solution (HBSS), Minimum Essential Medium (MEM), Opti-MEM I Reduced Serum Medium, Horse Serum (HS), Fetal Bovine Serum (FBS), L-glutamine, Penicillin-Streptomycin, Trypsin-EDTA (0.05%), Phosphate-Buffered Saline (PBS), Lipofectamine 2000, Lipofectamine 3000 were purchased from Thermo Fischer (Massachusetts, USA), Invitrogen (California, USA). Rabbit polyclonal anti-caspase 3, rabbit polyclonal anti-caspase 6, rabbit monoclonal anti-A β (17-42) antibody were purchased from Cell Signaling (Massachusetts, USA). Rabbit polyclonal anti-APP antibody was purchased from Ab-cam (Cambridge, UK).

5.2. Mice

Animals were kept under standard conditions of temperature, humidity and light, and were supplied with standard food and water *ad libitum*. Animals were handled in accordance with the recommendations of International Guidelines for Animal Research and the experimental protocol was approved by the Animal Care and Use Committee of “Federico II” University of Naples. All efforts were made to minimize animal suffering and to reduce the number of animal used. Heterozygous male Tg2576 mice and wild-type (WT) littermates, obtained backcrossing male Tg2576 mice with F1 WT female, were used for all experiments. Tg2576 mice, purchased from commercial source [B6;SJL-Tg(APP^{SWE})2576Kha, model 1349, Taconic, Hudson, NY], are well-established AD-related mouse model carrying the human APP Swedish 670/671 mutation (K670N e M671L; Hsiao *et al.*, 1996). F1 wild-type female (B6;SJL) littermates were obtained crossing female C57BL/6 with male SJL; C57BL/6 and SJL mice were purchased from Charles River.

5.2.2 Genotyping: PCR Analysis

Genomic DNA from mouse tails was isolated with salt precipitation method. Tails after the cut were incubated with tail digestion buffer (50 mM Tris-HCl pH 8.0, 100 mM EDTA pH 8.0, 100 mM NaCl, 1% SDS) supplemented with Proteinase K (Sigma Aldrich, Milan, Italy) at a final concentration of 0.5 mg/ml and placed in water bath at 55-60°C overnight with mixing. This step should result in the complete solubilization of the tail fragment. Embryonic brain tissue was kept during cerebral dissection and frozen immediately upon collection. After thawing, we added TRI Reagent to each sample in order to homogenize

the tissue. Subsequently one volume of phenol:chloroform:isoamyl alcohol (25:24:1) was added to each sample. After centrifugation, the mixture separated into 3 phases: an aqueous phase containing the RNA, the interphase containing DNA, and an organic phase containing proteins. We discarded and collected the interphase in a new centrifuge tube for each sample. After we proceeded to DNA precipitation with 100% ethanol; we centrifuged the sample at 4°C for 30 minutes at 16,000 × g to pellet the DNA. Carefully we remove the supernatant without disturbing the DNA pellet; after we added 70% ethanol and centrifuged each sample at 4°C for 2 minutes at 16,000 × g. We removed as much of the remaining ethanol as possible and we dried the DNA pellet at room temperature for 5–10 minutes. Finally we resuspended the DNA pellet in TE buffer (Tris-EDTA) by pipetting up and down 30–40 times. DNA concentration and purity of each sample was quantified using Nanodrop Spectrophotometer (Thermo Fisher Scientific, Wilmington, DE,US). We used following primers to amplify the DNA region with human APP Swedish mutation on both types of genomic DNA: 5'-CTGACCACTCGACCAGGTTCTGGGT-3' and 5'GTGGATAACCCCTCCCC AGCCTAGACCA-3' (Primm, Milan, Italy). 50 ng/μL of DNA were used for PCR reaction. The amplification protocol (30 cycles) was the following: 95°C for 45 s, 55°C for 60 s, 72°C for 60 s. Each 25-μL reaction contained: 1U of AmpliTaq DNA Polymerase (Lucigen, US) and 0.5 μM of each primer. The amplification products were visualized on agarose (2%) gel by loading approximately half (10 μL) of each reaction per lane. The band of 466bp indicated the transgenic genotype, whereas its absence indicated the wild type genotype.

5.2.3 Behavioural tests

AD is characterized by progressive decline in episodic memory and in cognitive abilities. Thus, a valid AD-transgenic model must reflect the behavioral changes observed in AD patients.

5.2.3.1 Open Field

The open field locomotion test is used primarily to examine motor function measuring spontaneous activity in an open field. It is also used to assess anxiety and exploration ability (in particular time spent in the center of the field). The circular or square open fields vary in size and are divided into distinct quadrants or sections. The animal is positioned in the open field and their movements are videotaped or monitored. We placed each mouse in the center of a chamber; mice are allowed to freely explore the chamber for the duration of the test session (5-minutes). Rodents typically spend a significantly greater amount of time exploring the periphery of the arena, usually in contact with the walls, than the center area. Mice that spend significantly more time exploring the unprotected center area demonstrate anxious behavior. Many software systems allow the researcher to designate center area, as well as multiple other regions of the test chamber, to track exploratory activity. The most commonly used measure to evaluate exploratory/locomotor activity is the total distance traveled.

5.2.3.2 T maze spontaneous alternation

The most extensively used paradigms for working memory in mice are maze (labyrinth) type tasks which require spatial working memory to solve. T-maze tasks are extensively used for cognitive behavioral testing in both mice and rats. These tasks are based on the natural exploratory behavior of rodents, in particular about the tendency to choose an alternative/new arm rather than familiar arm which has been previously explored. The T-maze is an apparatus in the form of a T placed horizontally. Animals are started from the base of the T and free to choose one of the goal arms. If two trials are given in quick succession, on the second trial the rodent tends to choose the arm not visited before, reflecting memory of the first choice. This is called “spontaneous alternation”. Spontaneous alternation is sensitive to dysfunction of the hippocampus, but other brain structures are also involved. Each trial should be completed in under 2 minutes, but the total number of trials required will vary (at least ten trials) (Deacon and Rawlins, 2006).

5.3 Cell Cultures

5.3.1 PC-12 Cells

Rat pheochromocytoma cells (PC-12 cells), a clonal cell line derived from a pheochromocytoma of the rat adrenal medulla, were grown in 100 mm plastic Petri dishes in 85% RPMI 1640, 10% HS and 5% heat-inactivated fetal FBS, containing penicillin (5U/mL) and streptomycin (5µg/mL), at 37°C with 5% CO₂. For electrophysiological experiments and morphological analysis, cells were seeded at low density on glass coverslips (Glaswarenfabrik Karl Hecht KG, Sondheim, Germany) coated with poly-L-lysine (50 µg/mL). Differentiation of

PC-12 cells was achieved by treatment with NGF 2.5S (50 ng/mL) for 7 days (Greene and Tischler 1976). In order to assess the differentiation status of the cells, in some experiments a “differentiation score” was calculated by means of phase contrast microscopy analysis (Eclipse E400 microscope; Nikon, Torrance, CA, USA). This was based on the number of neurites and the length of neuritic extension: 0, round cells; 1, cells with any extension of one or more neurite, each less than one body length; 2, extension of one or more neurites between one or two cell body lengths; and 3, at least one neurite of more than two body lengths in size (Pannaccione *et al.*, 2007). Moreover the expression of the axonal growth associated protein 43 (GAP-43) and the synaptic protein synapsin I could be evaluated by Western blot during cell differentiation (Das *et al.*, 2004).

5.3.2 Chinese Hamster Ovary Cells (CHO)

For our studies, we adopted as a heterologous expression system the Chinese Hamster Ovary Cells (CHO) cells. $K_v3.4$ and Mirp2 cDNAs were expressed in CHO cells by transient transfection. CHO cells were grown in 100 mm plastic Petri dishes in DMEM containing 10% FBS, penicillin (5 U/ml), and streptomycin (5 μ g/ml) at 37°C with 5% CO₂. For electrophysiological experiments, cells were seeded on glass coverslips (Glaswarenfabrik Karl Hecht KG, Sondheim, Germany) coated with poly-L-lysine (50 μ g/mL) and transfected the next day with the appropriate cDNAs using Lipofectamine 2000 (Invitrogen) according to guidelines for transfection. To dilute Lipofectamine 2000 it's recommended Opti-MEM I Reduced Serum Medium in the absence of antibiotics. Total cDNA in the transfection mixture was kept constant at 4 μ g: 2 μ g of $K_v3.4$ cDNA and 2 μ g of

MiRP2 cDNA. We performed electrophysiological experiments usually 48 hours after transfection.

5.3.3 Mouse Hippocampal Neurons

Primary neuronal cultures were prepared from Tg2576 and WT hippocampi of embryonic day (E). Embryonic age (E) was calculated by considering E0.5 the day when a vaginal plug was detected. Briefly, pregnant animals were anesthetized and sacrificed by cervical dislocation. Hippocampal tissues from embryos were dissected in ice-cold dissecting medium (HBSS supplemented with 27 mM glucose, 20 mM sucrose, 4 mM sodium bicarbonate), centrifuged, and the resulting pellet was mechanically dissociated with a fire polished glass pipette. Cells were resuspended in plating medium consisting in Eagle's MEM (MEM, Earle's salts, supplied bicarbonate-free) supplemented with 5% FBS, 5% HS, 2 mM L-glutamine, 20 mM glucose, 26 mM bicarbonate, and plated on 35mm culture dishes or onto 25 mm glass coverslips (Glaswarenfabrik Karl Hecht KG, Sondheim, Germany) coated with 100 µg/ml poly(D)-lysine at a density of one embryo hippocampi/1 ml. Three days after plating, non-neuronal cell growth was inhibited by adding 10µM of cytosine AraC. 24 hours after this treatment, the planting medium was replaced by growth medium (Eagle's Minimal Essential Medium with 20 mM glucose, 26 mM NaHCO₃ supplemented with 2mM L-glutamine and 10% HS. Neurons were cultured at 37°C in a humidified 5% CO₂ atmosphere. All the experiments were performed between 8-16 days *in vitro* (DIV).

5.3.4 Primary Astrocyte Cultures

Primary astrocyte cultures were obtained from 1-2-day-old rat pups. The animal was sacrificed by decapitation using the scissors. Their brains were then removed under aseptic conditions and placed in ice cold $\text{Ca}^{2+}/\text{Mg}^{2+}$ -free HBSS. Under a stereomicroscope, total brains were stripped of meningeal tissues and cut into small fragments. After we placed dissected brain tissues in DMEM containing 0.05% trypsin and 0.003% DNase and kept at 37°C for 30 minutes. The tissue was then mechanically dissociated using a Pasteur pipette and centrifuged at 1000 rpm for 10 minutes. The pellet was resuspended in a solution of DMEM containing only 0.003% DNase and again mechanically dissociated with a Pasteur pipette. After another centrifugation (1000 rpm, 10 minutes), the cells were resuspended in DMEM supplemented with 10% FBS, 100 U/mL penicillin, 100 $\mu\text{g}/\text{mL}$ streptomycin, and 2 mM L-glutamine and plated in flasks pre-coated with poly-L-lysine and cultured at 37°C in a 5% CO_2 incubator. The medium was changed 24 hours after plating and twice a week thereafter. Once became confluent, the cultures were shaken vigorously to remove non-adherent cells and subcultured 1:3. Upon becoming confluent again, the cells were then mechanically purified and subcultured again 1:4 before performing the experiments. This protocol produced 98% of GFAP-positive cells. For electrophysiological experiments and morphological analysis, astrocytes were seeded at low density on glass coverslips (Glaswarenfabrik Karl Hecht KG, Sondheim, Germany) coated with poly-L-lysine (50 $\mu\text{g}/\text{mL}$).

5.4 Solubilization of A β peptide and cellular treatments

The peptide used in our study was produced by chemical synthesis from Sigma Aldrich (Milan, Italy) or INBIOS (Naples, Italy) using the A β ₁₋₄₂ sequence of human APP [UniProtKB-P05067 (A4_HUMAN)]. Both sources yielded peptide of 95% purity, assessed with high performance liquid chromatography (HPLC) and demonstrated the correct molecular mass by mass spectrometry analysis. Lyophilized peptide was stored in sealed glass vials in desiccated containers at -20 °C. Prior to resuspension, each vial was allowed to equilibrate to room temperature for 30 min to avoid condensation upon opening the vial. The first step in resuspending the lyophilized peptide was treatment in 1,1,1,3,3,3-hexafluoro-2-propanol (HFIP; catalog number H8508; Sigma, Milan). Each vial of peptide was diluted in 100% HFIP to 1 mM. The clear solution containing the dissolved peptide was then aliquoted in microcentrifuge tubes and dried under vacuum in a SpeedVac until complete elimination of the solvent and recovery of the dried powder. Immediately prior to use, the HFIP-treated aliquots were carefully and completely resuspended to 5 mM in anhydrous dimethyl sulfoxide (Me₂SO; catalog number D-2650; Sigma).

5.4.1 A β ₁₋₄₂ Oligomers conditions

A β ₁₋₄₂ oligomers were prepared by diluting 5 mM A β ₁₋₄₂ in Me₂SO to 100 μ M in ice-cold cell culture medium (phenol red-free Ham's F-12), immediately vortexing for 30 s, and incubating at 4 °C for 24 h. At the end of 24 h, the solution containing A β ₁₋₄₂ oligomers was centrifuged at 14000 rpm at 4° C for 10 minutes. The supernatant, containing A β ₁₋₄₂ oligomers, was recovered and then aliquoted and stored at -20 °C (Stine *et al.*, 2003). Before all experiments,

we tested a pre-aggregated preparation of the A β ₁₋₄₂. SDS-PAGE was performed using rabbit monoclonal anti-A β -antibody (Cell signaling, Massachusetts, USA), which recognizes an epitope within residues 17-42 of human A β . Results showed that the oligomers between 12-15 kDa were the major species of A β ₁₋₄₂ peptide in the preparation. A β ₁₋₄₂ exposure was carried out in growth medium at the final concentration of 5 μ M. When we performed time-course experiments, the A β ₁₋₄₂ was added to culture medium at above mentioned concentration for 24 or 48 hours and kept throughout the experiment.

5.5 Electrophysiological recordings

K⁺ currents were recorded, by patch-clamp technique in whole-cell configuration, in the following experimental groups: **a)** NGF-differentiated PC-12; **b)** NGF-differentiated PC-12+K_v3.4 and Mirp2 cDNAs; **c)** CHO; **d)** CHO+K_v3.4 and Mirp2 cDNAs; **e)** WT hippocampal neurons; **f)** Tg2576 hippocampal neurons; **g)** astrocytes; **h)** astrocytes+A β ₁₋₄₂. Currents were filtered at 5 kHz and digitized using a Digidata 1322A interface (Molecular Devices). Data were acquired and analyzed using the pClamp software (version 9.0, Molecular Devices). All recordings were performed at room temperature (20-21°C). The pipette solution contained (in mM): 140 KCl, 2 MgCl₂, 10 HEPES, 10 glucose, 10 EGTA and 1 Mg-ATP, adjusted at pH 7.4 with KOH. The extracellular solution contained (in mM) 150 NaCl, 5.4 KCl, 3 CaCl₂, 1 MgCl₂ and 10 HEPES, adjusted pH 7.4 with NaOH. All experiments with neurons and astrocytes as cellular model were performed in the presence of nimodipine (10 μ M) to block L-type Ca²⁺-channels and TTX (50 nM) to block Na⁺-currents in the extracellular solution. To discriminate K⁺ current

components with distinct inactivation properties (namely an inactivating component I_A and a delayed rectifier non-inactivating component I_{DR}), appropriate electrophysiological protocols were used. The total outward K^+ current ($I_A + I_{DR}$) was measured by applying depolarizing voltage steps of 250 ms duration from a holding potential of -80 mV to +40 mV, preceded by conditioning pulses at -100 mV lasting 1.5 s, which allowed full recovery from inactivation of I_A . Following this protocol, I_{DR} was isolated by stepping from -80 to +40 mV for 250 ms, after conditioning pulses at -40 mV lasting 1.5 s to fully inactivate I_A . The I_A component was obtained by subtracting the isolated I_{DR} component from the total K^+ current. Current amplitudes were measured for I_A and I_{DR} at +40 mV, at the peak or at the end of the depolarizing pulse respectively. Steady-state properties of I_A inactivation were measured by a voltage protocol in which a 125-ms depolarizing pulse to a constant voltage of +40 mV was preceded by 1.5-s conditioning pulses from -120 to +40 mV. Possible changes in cell size were taken into account by measuring, in each cell, the membrane capacitance, which is directly related to membrane surface area, and by expressing the current amplitude data as current densities [picoamperes/picofarads (pA/pF)]. Capacitive currents were elicited by 5-mV depolarizing pulses from -80 mV and acquired at a sampling rate of 50 kHz. The capacitance of the membrane was calculated according to the following equation: $C_m = \tau_c / \Delta E_m (1 - I_\infty / I_o)$, where C_m is membrane capacitance, τ_c is the time constant of the membrane capacitance, I_o is the maximum capacitance current value, ΔE_m is the amplitude of the voltage step, and I_∞ is the amplitude of the steady-state current.

5.6 Western Blotting

To obtain total lysates for immunoblotting analysis, astrocytes, PC-12, CHO cells were washed in PBS and collected by gentle scraping in ice-cold RIPA buffer containing in mM: 50 Tris pH 7.4, 100 NaCl, 1 EGTA, 1 PMSF, 1 sodium orthovanadate, 1 NaF , 0.5% NP-40, and 0.2% SDS supplemented with protease inhibitor cocktail II (Roche Diagnostic, Monza, Italy). After sonication and incubation for 1 hour on ice, we centrifuged at 12,000 rpm at 4 °C for 30 minutes and collected the supernatants. Mice brain tissues from Tg2576 and WT were homogenized in a glass teflon grinder (10 strokes at 500 rpm in about 1 min) using a lysis buffer containing (in mM): 250 sucrose, 10 KCl, 1.5 MgCl₂, 1 EDTA, 1 EGTA, 1 dithiothreitol, 20 HEPES, pH 7.5, (Angulo *et al.* 2004) and completed with Protease Inhibitor Cocktail II (Roche Diagnostic, Monza, Italy). Tissue suspensions were then sonicated and incubated for 1 hour on ice. After centrifugation at 12,000 rpm at 4 C for 5 min, the supernatants were collected. The protein content of resulting supernatant was determined using the Bradford reagent. 70 µg of proteins were mixed with a Laemmli sample buffer; then, they are applied and resolved on SDS-PAGE polyacrylamide gels. Following transfer onto nitrocellulose membranes (Hybond-ECL, Amersham Bioscience, UK), non-specific binding sites were blocked by incubation for 2 hrs at 4°C with 5% non-fat dry milk (Bio-Rad Laboratories, Milan, Italy) in TBS-T buffer; subsequently, incubated with primary antibodies overnight at 4°C. After three 10-min washes with TBS-T, the membranes were incubated 1h with the appropriate secondary antibody. Excessive antibodies were then washed away three times (10 min) with TBS-T. Immunoblots were visualized by enhanced chemiluminescence (ECL) (Amersham-Pharmacia-Biosciences, UK). Films were developed using a standard photographic procedure and the relative levels of immunoreactivity

were determined by densitometry using ImageJ Software (NIH, Bethesda, MA, USA). Primary antibodies used were: rabbit polyclonal anti-K_v3.4 (1:1000 Alomone Labs), rabbit polyclonal anti-GFAP (1:8000, Sigma Aldrich), monoclonal anti-human β -Amyloid (1-17) (1:1000, 4G8, Sigma Aldrich), polyclonal anti β -Amyloid (D54D2) XP rabbit mAb (1:1000 Cell Signaling), rabbit polyclonal anti-cleaved caspase-3 (1:1000, Cell Signaling), rabbit polyclonal Caspase-6 (1:1000, Cell Signaling), rabbit polyclonal anti-APP (Ab-cam) and mouse monoclonal anti-Tubulin (1:3000; Sigma Aldrich). Immunoreactive bands were detected using the chemiluminescence system (Amersham-Pharmacia-Biosciences, UK). Proteins were visualized with peroxidase-conjugated secondary antibodies, using the enhanced chemiluminescence system (Amersham-Pharmacia Biosciences LTD, Uppsala, Sweden). The software Image J (NIH) was used for densitometric analysis..

5.7 Immunoprecipitation

Immunoprecipitation (IP) is the affinity purification of antigens using a specific antibody immobilized to a solid support (agarose beads). Immunoprecipitation is one methods to isolate proteins from cell or tissue lysates for the detection by Western Blot and other techniques. The first phase of IP was the preclearing, designed to remove potentially reactive, non-specific components from the lysate prior to the immunoprecipitation procedure. The approach to preclear the lysate was to incubate the sample with a nonspecific antibody or serum from the same host species as the IP antibody. Therefore agarose beads were used to remove nonspecific binding. We added 0,25 μ g of irrelevant antibody of the same species and isotype as the IP antibody, or normal serum to 1 mL of the lysate with 20 μ L of agarose beads (*Protein A-Agarose*, *Protein G-Agarose*,

Protein A/G-Agarose or Protein L-Agarose); we incubated for 1 hour at 4° C. We centrifuged at 3000 rpm for 30 seconds, discarded beads pellet and kept supernatant for immunoprecipitation. In a new tube we added 100-1000 µg of the lysate plus the recommended amount of antibody. The amounts will be chosen depending on the abundance of the protein and the affinity of the antibody for the protein. We incubated the sample with the antibody 1-2 hours at 4°C under rotary agitation. Then we mixed 20 µL of the beads to each sample; beads will tend to stick to the sides of the tip so we try to minimize the movement in the pipette, thus it's recommended to use a tip cut 5mm from the top. We incubated the lysate-beads mixture at 4°C overnight under rotary agitation. When the incubation time is over, we centrifuged the tubes at 3000 rpm for 30 seconds, we removed the supernatant and washed the beads in lysis buffer three times (each time centrifuging at 4°C and removing the supernatant). We removed the supernatant and added 40 µL of 2X loading buffer (Laemmli) and boiled at 95-100° C for 5 minutes to denature the protein and separated it from the beads. At the end we performed SDS-PAGE.

5.8 Assessment of nuclear morphology

Nuclear morphology in PC-12 and astrocytes was evaluated by staining the nucleus with the fluorescent DNA-binding dye Hoechst-33258 (Sigma, Milan, Italy). Astrocytes morphology was evaluated by cytoskeletal F-actin with rhodamine phalloidin (Sigma, Milan Italy). To this aim, PC-12 cells and astrocytes in the presence or in the absence of 5µM Aβ₁₋₄₂ were fixed in 4% paraformaldehyde, washed in PBS and incubated for 20 min in PBS containing 1 µg/ml Hoechst-33258 at 37°C. Astrocytes were incubated also with rhodamine phalloidin (1:200). Coverslips were mounted on glass slides and

observed by fluorescence microscopy on a Nikon Eclipse E400 microscope (Nikon, Torrance, CA, USA). Digital images were taken with a CoolSnap camera (Media Cybernetics Inc., Silver Spring, MD, USA), and analyzed with the Image-Pro Plus 4.5 software (Media Cybernetics Inc., Silver Spring, MD, USA). Pathological nuclei were characterized by chromatin condensation (pyknosis), fragmentation, or by a decrease in size. The number of pathological nuclei of both PC-12 cells and astrocytes and the number of processes of astrocytes under control conditions and 48 hours after $A\beta_{1-42}$ exposure were analyzed.

5.9 Immunocytochemistry

Cell cultures were fixed in 4% paraformaldehyde for 30 minutes at room temperature and then we washed the cells three times with PBS. The cells can be stored in 0.02% (w/v) sodiumazide in PBS at 4°C for several days or incubated immediately with primary antibody. After blocking in Bovine Serum Albumin (BSA) cells were incubated with primary antibodies for 24 or 48 hours. The primary antibodies used in these experiments were the following: rabbit polyclonal anti-K_v3.4, mouse monoclonal anti-K_v3.4 (Ab Nova, Taiwan), rabbit polyclonal anti-GFAP. Subsequently, they were incubated in a mixture of fluorescent-labeled secondary antibodies. Images were observed using a Zeiss LSM510 META/laser scanning confocal microscope. Single images were taken with an optical thickness of 0.7 μm and a resolution of 1024x1024. Nuclear morphology was evaluated by using the fluorescent DNA-binding dye Hoechst-33258. All images were obtained with an x40 objective with identical laser power settings.

5.10 RNA interfering

For transfection of cells with siRNA we used HiPerFect Transfection Reagent (QIAGEN). We tested two siRNA specific for rat $K_V3.4$ genes named Rn_LOC684516_1 and Rn_LOC684516_2, in rat hippocampal neurons at 10nM and 20nM. After 48 hours we evaluated the silencing efficiency by Western Blot analysis. Moreover we tested three siRNA specific for mouse $K_V3.4$ genes named Mm_Kcnc4_4, Mm_Kcnc4_5, Mm_Kcnc4_6, in mouse hippocampal neurons at 20nM. The ratio of HiPerFect Transfection Reagent to siRNA should be optimized to obtain higher silencing efficiency. We used a specific ratio: 5 nM siRNA and 3 μ l HiPerFect Transfection Reagent. For our experiments we used AllStars Negative Control siRNA (QIAGEN) that provided minimal nonspecific effects on gene expression. Silencing of $K_V3.4$ in WT and Tg2576 mice was performed through intracerebroventricular (i.c.v.) infusion of specific siRNA (Pignataro *et al.*, 2011; Pignataro *et al.*, 2012). In brief, anesthetized mice were first positioned on a stereotaxic frame, and then a 26-g stainless steel guide cannula (23 Gauge, Plastic One), connected to an osmotic pump (Alzet), was implanted into the right lateral ventricle using the following stereotaxic coordinates from bregma: AP -0.1mm caudal; LL -0,75mm lateral; 2,1 mm below the dura. Next, siRNAs, at a final concentration of 1 μ M, were intracerebroventricularly (i.c.v.) infused every 24 hours for three consecutive days. Finally, at the end of 72 hours mice were sacrificed and brain samples collected for immunoblotting.

5.11 Statistical Analysis

Statistical analysis were performed with ANOVA followed by Newman test or Student t-test. Differences were considered to be statistically significant at $p < 0.05$.

RESULTS

Chapter 6: Results

6.1 A β ₁₋₄₂ peptide aggregates to form low molecular weight oligomers (dimers and trimers) in Tg2576 mice at the early stages of AD.

The Tg2576 mouse model overexpresses a human APP transgene containing the Swedish FAD mutation (K670N/M671L) that causes the increase in β A levels. Furthermore, transgenic APP mice showed pathogenic β A aggregates that initiate a cascade of molecular events culminating in extensive neurodegeneration. In this study, principally, we investigated the events occurring in the early phase of AD. First we measured the deposition of β A aggregates, in particular β -amyloid trimers (β A₁₋₄₂ trimers) in brain tissue obtained from Tg2576 mice compared to age-matched Wild-Type (WT) mice. Western Blot analysis showed a specific band of 15 kDa corresponding to β A₁₋₄₂ trimers only in Tg2576 brain tissue, whereas no band at 15 kDa was observed in age-matched Wild-Type (WT) mice (**Fig. 5A**). Furthermore we dissected Tg2576 and WT brain tissue in: cerebellum, cerebral cortex, striatum and hippocampus. In each area of Tg2576 mice we observed β A₁₋₄₂ trimers deposition. We evaluated also the APP protein expression in Tg2576 and WT mice. We found a specific band of 100 kDa corresponding to APP both in WT and Tg2576 brain tissue. As expected, in Tg2576 brain tissue APP protein expression was significantly augmented (**Fig. 5A**).

6.2 A β_{1-42} trimers deposition in young Tg2576 mice correlates with the overexpression of K_v3.4 Channel Subunits and its accessory subunit MiRP2

Immunoblot analysis performed with a K_v3.4 specific antibody on protein extracts from WT and Tg2576 hippocampal tissue revealed one band at 110 kDa corresponding to native subunit monomer (McMahon *et al.*, 2004), (**Fig. 5B**). We analyzed the K_v3.4 protein expression at different stages of AD pathology evolution; in particular we selected Tg2576 and age-matched WT mice at the early (3 months of age), middle (8 months of age) and late (12 months of age) stages of AD (Braak and Braak, 1997). Densitometric analysis showed that the band at 110 kDa was significantly more intense in hippocampal tissue obtained from 3 months old Tg2576 mice compared to age-matched WT mice (**Fig. 5C**). Moreover, in the hippocampus of 8 months old Tg2576 mice we still observed a significant increase in K_v3.4 protein expression compared to age-matched WT mice. Conversely, in the hippocampus of elderly Tg2576 mice (12 months of age) we observed a significant down regulation of K_v3.4 protein expression (**Fig. 5C**). These data highlighted that the maximal increase in K_v3.4 protein expression occurred in the hippocampus of young transgenic mice. K_v3.4 subunits can form stable complexes with MiRP2; this interaction modifies the voltage-dependence of activation, speeds the recovery from inactivation, reduces the cumulative inactivation, and affects the conductance of K_v3.4 channels (Pannaccione *et al.*, 2007). Thus we performed immunoblot analysis with a MiRP2-specific antibody on protein extracts from WT and Tg2576 hippocampal tissue that revealed one band at 20 kDa, corresponding to MiRP2 (Abbott *et al.*, 2001)

(**Fig. 5D**). Densitometric quantification showed that MiRP2 followed the same tendency of $K_v3.4$ protein expression; in fact we observed a significant increase in MiRP2 protein expression in younger Tg2576 mice compared to age-matched WT (**Fig. 5E**). Thus, we observed the modulation both of $K_v3.4$ and its accessory component in Tg2576 mice.

Fig. 5

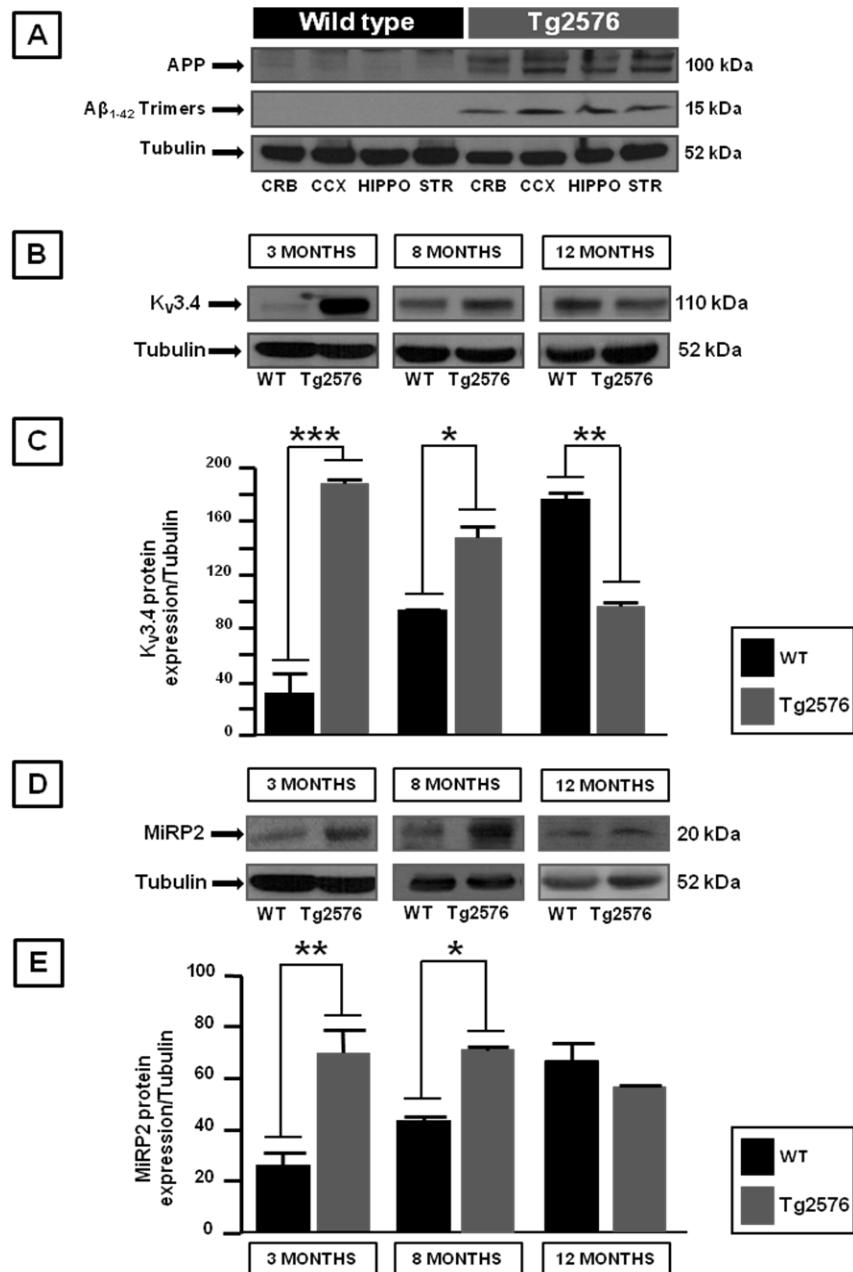


Fig. 5 Aβ₁₋₄₂ trimers deposition in young Tg2576 mice correlates with the over expression of Kv3.4 Channel Subunits and its accessory subunit MiRP2. **(A)** Western Blot of Aβ₁₋₄₂ trimers deposition and APP protein expression in young WT and Tg2576 mice evaluated in cerebellum, cerebral cortex, hippocampus and striatum. **(B)** Western Blot of Kv3.4 protein expression evaluated in the hippocampus of WT and Tg2576 mice at different AD stages. **(C)** Densitometric analysis of Kv3.4 protein expression normalized to α-tubulin levels. **(D)** Western Blot of MiRP2 protein expression evaluated in the hippocampus of WT and Tg2576 mice at different AD stages. **(E)** Densitometric analysis of MiRP2 protein expression normalized to α-tubulin levels. The values are expressed as mean±SEM of 3 independent experimental sections. **p*≤ 0.05 versus their respective control, ***p*≤ 0.01 versus their respective control, *** *p*≤ 0.001 versus their respective control (*Student's t test and ANOVA*).

6.3 Changes in K_v3.4 and in its accessory subunit MiRP2 protein expression are related to disease stage

To confirm the involvement of K_v3.4 in the early stages of AD, we performed Western Blot experiments on protein extracts obtained from elderly Tg2576 mice (14, 16 and 18 months of age). We observed that the specific band at 110 kDa, corresponding to native K_v3.4, was reduced in the hippocampus of 14 months old Tg2576 mice compared to age-matched WT mice (**Fig. 6B, 6C**). By contrast K_v3.4 protein expression was unchanged in 16 and 18 old Tg2576 mice compared to age-matched WT mice (**Fig. 6B, 6C**). In addition we performed immunoblot analysis with a MiRP2-specific antibody on protein extracts from elderly Tg2576 mice (**Fig. 6D**). Densitometric analysis showed that MiRP2 protein expression was unchanged in 16 and 18 old Tg2576 mice compared to age-matched WT mice (**Fig. 6E**). Moreover we evaluated the APP protein expression in the hippocampus of elderly Tg2576 mice compared to age-matched WT. As expected, we observed a significant enhance in APP protein expression in Tg2576 hippocampus compared to age-matched WT (**Fig. 6A**). Interestingly, in the late phase of AD we find the accumulation of high-molecular weight A β ₁₋₄₂ oligomers, protofibrils/fibrils and lastly plaques; whereas in the early phase of AD the predominant A β species are low-molecular weight A β ₁₋₄₂ oligomers, specially A β ₁₋₄₂ dimers and trimers (**Fig. 5A**). Thus, we performed immunoblot analysis to evaluate the species of A β ₁₋₄₂ oligomers more prevalent in elderly Tg2576 mice. In particular we detected through a specific anti-A β ₁₋₄₂ antibody, A β ₅₆, nonamers and dodecamers of A β ₁₋₄₂ oligomers in Tg2576 hippocampus compared to age-matched WT (**Fig. 6A**). We observed also a time dependent increase in A β ₁₋₄₂ oligomers

deposition in Tg2576 hippocampus. Collectively the data obtained showed that: **1)** K_v3.4 had a specific role in the early stages of AD; and **2)** only low-molecular weight A β ₁₋₄₂ oligomers were able to elicit a deregulation of K_v3.4.

Fig. 6

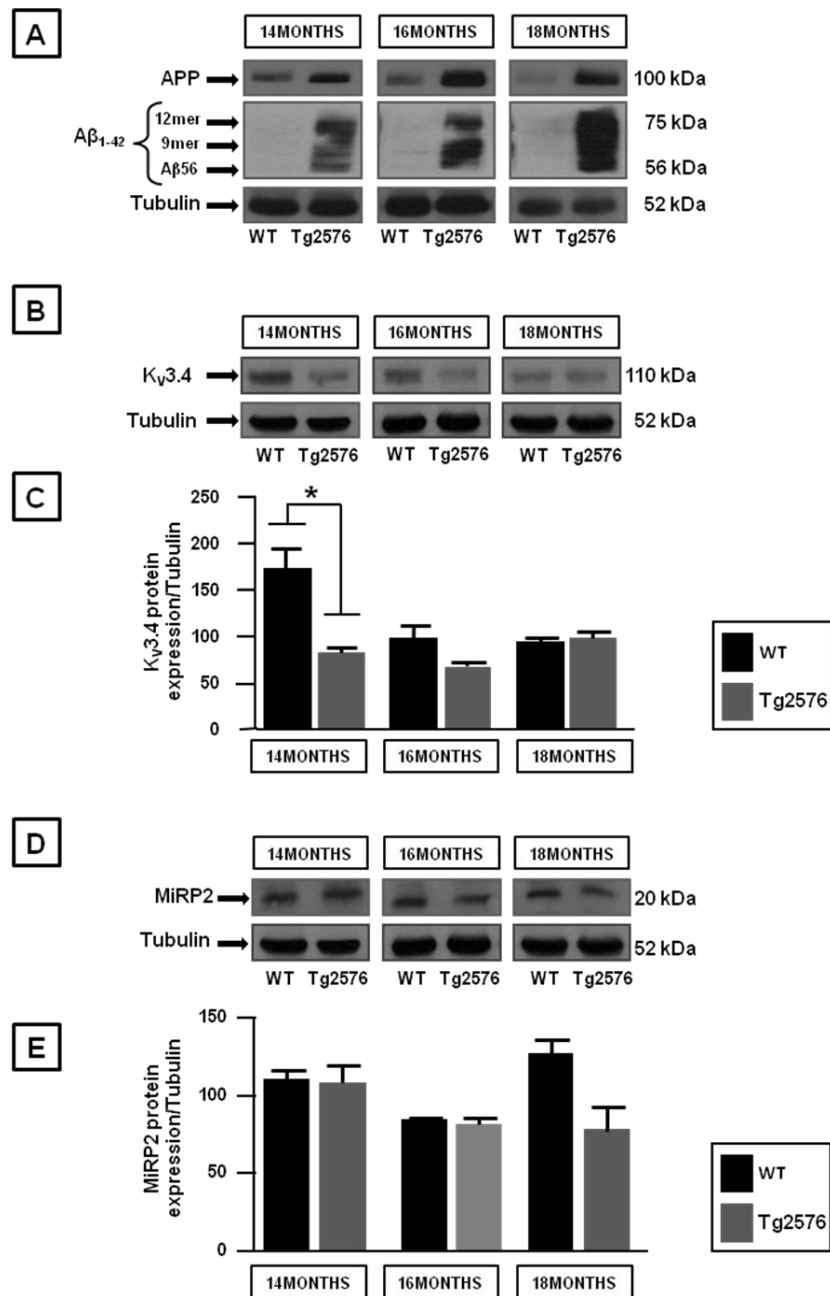


Fig. 6 Changes in K_v3.4 and in its accessory subunit MiRP2 protein expression are related to disease stage . (A) Western Blot of Aβ₁₋₄₂ oligomers deposition and APP protein expression in the hippocampus of Tg2576 mice compared to age-matched WT. **(B)** Western Blot of K_v3.4 protein expression evaluated in the hippocampus of WT and Tg2576 mice at different AD stages. **(C)** Densitometric analysis of K_v3.4 protein expression normalized to α-tubulin levels. **(D)** Western Blot of MiRP2 protein expression evaluated in the hippocampus of WT and Tg2576 mice at different AD stages. **(E)** Densitometric analysis of MiRP2 protein expression normalized to α-tubulin levels. The values are expressed as mean±SEM of 3 independent experimental sections. **p*≤ 0.05 versus their respective control, ***p*≤ 0.01 versus their respective control, *** *p*≤ 0.001 versus their respective control (*Student's t test and ANOVA*).

6.4 K_v3.4 activity increases in hippocampal neurons obtained from Tg2576 mice

To correlate the increase of K_v3.4 protein expression in Tg2576 mice with electrophysiological activity we performed patch clamp experiments in whole cell configuration. In particular, we recorded hippocampal neurons obtained from WT and Tg2576 embryos at different days in vitro (DIV). We observed a significant increase of total potassium currents I_k in Tg2576 hippocampal neurons compared to WT (**Fig. 7A**). Interestingly, the isolation of I_A component from total potassium currents, showed the significant increase of this component in Tg2576 hippocampal neurons compared to WT hippocampal neurons (**Fig. 7A-7C**). Time-course experiments at different DIV (8-12-15 DIV) revealed that transgenic hippocampal neurons displayed an early increase of K⁺ current density compared to WT hippocampal neurons. We found, that K⁺ current density was significantly increased already at 8 DIV in culture, reached the maximal value at 12 DIV, and showed a less pronounced, but still significant, increase at 15 DIV (**Fig. 7D**) in the transgenic neurons respect WT. The up-regulated I_A currents recorded in Tg2576 hippocampal neurons were inhibited by BDS-I, a well known blocker of K_v3 family (Diochot *et al.*, 1998; Yeung *et al.*, 2005). The percentage of the BDS-I inhibition was higher in Tg2576 hippocampal neurons compared to WT (**Fig. 7E**). In addition we performed immunocytochemical analysis to measure the expression levels of K_v3.4 in Tg2576 and WT hippocampal neurons at 12DIV, when we observed the maximal increase of K_v3.4 activity. We observed an increase in the expression of K_v3.4 in Tg2576 hippocampal neurons compared to WT. More interestingly, K_v3.4 immunosignal pattern was more different between WT and

Tg2576 cultured hippocampal neurons; in fact, we observed a plasma membrane localization and a punctuated staining pattern mostly confined throughout the neuropil in WT hippocampal neurons, whereas, in Tg2576 hippocampal cells, the $K_V3.4$ immunosignal was more confined to the soma plasma membrane (**Fig. 7F**).

Fig. 7

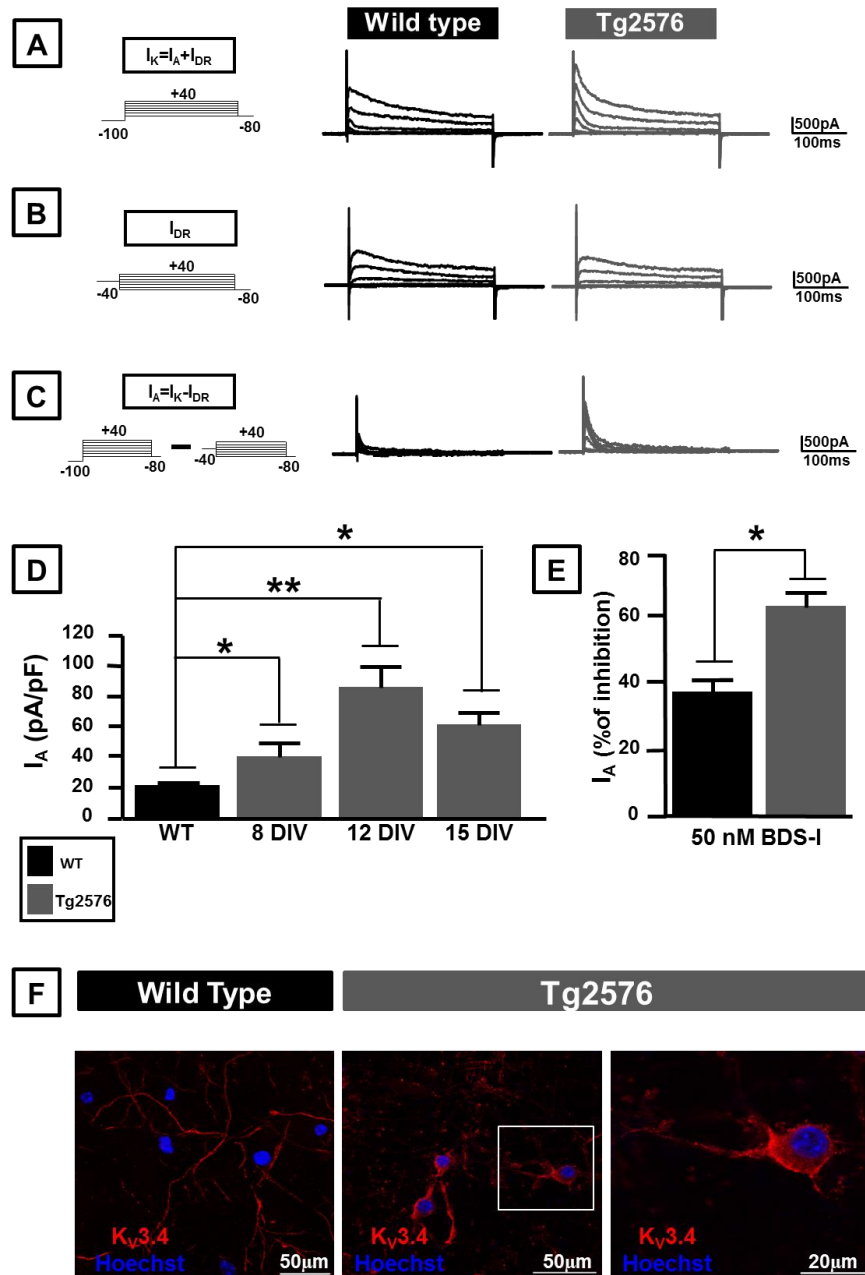


Fig. 7 $K_v3.4$ activity increases in hippocampal neurons obtained from Tg2576 mice. **(A)** Total outward K^+ currents recorded from WT and Tg2576 hippocampal neurons in 12 DIV. **(B)** I_{DR} currents recorded from WT and Tg2576 hippocampal neurons in 12 DIV. **(C)** I_A currents obtained upon subtraction of I_{DR} from I_K currents recorded from WT and Tg2576 hippocampal neurons in 12 DIV. **(D)** Quantification of I_A currents recorded in different DIV in Tg2576 hippocampal neurons compared to WT. **(E)** Quantification of I_A currents recorded in Tg2576 hippocampal neurons expressed as a percentage of inhibition induced by 50 nM of BDS-I compared to WT. **(F)** Immunofluorescence images of Tg2576 and WT hippocampal neurons in 12 DIV displaying both $K_v3.4$ protein expression and Hoechst-33258 staining. The values are expressed as mean \pm SEM of 3 independent experimental sections. * $p \leq 0.05$ versus their respective control, ** $p \leq 0.01$ versus their respective control, *** $p \leq 0.001$ versus their respective control (*Student's t test and ANOVA*).

6.5 K_V3.4 over expression induces caspase-3 activation culminating in neuronal death

We performed in vitro experiments to induce K_V3.4 over expression in mouse hippocampal neurons, through transient transfection of K_V3.4 and MiRP2 cDNAs. At first, we assessed K_V3.4 activity both in control hippocampal neurons and overexpressing K_V3.4 and MiRP2 cDNAs. We observed a significant up-regulation in K_V3.4 currents in neurons over expressing K_V3.4 and MiRP2 cDNAs compared to control (**Fig. 8A-8B**). The increase in K_V3.4 activity correlated with K_V3.4 protein expression, indeed we found a significant raise in hippocampal neurons over expressing K_V3.4 (**Fig. 8C**). It is well known that the cytoplasmic K⁺ loss promotes caspases and nucleases activation, which lead to apoptosis. Thus, we performed Western Blot analysis to evaluate caspase-3 activation, a specific key mediator of apoptosis in neuronal cells (D'Amelio *et al.*, 2003). In hippocampal neurons over expressing K_V3.4 we observed a significant augment in caspase-3 activation (**Fig. 8D**), thus the deregulation of intracellular K⁺ concentration mediated by an increase of K_V3.4 activity correlated with apoptosis. Subsequently, we analyzed caspase-3 activation in the hippocampus of young WT and Tg2576 mice in which we observed the increase in K_V3.4 protein expression. Interestingly, we found an increase in pro-caspase 3 expression in the hippocampus of young Tg2576 mice compared to age-matched WT; furthermore we detected a specific band of 17 kDa corresponding to cleaved caspase-3 only in Tg2576 mice (**Fig. 8E**).

Fig. 8

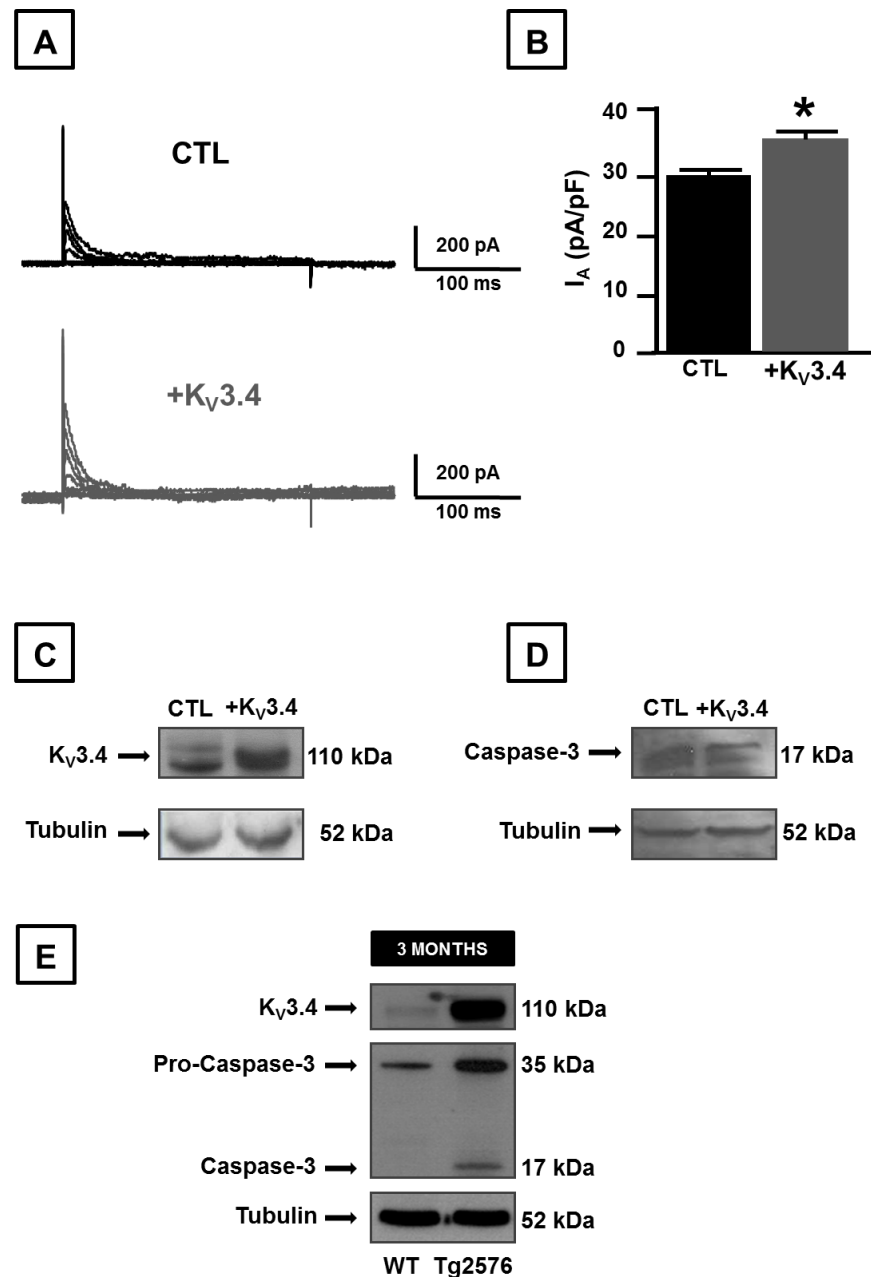


Fig. 8 Kv3.4 over expression induces caspase-3 activation. (A) I_A currents obtained upon subtraction of I_{DR} from I_K currents in control hippocampal neurons and over-expressing $K_V3.4$ and MiRP2 cDNAs. (B) Quantification of I_A currents recorded in control hippocampal neurons and over-expressing $K_V3.4$ and MiRP2 cDNAs. (C) Western Blot of $K_V3.4$ protein expression on protein extracts obtained from control hippocampal neurons and over-expressing $K_V3.4$ and MiRP2 cDNAs. (D) Western Blot of caspase-3 protein expression on protein extracts obtained from control hippocampal neurons and over-expressing $K_V3.4$ and MiRP2 cDNAs. (E) Western Blot of $K_V3.4$ protein expression and caspase-3 on hippocampal tissue obtained from three old Tg2576 mice compared to age-matched WT. The values are expressed as mean \pm SEM of 3 independent experimental sections. * $p \leq 0.05$ versus their respective control, ** $p \leq 0.01$ versus their respective control, *** $p \leq 0.001$ versus their respective control (*Student's t test and ANOVA*).

6.6 K_v3.4 selective knockdown effect on K_v3.4 protein expression in rat and mouse hippocampal neurons

In order to verify the involvement of K_v3.4 overexpression in caspases activation and in the apoptotic cell death, we selectively knockdown K_v3.4 through gene silencing using RNA interfering (RNAi). We tested specific siRNA in two different *in vitro* models. Firstly we performed K_v3.4 silencing in rat hippocampal neurons to identify the siRNA able to target rat K_v3.4 genes. We transfected rat hippocampal neurons with two siRNA specific for rat *Kcnc4* genes: Rn_LOC684516_1 and Rn_LOC684516_2. We incubated neurons for 48 hours with two different concentrations (10nM and 20nM) for each siRNA. Western Blot analysis showed a significant down-regulation of K_v3.4 protein expression in hippocampal neurons with the siK_v3.4 Rn_LOC684516_2 compared to control neurons (**Fig. 9A**). Densitometric analysis showed the maximal reduction in K_v3.4 protein expression in presence of 20nM of siK_v3.4 Rn_LOC684516_2 (**Fig. 9A**). By contrast, we did not observe a difference in K_v3.4 protein expression in hippocampal neurons treated with siK_v3.4 Rn_LOC684516_1 compared to control neurons (**Fig. 9B**). In addition we transfected mouse hippocampal neurons with three siRNA specific for mouse *Kcnc4* genes: Mm_Kcnc4_4, Mm_Kcnc4_5, Mm_Kcnc4_6. We incubated neurons for 48 hours with 20nM of each siRNA. Western Blot analysis revealed that the siRNA with the maximal efficacy to reduce K_v3.4 protein expression was Mm_Kcnc4_5 (**Fig. 9C**). In fact, densitometric analysis showed a significant reduction in K_v3.4 protein expression in presence of 20nM of siK_v3.4 Mm_Kcnc4_5 compared to control neurons (**Fig. 9C**).

Fig. 9

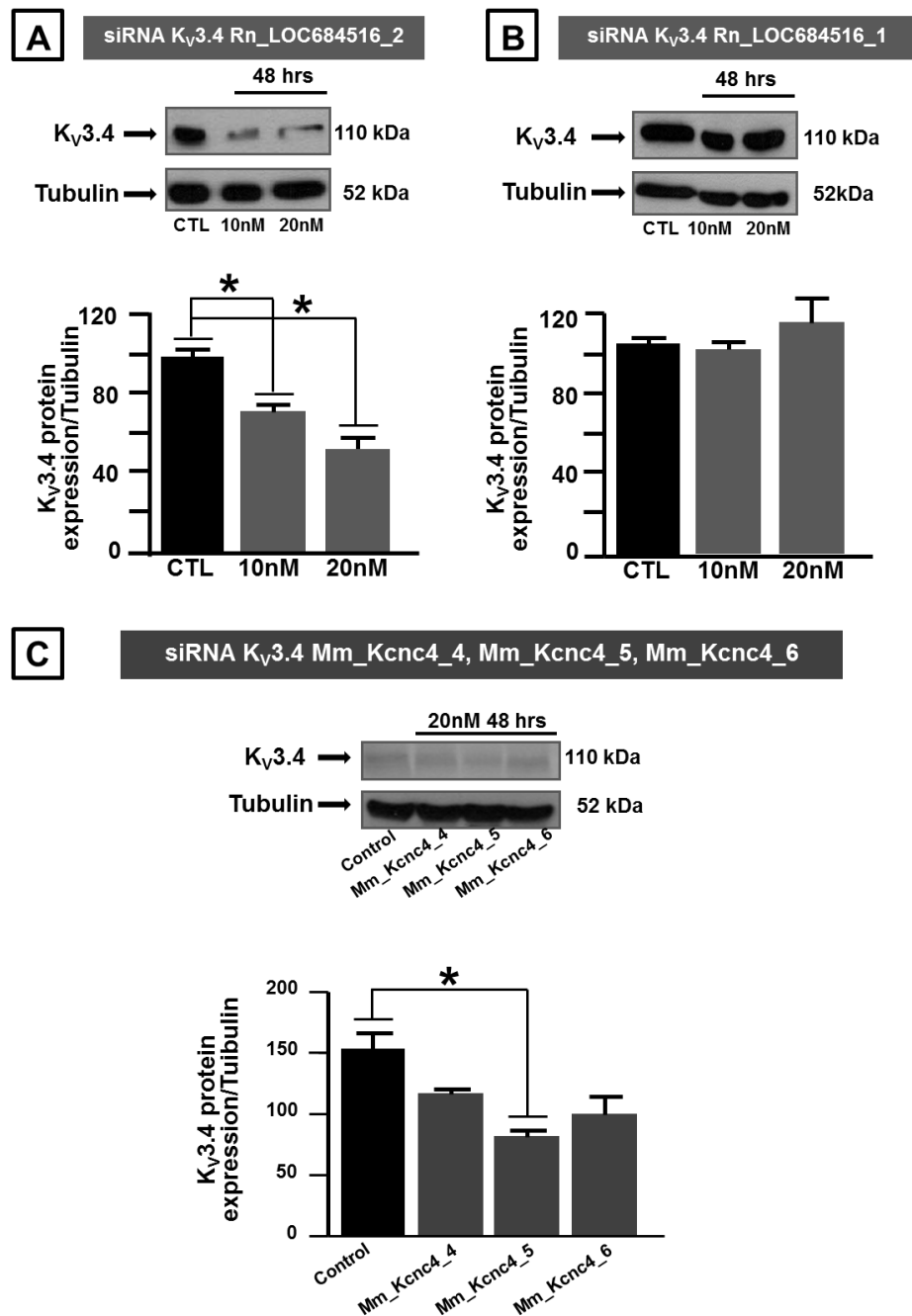


Fig. 9 Effect of $K_v3.4$ selective knockdown on $K_v3.4$ protein expression in rat and mouse hippocampal neurons. (A) Western Blot and densitometric analysis of $K_v3.4$ protein expression in rat hippocampal neurons treated with siRNA Rn_LOC684516_2. **(B)** Western Blot and densitometric analysis of $K_v3.4$ protein expression in rat hippocampal neurons treated with siRNA Rn_LOC684516_1. **(C)** Western Blot and densitometric analysis of $K_v3.4$ protein expression in mouse hippocampal neurons treated with siRNA Mm_Kcnc4_4, Mm_Kcnc4_5, Mm_Kcnc4_6. The values are expressed as mean \pm SEM of 3 independent experimental sections. * $p \leq 0.05$ versus their respective control, ** $p \leq 0.01$ versus their respective control, *** $p \leq 0.001$ versus their respective control (*Student's t test and ANOVA*).

6.7 K_V3.4 selective knockdown prevents caspase-3 activation and apoptotic events in Tg2576 mice

To investigate the role of K_V3.4 over-expression in the induction of apoptotic cell death we performed *in vivo* experiments in order to knockdown K_V3.4 gene. We silenced K_V3.4 by intracerebroventricular (icv) administration of siK_V3.4 Mm_Kcnc4_5, specific to mouse K_V3.4 genes, previously tested in *in vitro* models. We treated three months old WT and Tg2576 mice with 5 μ M of siK_V3.4 Mm_Kcnc4_5 for 72 hours; the experimental procedure required multiple administration, at least one every 24 hours. At the end of 72 hours animals were sacrificed, brains were collected and homogenized with a specific lysis buffer in order to obtain total protein lysate. Western Blot analysis on protein extracts showed that siK_V3.4 Mm_Kcnc4_5 also *in vivo* was able to knockdown K_V3.4. In particular, we observed a reduction in K_V3.4 protein expression both in WT and Tg2576 mice treated with siRNA compared to WT mice without siK_V3.4 (**Fig. 10A**) and Tg2576 mice without siK_V3.4, respectively (**Fig. 10B**). Furthermore, we studied caspases activation in the presence and in the absence of siK_V3.4. In Tg2576 mice we observed: **1)** the increase of pro-caspase 3 protein expression compared to age-matched WT mice; **2)** the presence of active caspase-3 (**Fig. 10C-10D**). Interestingly, densitometric quantification showed that the treatment with siK_V3.4 counteracted pro-caspase 3 increase (**Fig. 10E**). and caspase 3 activation observed in Tg2576 mice. Upon apoptotic stimulation, initiator caspases, such as caspase-9 are activated. The activated upstream caspases further process downstream executioner caspases: caspase 3 and caspase 6, thereby initiating caspase cascade leading to apoptosis. Thus, we also evaluated the effect of siK_V3.4 on

pro-caspase 6. In Tg2576 mice we observed the rise of pro-caspase 6 protein expression compared to age-matched WT mice (**Fig. 10C-10D**). Interestingly, densitometric quantification showed that the treatment with siK_v3.4 neutralized pro-caspase 6 increase observed in Tg2576 mice (**Fig. 10F**).

Fig. 10

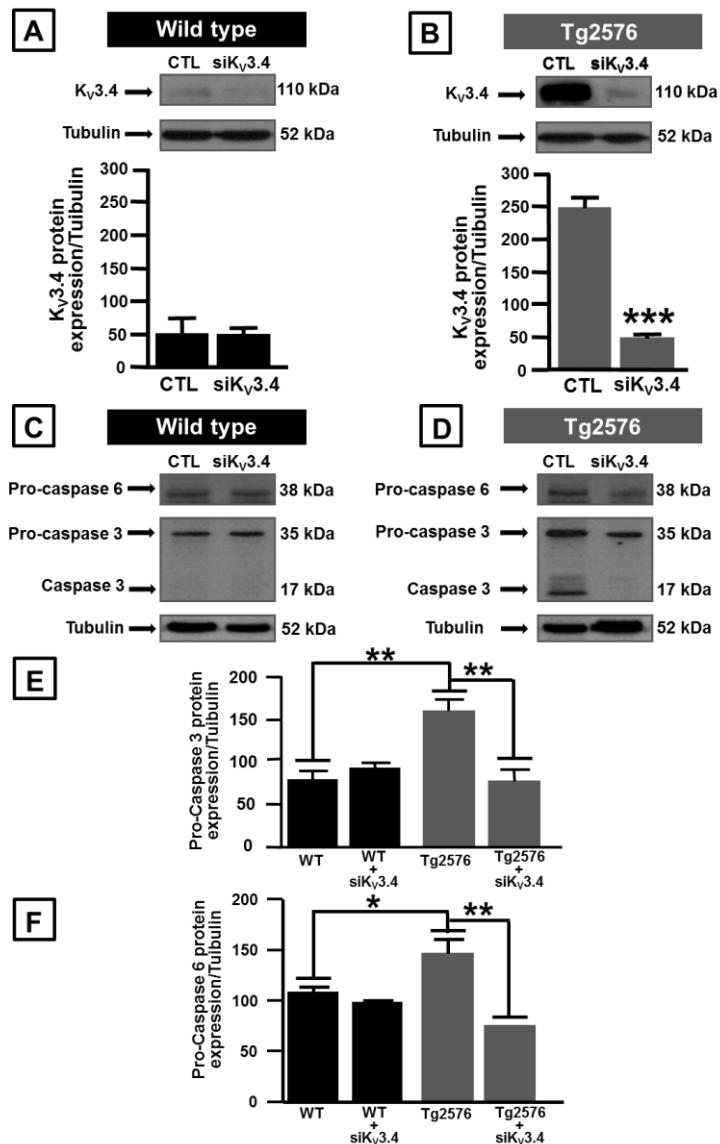


Fig. 10 K_v3.4 selective knockdown prevents caspase-3 activation and apoptotic events in Tg2576 mice. (A) Western Blot and densitometric analysis of K_v3.4 protein expression on protein extracts obtained from three months old WT mice in the presence and in the absence of siK_v3.4. (B) Western Blot and densitometric analysis of K_v3.4 protein expression on protein extracts obtained from three months old Tg2576 mice in the presence and in the absence of siK_v3.4. (C) Western Blot of pro-caspase 6, pro-caspase 3 and caspase 3 protein expression on protein extracts obtained from three months old WT mice in the presence and in the absence of siK_v3.4. (D) Western Blot of pro-caspase 6, pro-caspase 3 and caspase 3 protein expression on protein extracts obtained from three months old Tg2576 mice in the presence and in the absence of siK_v3.4. (E) Densitometric analysis of pro-caspase 3 protein expression on protein extracts obtained from three months old WT and Tg2576 mice, in the presence and in the absence of siK_v3.4. (F) Densitometric analysis of pro-caspase 6 protein expression on protein extracts obtained from three months old WT and Tg2576 mice, in the presence and in the absence of siK_v3.4. The values are expressed as mean±SEM of 3 independent experimental sections. **p*≤ 0.05 versus their respective control, ***p*≤ 0.01 versus their respective control, *** *p*≤ 0.001 versus their respective control (*Student's t test and ANOVA*)

6.8 K_v3.4 selective knockdown reduces A β production and trimers deposition in Tg2576 mice, improving memory performance

Caspases display primary specificity for aspartic acid residues. To date, more than 280 proteins have been shown to be substrates of caspases in mammalian cells (Fischer *et al.*, 2003; Tesco *et al.*, 2003). Among them we find proteins involved in cell death, cell cycle regulation, cytoskeleton organization, DNA and RNA metabolism, signal transduction, cytokine maturation, and gene transcription. Recently, it has been demonstrated that APP is also a substrate for caspase cleavage, leading to an increase in A β production (Gervais *et al.*, 1999; Lu *et al.*, 2003; D'Amelio *et al.*, 2010). Thus we evaluated if the silencing of K_v3.4 could modify A β production and trimers deposition in Tg2576 mice. We measured by Western Blot experiments the levels of A β ₁₋₄₂ trimers in the absence and in the presence of siK_v3.4 in Tg2576 mice. Firstly, we observed a specific band of 15 kDa corresponding to A β ₁₋₄₂ trimers only in Tg2576 mice whereas in WT mice we did not observe A β deposition (**Fig. 11A**). Notably, in the presence of siK_v3.4 we found a significant reduction in the levels of A β ₁₋₄₂ trimers in Tg2576 (**Fig. 11A**). We could assume the existence of indirect link between K_v3.4 overexpression, caspases activation and A β ₁₋₄₂ trimers deposition. In fact, the silencing of K_v3.4 prevented caspases activation, reduced APP alternative cleavage by caspases and in turn reduced A β ₁₋₄₂ formation in Tg2576 mice. A β aggregation has been recognized as a necessary condition for toxicity and it has been hypothesized that dimers and trimers of A β are the principal toxic species (Hung *et al.*, 2008). Moreover, recent studies showed that A β oligomers can

inhibit hippocampal LTP and that A β ₁₋₄₂ dimers and trimers accumulate at the same time as memory impairment begins in Tg2576 mice (Kawarabayashi *et al.*, 2004). Thus, we evaluated memory performance of Tg2576 mice in the presence and in the absence of K_v3.4 silencing, by T-Maze spontaneous alternation test. This behavioral test (described in detail in Chapter 5: Materials and Methods) allows the evaluation of exploratory ability and memory performance, especially the spatial and working memory. We observed that Tg2576 mice exhibited impaired exploration ability, spatial learning and memory abilities, as indicated by fewer alternative choices and longer latency in the T-maze test. Interestingly, the silencing of K_v3.4 ameliorated exploration ability and memory performance in Tg2576 mice. In fact, Tg2576 mice in the presence of K_v3.4 silencing showed an increase in the percentage of alternation compared to Tg2576 mice without siK_v3.4 (**Fig. 11B**); Tg2576 mice with siK_v3.4 showed a reduction in the latency time necessary to reach the goal arm compared to Tg2576 mice without siK_v3.4 (**Fig. 11B**). Furthermore, APP transgenic models show not only cognitive decline but also non-cognitive symptoms associated with the disease, including anxiety, aggression, locomotor hyperactivity (Walker *et al.*, 2011). Therefore, we investigated simultaneously locomotion, exploration and anxiety with Open Field Test (described in detail in Chapter 5: Materials and Methods). Tg2576 mice travelled a greater average distance in comparison with WT mice, indicating a locomotor hyperactivity of transgenic mice. Tg2576 mice in the presence of siK_v3.4 displayed a significant reduction in the total distance traveled compared to Tg2576 without siK_v3.4 (**Fig. 11C**).

Fig. 11

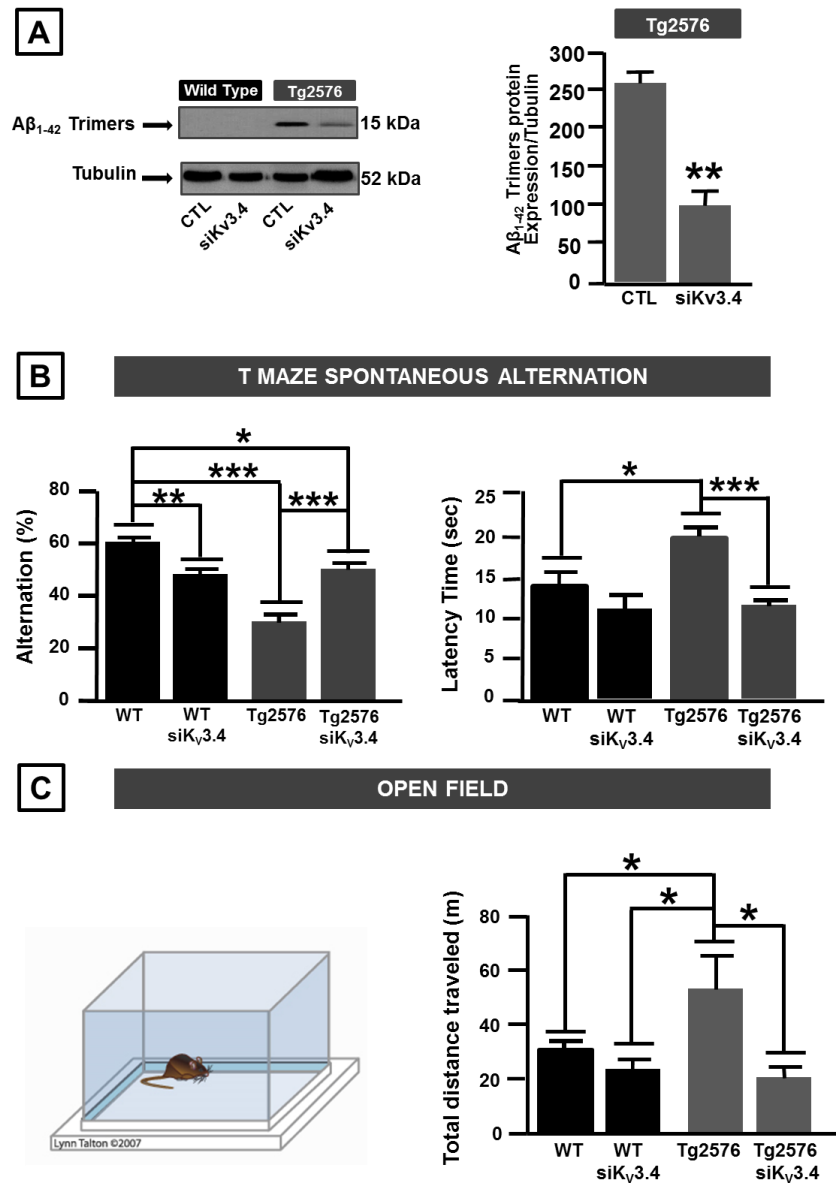


Fig. 11 Kv3.4 selective knockdown reduces Aβ production and trimer deposition in Tg2576 mice, improving memory performance. (A, left panel) Western Blot of Aβ₁₋₄₂ trimers protein expression on protein extracts obtained from three months old WT and Tg2576 mice in the presence and in the absence of siKv3.4. **(A, right panel)** Densitometric analysis of Aβ₁₋₄₂ trimers protein expression on protein extracts obtained from three months old Tg2576 mice in the presence and in the absence of siKv3.4 **(B, left panel)** Evaluation of the percentage of alternation (number of turns in each goal arm) in the T-Maze Spontaneous Alternation Test. **(B, right panel)** The latency time necessary to reach the goal arm calculate for each experimental groups in the T-Maze Spontaneous Alternation Test. **(C)** Evaluation of total distance traveled by animals in the Open Field Test calculate for each experimental groups. The values are expressed as mean±SEM of 3 independent experimental sections. *p≤ 0.05 versus their respective control, **p≤ 0.01 versus their respective control, *** p≤ 0.001 versus their respective control (*Student's t test and ANOVA*).

6.9 BDS 1-8 fragment, obtained from full length BDS-I toxin, could be an innovative pharmacological strategy to block K_v3.4 in Tg2576 mice

Sea anemone venom contains toxins that are able to active voltage-sensitive Na⁺ channels or block K⁺ channels. In particular *Anemonia sulcata* produced two toxins, BDS-I and BDS-II, which differ in only two positions (Ser-7 instead of Pro and Gly-11 instead of Asp). Both peptides have 43 aminoacids and are cross-linked by three disulfide bridges. BDS-I, but not BDS-II, is able to inhibit K_v3.4 currents in a reversible manner, with an IC₅₀ value of 47 nM (Diochot *et al.*, 1998). To find an innovative strategy to inhibit K_v3.4 potassium channel, we synthesized more fragments from full length BDS-I in order to identify the smaller portion of toxin that preserves the ability to block K_v3.4 currents. We chose CHO cell line as host cells for K_v3.4 and MiRP2 cDNAs transient transfection. First of all we evaluated the transfection efficiency by Western Blot analysis on protein extracts from control CHO cells and CHO cells plus K_v3.4 and MiRP2 cDNAs. K_v3.4-specific antibody revealed two band, at 75 kDa and 110 kDa, that correspond to immature and mature K_v3.4 subunit respectively, only in CHO cells plus K_v3.4 and MiRP2 cDNAs (**Fig. 12A**). Electrophysiological experiments showed a typical K⁺ currents mediated by K_v3.4, only in CHO cells plus K_v3.4 and MiRP2 cDNAs (**Fig. 12A**). BDS1-8 fragment, containing the first eight aminoacids from full BDS-I, has been the first fragment tested. We supposed that this fragment could have a critical role in the inhibition of K_v3.4 currents because contained one of two positions which differ between BDS-I and BDS-II. In particular, Proline in position 7 of BDS-I which differ from Serine in position 7 of BDS-II could explain the

property of BDS-I, but not of BDS-II, to block $K_V3.4$ currents. Electrophysiological experiments performed in CHO cells plus $K_V3.4$ and MiRP2 cDNAs showed that BDS1-8 fragment was able to inhibit $K_V3.4$ currents in a concentration dependent manner (**Fig. 12B**). Interestingly, 30nM of BDS1-8 were able to inhibit $K_V3.4$ currents; moreover 100nM of BDS-I were able to totally block $K_V3.4$ activity (**Fig. 12B**). Pannaccione and colleagues (2007), demonstrated that BDS-I prevented $A\beta_{1-42}$ -induced apoptosis in NGF-differentiated PC-12 cells and in hippocampal neurons. Thus we tested the ability of BDS1-8 fragment to prevent apoptotic mechanisms in presence of a death stimulus, such as $A\beta_{1-42}$ treatment that triggers an increase in $K_V3.4$ expression and activity. BDS 1-8 (100 nM), was able to significantly prevent the abnormal nuclear morphology induced by the exposure of NGF-differentiated PC-12 cells to $A\beta_{1-42}$ (5 μ M for 24 h), as detected by the Hoechst 32258 dye staining (**Fig. 12C**). Interestingly, BDS1-8 prevention of $A\beta_{1-42}$ -induced apoptosis occurred through its ability to inhibit $K_V3.4$ activity. Nuclear morphology quantification assessment with Hoechst 33258 dye staining revealed that BDS1-8 was able to avoid the increase in the percentage of abnormal nuclei induced by $A\beta_{1-42}$ treatment (**Fig. 12E**). Moreover BDS1-8 treatment was also able to prevent caspase-3 activation that we observed after $A\beta_{1-42}$ exposure (**Fig. 12E**).

Fig. 12

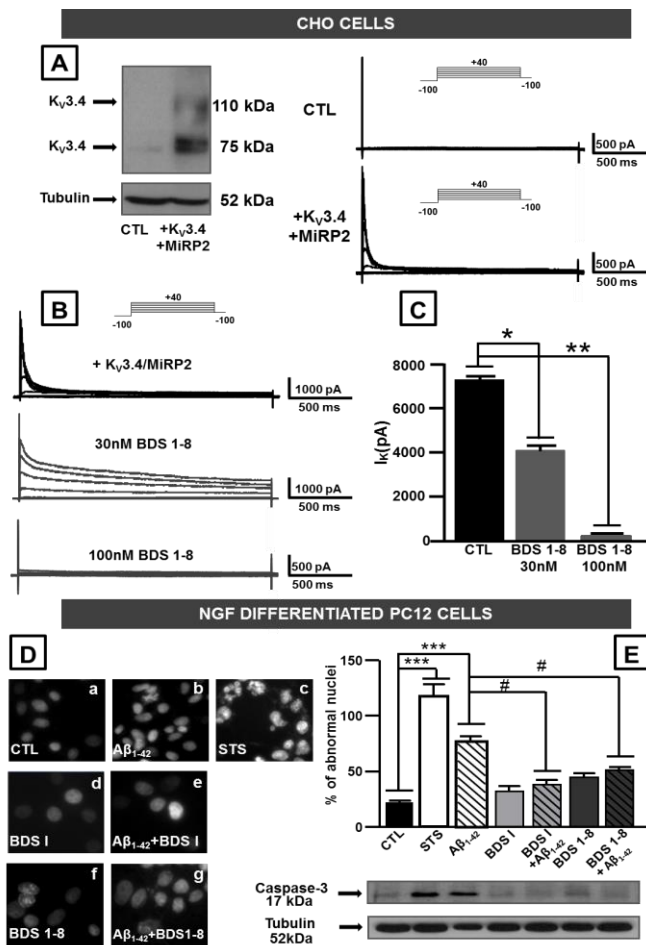


Fig. 12 BDS 1-8 fragment, obtained from full BDS-I toxin, could be an innovative pharmacological strategy to block K_V3.4 in Tg2576 mice. (A, left panel) Western Blot analysis of K_V3.4 protein expression on protein extracts obtained from control CHO cells and CHO cells plus K_V3.4 and MiRP2 cDNAs. **(A, right panel)** Total outward K⁺ currents recorded from control CHO cells and CHO cells plus K_V3.4 and MiRP2 cDNAs. **(B)** Total outward K⁺ currents recorded from CHO cells plus K_V3.4 and MiRP2 cDNAs in the absence and in the presence of 30nM, 100nM of BDS1-8 fragment. **(C)** Quantification of total outward K⁺ currents recorded from CHO cells plus K_V3.4 and MiRP2 cDNAs in the absence and in the presence of 30nM, 100nM of BDS1-8 fragment. **(D)** Assessment of nuclear morphology with Hoechst-33258 in NGF-differentiated PC-12 cells exposed for 24h to only Staurosporine, to only 5 μM Aβ₁₋₄₂, to only 50nM BDS-I, to only 100nM BDS1-8, to Aβ₁₋₄₂ + 50nM BDS-I, to Aβ₁₋₄₂ + 100nM BDS1-8. **(E)** Quantification of abnormal nuclear morphology and evaluation of caspase-3 activation in NGF-differentiated PC-12 cells exposed for 24h to only Staurosporine, to only 5 μM Aβ₁₋₄₂, to only 50nM BDS-I, to only 100nM BDS1-8, to Aβ₁₋₄₂ + 50nM BDS-I, to Aβ₁₋₄₂ + 100nM BDS1-8. The values are expressed as mean±SEM of 3 independent experimental sections. *p≤ 0.05 versus their respective control, **p≤ 0.01 versus their respective control, *** p≤ 0.001 versus their respective control, #p≤ 0.001 versus Aβ₁₋₄₂ groups (*Student's t test and ANOVA*).

6.10 A β ₁₋₄₂ exposure increases K_v3.4 expression and induces the astrocytes activation.

K_v channels are found in both excitable and non-excitable cell types. They have a critical role in neuronal and muscular excitability, in the regulation of action potential frequency and membrane potential, in the neurotransmitter release. However, their role in the non-excitable glial cell type remain yet unclear. Astrocytes, the most abundant glial cell type in CNS, serve as neuronal support and also as homeostasis regulators. Bekar and colleagues (2005), through immunocytochemical evaluation and RT-PCR analysis, has been demonstrated the presence of K_v3.4 subunit in hippocampal astrocyte cultures (Bekar *et al.*, 2005). However its expression and activity under AD pathology was never explored. Thus we studied the expression and the functional role of K_v3.4 subunit in astrocyte cultures treated with A β ₁₋₄₂ peptide. Firstly we performed Western Blot analysis in order to evaluate K_v3.4 and GFAP protein expression in astrocytes after A β ₁₋₄₂ exposure. We found a significant increase in K_v3.4 (**Fig. 13A**) and GFAP (**Fig. 13B**) protein expression in astrocytes treated with 5 μ M of A β ₁₋₄₂ for 48 hours compared to control astrocytes. We performed experiments with the cytoskeletal marker phalloidin in order to assess the astrocytes morphology and the nuclear dye Hoechst- 33342 in order to evaluate nuclear changes following A β ₁₋₄₂ treatment. Primary cultured astrocytes exposed to 5 μ M of A β ₁₋₄₂ for 48 hours showed more main cellular processes than untreated astrocytes (**Fig. 13C**). Moreover, little changes were detected in their nuclear morphology (**Fig. 13C**) but no apoptotic damage was observed in astrocytes after 48 hours of A β ₁₋₄₂. Thus, A β ₁₋₄₂ elicited astrocytes activation, as confirmed by the increase in

GFAP protein expression. Double immunofluorescence experiments with the anti-K_v3.4 and anti-GFAP antibodies revealed a more pronounced immunoreactivity for both K_v3.4 and GFAP when astrocytes were exposed to A β ₁₋₄₂ for 48 hours (**Fig. 13D**). Interestingly, immunocytochemistry experiments revealed that the K_v3.4 and GFAP immunosignals overlapped both in control astrocytes (**Fig. 13D, c**) and in A β ₁₋₄₂-treated astrocytes (**Fig. 13D, f**). Furthermore the exposure to A β ₁₋₄₂ induced an improve in the co-expression of K_v3.4 and GFAP proteins. To assess whether the overlap between GFAP and K_v3.4 immunostaining in the astrocytes was due to a direct binding between the two proteins, cell lysates from control and A β ₁₋₄₂-treated astrocytes were immunoprecipitated with anti-GFAP or anti-K_v3.4 antibodies and immunoblotted with anti-K_v3.4 antibodies or anti-GFAP, respectively. When we immunoprecipitated for K_v3.4 and then immunoblotted for GFAP we revealed a specific band at 50 kDa corresponding to GFAP both in control conditions and in A β ₁₋₄₂-treated astrocytes (**Fig. 13E**). Whereas when we immunoprecipitated for GFAP and then immunoblotted for K_v3.4 we found a specific band at 75 kDa corresponding to K_v3.4 both in control conditions and in A β ₁₋₄₂-treated astrocytes (**Fig. 13E**).

Fig. 13

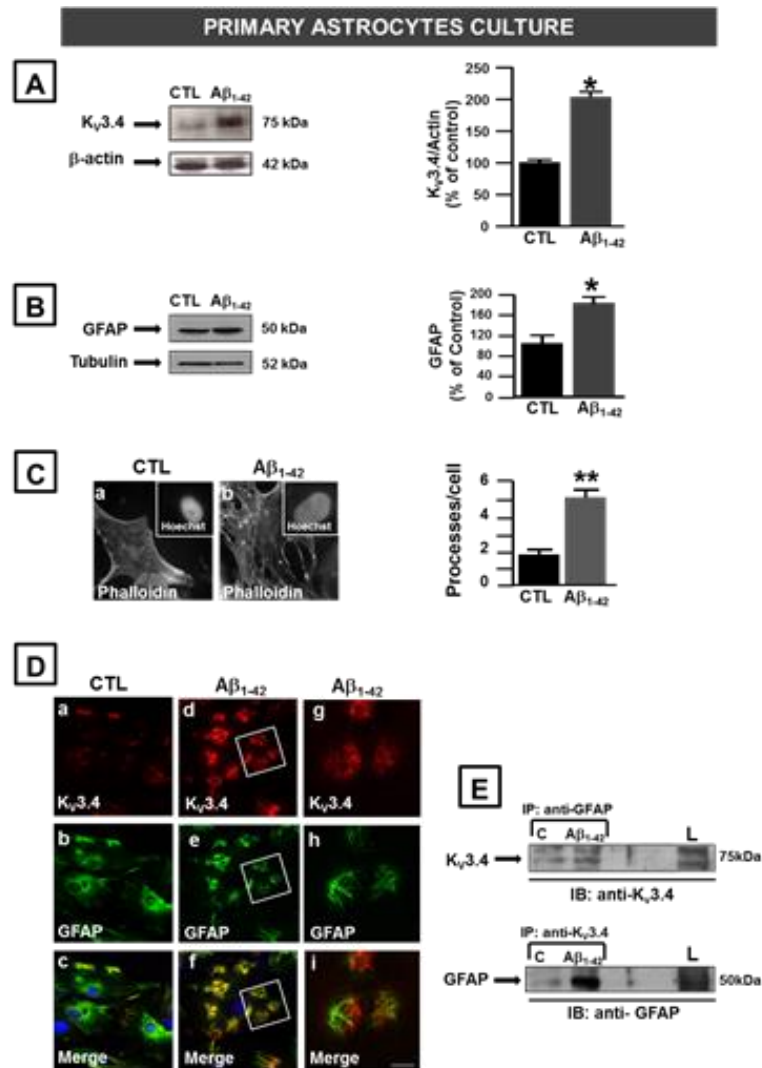


Fig. 13 Aβ₁₋₄₂ exposure increases Kv3.4 expression and induces the astrocytes activation. (A) Western Blot analysis and densitometric analysis of Kv3.4 protein expression on protein extracts obtained from primary astrocytes under control conditions or 48 hours after Aβ₁₋₄₂ exposure. **(B)** Western Blot analysis and densitometric analysis of GFAP protein expression on protein extracts obtained from primary astrocytes under control conditions or 48 hours after Aβ₁₋₄₂ exposure. **(C, left panel)** Light microscopy images displaying phalloidin and Hoechst-33258 double-labeling in single representative primary astrocytes under control conditions (a) or 48 hours after Aβ₁₋₄₂ exposure (b). The top frames in a-b show the nuclear morphology. **(C, right panel)** Quantitative analysis of the number of astrocytic processes for cell detected with phalloidin labeling under control conditions or 48 hours after Aβ₁₋₄₂ exposure. **(D)** Confocal double immunofluorescence images of primary astrocytes displaying both Kv3.4 (red) and GFAP (green) immunoreactivities under control conditions (a-c) or 48 hours after Aβ₁₋₄₂ exposure (d-i). **(E)** Total astrocyte cell extract (1mg) was immunoprecipitated with anti-GFAP or anti-Kv3.4 antibodies and then immunoblotted with anti-Kv3.4 or anti-GFAP antibodies respectively. L, lysates; C, control. The values are expressed as mean±SEM of 3 independent experimental sections. *p≤ 0.05 versus their respective control, **p≤ 0.01 versus their respective control, *** p≤ 0.001 versus their respective control (*Student's t test and ANOVA*).

6.11 $A\beta_{1-42}$ exposure increases $K_v3.4$ activity in primary astrocytes, whereas the $K_v3.4$ silencing prevents $A\beta_{1-42}$ effect.

Electrophysiological recordings by patch clamp in astrocytes exposed for 48 hours to $A\beta_{1-42}$ displayed a significant up-regulation of the transient outward potassium currents I_A compared to control cells (**Fig. 14A**). Upon bath-application of the selective blocker of $K_v3.4$ channels, BDS-I (50nM), we observed a significant inhibition of I_A currents both in control and in $A\beta_{1-42}$ -treated astrocytes (**Fig.14B**). We observed a significant inhibition of $K_v3.4$ currents in presence of BDS-I both in control astrocytes and in $A\beta_{1-42}$ -treated astrocytes (**Fig. 14B**). To further confirm the contribution of $K_v3.4$ function to the upregulated I_A currents in astrocytes exposed to $A\beta_{1-42}$ we knockdown $K_v3.4$ subunits with a selective siRNA in the presence or in the absence of amyloid fragment. Electrophysiological recordings revealed that $K_v3.4$ silencing was able to avoid the up-regulation of the I_A currents triggered by $A\beta_{1-42}$ treatment (**Fig. 14C**). Quantification of I_A currents showed a significant reduction of I_A component of I_K currents in astrocytes in the presence of selective $K_v3.4$ siRNA (**Fig. 14D**). Moreover, we observed a more pronounced decrease in I_A currents in astrocytes with the silencing of $K_v3.4$, treated with $A\beta_{1-42}$ peptide (**Fig. 14D**).

Fig. 14

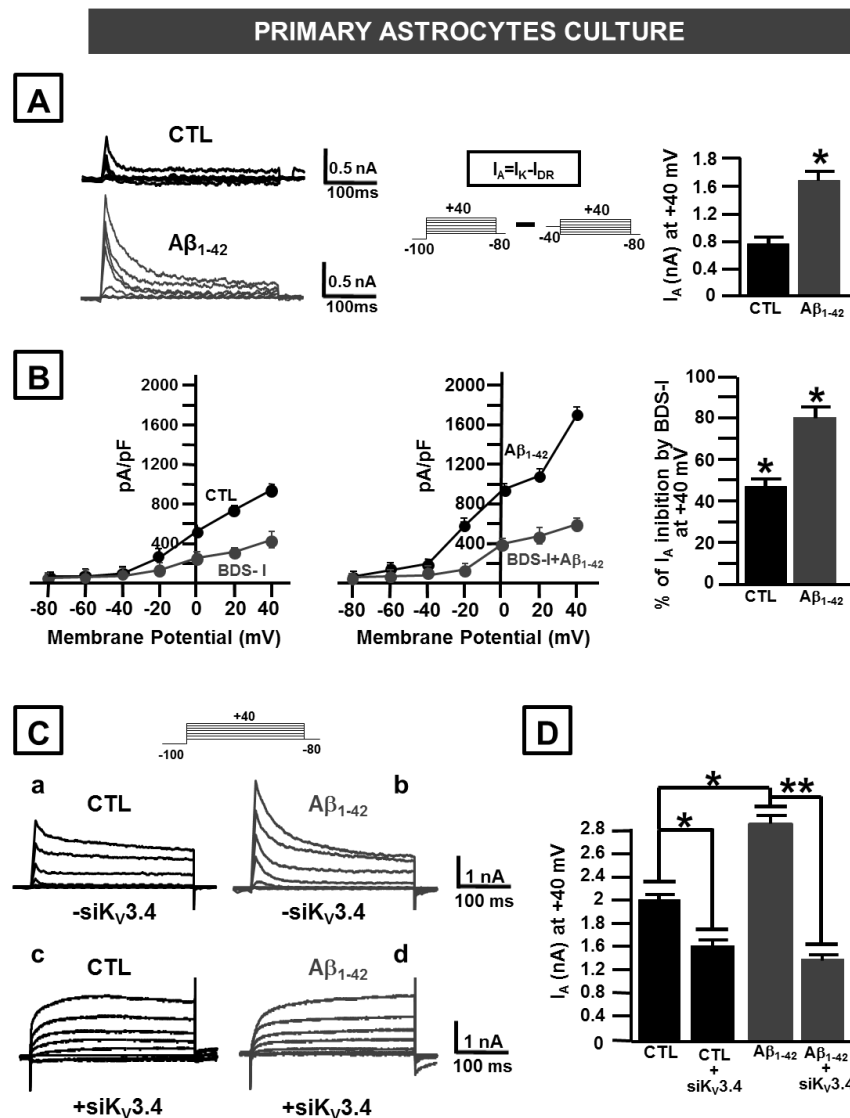


Fig. 14 Aβ₁₋₄₂ exposure increases K_v3.4 activity in primary astrocytes, whereas the K_v3.4 silencing prevents Aβ₁₋₄₂-effect. **(A, left panel)** Representative traces of voltage-isolated fast inactivating currents (I_A) recorded from primary astrocytes under control conditions and 48 hours after Aβ₁₋₄₂ exposure. **(A, right panel)** I_A currents quantification represented in the left panel. **(B, left panel)** current-voltage relationships for isolated I_A under control conditions and 48 hours after Aβ₁₋₄₂ exposure both in the presence or in the absence of 50nM BDS-I. **(B, right panel)** I_A currents quantification represented in the left panel. **(C, left panel)** Representative traces of the outward K⁺ currents (I_K) recorded from control **(a)**, control plus siK_v3.4 **(c)**, after Aβ₁₋₄₂ for 48 hours **(b)**, after Aβ₁₋₄₂ for 48 hours plus siK_v3.4 **(d)** in primary astrocytes. **(C, right panel)** quantification of I_A currents recorded from control, control plus siK_v3.4, after Aβ₁₋₄₂ for 48 hours, after Aβ₁₋₄₂ for 48 hours plus siK_v3.4 in primary astrocytes. The values are expressed as mean±SEM of 3 independent preparation of primary astrocyte cultures (n=12 cells in each cell culture and for each group). *p≤ 0.05 versus their respective control, **p≤ 0.01 versus their respective control, *** p≤ 0.001 versus their respective control (*Student's t test and ANOVA*).

6.12 Silencing of K_v3.4 significantly reduced astrocytes activation in Tg2576 mice in the early stages of AD.

To test the contribution of K_v3.4 increased expression and activity to the early astrocytes activation in Tg2576 mouse brain, we explored *in vivo* whether the selective knockdown of the K_v3.4 gene could affect astrocyte activation. To this aim, we silenced K_v3.4 subunits with a selective siRNA and analyzed GFAP protein levels in brain lysates from both Tg2576 and WT mice. Western Blot analysis revealed that GFAP protein levels was upregulated in Tg2576 mice compared to age-matched WT (**Fig. 15A**) By contrast, intracerebral ventricular infusion of siRNA significantly reduced astrocytes activation in Tg2576 mice as detected by the significant decrease in the optical density of the 50kDa band (GFAP) (**Fig. 15C**).

Fig. 15

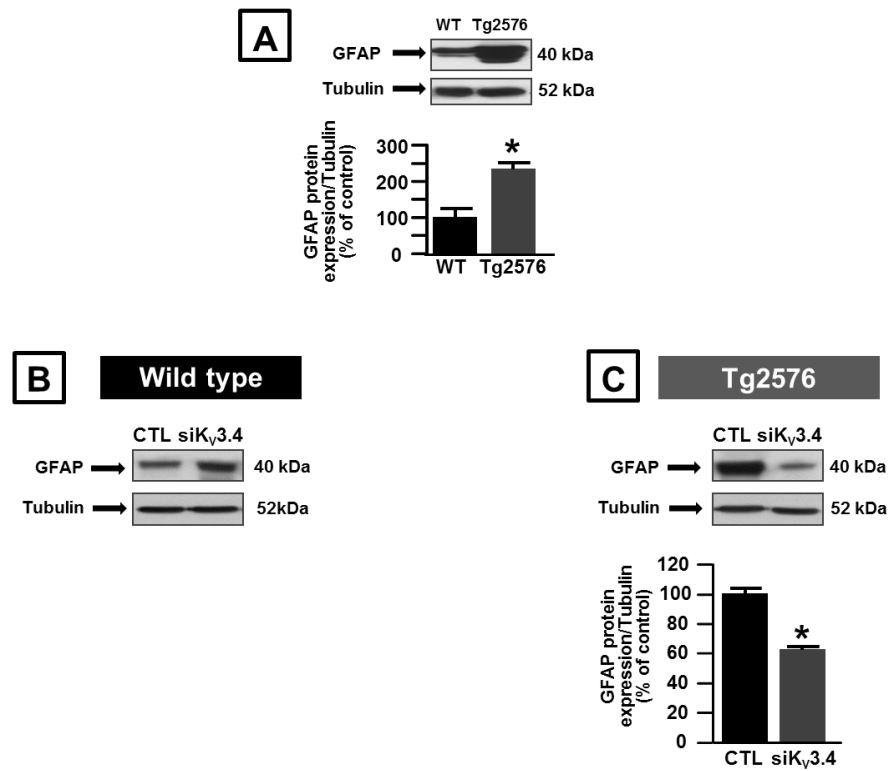


Fig. 15 Silencing of K_v3.4 significantly reduced astrocyte activation in Tg2576 mice in the early stages of AD. (A) Western Blot analysis and densitometric analysis of GFAP protein expression in the brain of WT and Tg2576 mice. **(B)** Western blot analysis of GFAP in the brain of WT mice in the absence or in the presence of siK_v3.4. **(C)** Western blot analysis and densitometric analysis of GFAP protein expression in the brain of Tg2576 in the absence or in the presence of siK_v3.4. The values are expressed as mean±SEM of 3 independent experimental sections. *p≤ 0.05 versus their respective control, **p≤ 0.01 versus their respective control, *** p≤ 0.001 versus their respective control (*Student's t test and ANOVA*).

DISCUSSION

Chapter 7: Discussion

This PhD thesis demonstrated that $K_V3.4$ potassium channel subunit has a critical role in the early stages of AD. In fact we observed an increase in $K_V3.4$ protein expression in the hippocampus of young Tg2576 mice (3 months old), whereas we did not observe a significant modification in elderly Tg2576 mice (14-18 months old). In addition we observed a singular tendency of $K_V3.4$ expression in WT and Tg2576 mice. In the hippocampus of 3 months old WT mice we found the lower levels of $K_V3.4$, whereas in the hippocampus of 12 months old WT mice $K_V3.4$ expression reached the peak, suggesting a key role of $K_V3.4$ in the adulthood and aging. Progressive increase in the expression and the achievement of a peak in adulthood suggested that $K_V3.4$ could contribute to the maturation of the neuronal electrical activity. Moreover, in Tg2576 mice we reported an anticipation of the events described in WT mice. In fact $K_V3.4$ maximal protein expression occurred in the hippocampus of 3 months old Tg2576 mice, whereas in 12 months old transgenic mice we noted a significant reduction. In addition, we investigated the protein expression of MiRP2, a neuronal β -subunit co-assembling with $K_V3.4$ that plays a central role in the control of its biophysical properties and pharmacological profile (Abbott *et al.*, 2001). MiRP2 protein expression followed the same trend of $K_V3.4$; in fact we observed its modulation only in the early stages of AD pathogenesis. Pannaccione *et al* (2007) found in *in vitro* models that $A\beta_{1-42}$ exposure induced the simultaneously modulation of $K_V3.4$ and its accessory component. Our results, obtained in an *in vivo* model of AD, such as Tg2576 mice, were in agreement with those performed *in vitro* with $A\beta_{1-42}$ treatment. In the early phase of AD we found the deposition of $A\beta_{1-42}$

oligomers of low molecular weight such as dimeric and trimeric forms (Kawarabayashi *et al.*, 2004). In particular, we found A β ₁₋₄₂ trimers deposition in 3-months old transgenic mice when we observed the maximal increase in K_v3.4 and MiRP2 expression, suggesting the deleterious effects triggered by trimers deposition in AD brain. Recently, it has been demonstrated that primary neurons from Tg2576 mice recapitulate the *in vivo* localization and accumulation of A β ₁₋₄₂ with time in culture (Takahashi *et al.*, 2004). Thus we measured K_v3.4 activity by patch clamp in hippocampal neurons obtained from WT and transgenic embryos at different DIV. Electrophysiological recordings displayed a substantial increase in total outward K⁺ currents in transgenic hippocampal neurons compared to WT neurons. In addition we found an increase in I_A amplitude, previously isolated with the voltage subtraction protocol from I_K currents, in transgenic neurons. Interestingly, we found an early increase in transgenic neurons at 8 and 12 DIV whereas at 15 DIV we observed a down-regulation in I_A currents. These results supported the concept that K_v3.4 has a key role in early stages of AD, contributing to neuronal hyperexcitability. It has been hypothesized that A β ₁₋₄₂ accumulation makes neurons hyperexcitable and susceptible for epileptiform activity. In APP transgenic mice it has been found the onset of spontaneous non-convulsive seizure in cortical and hippocampal networks (Palop *et al.*, 2007). Moreover, AD patients also have a higher incidence of seizures compared to normal populations. Indeed, the epileptic activity is predominantly in AD patients with early-onset dementia and during the earlier stages of the disease. Interestingly, mice overexpressing human WT or mutated APP showed premature death, with a peak around 3-4 months of age before the finding of first plaques. Minkeviciene and colleagues (2009) reported that epileptic

seizure may trigger premature death in APP transgenic mice. In agreement with biochemical and electrophysiological results, the immunocytochemical analysis confirmed that in transgenic mice there was an increase in K_v3.4 expression associated with an altered subcellular distribution of this protein. In fact in transgenic hippocampal neurons we observed a more intense K_v3.4 immunosignal mainly confined to the somatic plasma membrane, in comparison with WT hippocampal neurons in which the fluorescent signal was mostly distributed through the neuropil. This different K_v3.4 distribution could be induced by the alteration of the cytoskeletal integrity provoked by A β ₁₋₄₂ accumulation. Intriguingly, it has been demonstrated that [K⁺]_i play a key role in cell survival. Cytoplasmic K⁺ loss has been shown to favor activation of caspases and nucleases, which lead to apoptosis (Hughes *et al.*, 1997; Cain *et al.*, 2001). K⁺ efflux has been proposed to be a pro-apoptotic factor, consequently plasma membrane potassium channels represent good candidates for apoptosis regulation. Pannaccione and colleagues (2007) have demonstrated that A β ₁₋₄₂ peptide induced a selective up-regulation of K_v3.4 channel subunits and that this event was associated with an increase in K_v3.4 currents. In addition, hippocampal neurons and NGF-differentiated PC-12 cells over expressing K_v3.4 showed an apoptotic nuclear process, as revealed by caspase-3 activation and by Hoechst 33258-monitored abnormal nuclear morphology, thus suggesting a possible link between the enhanced expression and function of this K⁺ channel and the neurotoxic consequences of A β exposure. Intriguingly in Tg2576 mice, in the early phase of AD, the up-regulation of K_v3.4 expression and activity was accompanied by the increase in pro-caspase 3 and the activation of caspase-3. Thus K_v3.4 potassium channel subunit was implicated in AD pathogenesis, in particular had a pivotal

role in the onset of AD symptoms. Consistently with this hypothesis we provided evidence that the silencing of $K_v3.4$ in the brain of early Tg2576 mice (3 months old) strongly reducing $K_v3.4$ expression, prevented the activation of caspase-3. In addition, in Tg2576 mice we observed the rise of pro-caspase 6 protein expression and that si $K_v3.4$ was able to prevent this increase. Recently, several studies have demonstrated that APP is also a substrate for caspases cleavage, suggesting an additional role of caspases in the neurodegeneration characteristic of AD. In fact, a second mechanism for APP processing involves caspase-induced cleavage of APP. Furthermore, caspases activation leads to an increase of amyloidogenic fragments and $A\beta$ peptide (Gervais *et al.*, 1999; Lu *et al.*, 2003; D'Amelio *et al.*, 2010). Thus we evaluated if the silencing of $K_v3.4$ could modify $A\beta$ production and trimers deposition in Tg2576 mice. Notably, in the presence of si $K_v3.4$ we found a significant reduction in the levels of $A\beta_{1-42}$ trimers in Tg2576 mice. We could assume the existence of an indirect link between $K_v3.4$ over-expression, caspases activation and $A\beta_{1-42}$ trimers deposition. In fact, the silencing of $K_v3.4$ in Tg2576 mice prevented caspases activation, reduced APP alternative cleavage by caspases and in turn reduced $A\beta_{1-42}$ formation. $A\beta$ aggregation has been recognized as a necessary condition for toxicity and it has been hypothesized that dimers and trimers of $A\beta$ are the principal toxic species (Hung *et al.*, 2008). Moreover, recent studies showed that $A\beta$ oligomers can inhibit hippocampal LTP and that $A\beta_{1-42}$ dimers and trimers accumulate in Tg2576 mice in the same time when memory impairment begins (Kawarabayashi *et al.*, 2004). Thus, we evaluated memory performance of Tg2576 mice through T-Maze spontaneous alternation test. Tg2576 mice exhibited impaired exploration ability, spatial learning and memory abilities, as

indicated by fewer alternative choices and longer latency. Interestingly, the silencing of $K_v3.4$ ameliorated exploration ability and memory performance. In fact, Tg2576 mice in the presence of $K_v3.4$ silencing showed an increase in the percentage of alternation and a reduction in the latency time necessary to reach the goal arm, compared to Tg2576 mice without si $K_v3.4$. Furthermore, APP transgenic models show not only cognitive decline but also non-cognitive symptoms associated with the disease, including anxiety, aggression, locomotor hyperactivity (Walker *et al.*, 2011). Furthermore we investigated simultaneously locomotion, exploration and anxiety with Open Field test. Tg2576 mice travelled a greater average distance in comparison with WT mice, demonstrating a locomotor hyperactivity. Tg2576 mice in the presence of si $K_v3.4$ displayed a significant reduction in the total distance travelled compared to Tg2576 without si $K_v3.4$. These results suggested a critical role of $K_v3.4$ in the progression and development of AD. Intriguingly, si $K_v3.4$ ameliorating memory performance and non-cognitive symptoms associated with AD could become a new pharmacological target in the care of AD. To achieve this aim we found a new synthetic compound, BDS1-8, containing the first eight aminoacids from full length BDS-I that as well known blocks $K_v3.4$ currents. Electrophysiological experiments performed in CHO cells plus $K_v3.4$ and MiRP2 cDNAs showed that BDS1-8 fragment was able to inhibit $K_v3.4$ currents in a concentration dependent manner. Furthermore BDS1-8 was able to significantly prevent the abnormal nuclear morphology induced by $A\beta_{1-42}$ exposure (5 μ M for 24 h) in NGF-differentiated PC-12 cells, as detected by Hoechst 32258 dye staining. Nuclear morphology assessment with Hoechst 33258 dye staining revealed that BDS1-8 was able to avoid the increase in the percentage of abnormal nuclei induced by $A\beta_{1-42}$ treatment. Moreover BDS1-8

treatment was also able to prevent caspase-3 activation that we observed after $A\beta_{1-42}$ exposure. Based on these observations, we proposed that reducing the elevated levels of $K_v3.4$ we may provide a promising strategy to slowing down AD development and progression. In the last years the new pharmacological strategies for AD treatment are focused on the possibility to block or modify the course of AD. To block the progression of the disease the new pharmacological strategies should interfere with the pathogenic steps responsible for the clinical symptoms, including the deposition of $A\beta_{1-42}$ peptide. Thus the inhibition of $K_v3.4$ in the early stages of AD could become a promising strategy to slowing down $A\beta_{1-42}$ formation. In the last phase of our study we investigated the role of $K_v3.4$ in astrocytes. Bekar and colleagues (2005) have demonstrated the presence of $K_v3.4$ subunit in hippocampal astrocyte cultures (Bekar *et al.*, 2005). However their expression and activity under AD pathology was never explored. Thus we studied the expression and the functional role of $K_v3.4$ subunit in astrocyte cultures treated with $A\beta_{1-42}$ peptide. We found a significant increase in $K_v3.4$ and GFAP protein expression in astrocytes treated with $5\mu\text{M}$ of $A\beta_{1-42}$ for 48 hours compared to control astrocytes. Moreover, primary cultured astrocytes exposed to $5\mu\text{M}$ of $A\beta_{1-42}$ for 48 hours showed more main cellular processes than untreated astrocytes, little changes were detected in their nuclear morphology but no apoptotic damage was observed. Thus, $A\beta_{1-42}$ elicited astrocytes activation, as confirmed by the increase in GFAP protein expression. Double immunofluorescence experiments with the anti- $K_v3.4$ and anti-GFAP antibodies revealed a more pronounced immunoreactivity for both $K_v3.4$ and GFAP when astrocytes were exposed to $A\beta_{1-42}$ for 48 hours. Interestingly, immunocytochemistry experiments revealed the presence of intense overlap

between $K_V3.4$ and GFAP immunosignals in control astrocytes and in $A\beta_{1-42}$ -treated astrocytes. Furthermore the exposure to $A\beta_{1-42}$ induced an improvement in the co-expression of $K_V3.4$ and GFAP proteins. Immunoprecipitation experiments performed with anti-GFAP or anti- $K_V3.4$ antibodies demonstrated that the overlap between GFAP and $K_V3.4$ immunostaining in the astrocytes was due to a direct binding between the two proteins. Electrophysiological recordings by patch clamp in astrocytes exposed for 48 hours to $A\beta_{1-42}$ displayed a significant up-regulation of the transient outward potassium currents I_A compared to control cells. The treatment with the selective blocker of $K_V3.4$ channels, BDS-I (50nM), and the silencing of $K_V3.4$ were able to prevent the current increase induced by the amyloid fragment. Thus we confirmed the contribution of $K_V3.4$ function to the up-regulated I_A currents in astrocytes exposed to $A\beta_{1-42}$. To test the involvement of increased $K_V3.4$ expression and activity in the early astrocytes activation in Tg2576 mouse brain, we explored *in vivo* whether the selective knockdown of the $K_V3.4$ genes could affect astrocytes activation. To this aim, we silenced $K_V3.4$ subunits with a selective si $K_V3.4$ and analyzed GFAP protein levels in brain lysates from both Tg2576 and WT mice. Western Blot analysis revealed that GFAP protein levels were up-regulated in Tg2576 mice compared to age-matched WT and that the si $K_V3.4$ significantly reduced astrocytes activation in Tg2576 mice. In astrocytes, the role of the interaction between a cytoskeleton protein, GFAP, and potassium channels remains still unclear. We could speculate that this link has a role in the channels trafficking to membrane. In fact, GFAP in astrocytes might promote channel addressing in precise domains of the membrane in order to facilitate the accumulation of $K_V3.4$ channel and, in turn, the increase of potassium ions necessary to

activate specific cellular mechanisms. The position and localization of the cytoskeleton strongly reflect the corresponding position of the specific ionic gradients and the related binding proteins. Furthermore supporting evidence demonstrated the role of Ca^{2+} in the remodeling of the cytoskeleton (Hepler, 2016), as well as K^+ ions could promote the activation or inhibition of specific mechanisms in activated astrocytes.

REFERENCES

- Abbott GW, Butler MH, Bendahhou S, Dalakas MC, Ptacek LJ and Goldstein SA. **MiRP2 Forms Potassium Channels in Skeletal Muscle with Kv3.4 and Is Associated with Periodic Paralysis.** *Cell* 2001; 104:217-231.
- Abbott GW, Goldstein SA, Sesti F. **Do all voltage-gated potassium channels use MiRPs.** *Circulation Research* 2001b; 88:981-983.
- Albert MS, DeKosky ST, Dickson D, Dubois B, Feldman HH, Fox NC, Gamst A, Holtzman DM, Jagust WJ, Petersen RC, Snyder PJ, Carrillo MC, Thies B and Phelps CH. **The diagnosis of mild cognitive impairment due to Alzheimer's disease: Recommendations from the National Institute on Aging-Alzheimer's Association workgroups on diagnostic guidelines for Alzheimer's disease.** *Alzheimer's & Dementia* 2011; 7(3):270-279.
- Alkon DL. **Ionic conductance determinants of synaptic memory nets and their implications for Alzheimer's disease.** *J. Neurosci. Res.*, 1999; 58:24–32.
- Alzheimer A. **Über eine eigenartige Erkrankung der Hirnrinde.** *Allg Z Psychiatr* 1907; 64:146–148.
- Araque A, Parpura V, Sanzgiri RP., and Haydon P.G. **Tripartite synapses: glia, the unacknowledged partner.** *Trends Neurosci.* 1999; 22:208–215
- Baner C, Brunner C, Lassmann H, Budka H, Jellinger K, Wiche G, Seitelberger F, Grundke-Iqbal I, Iqbal K, Wisniewski HM. **Accumulation of abnormally phosphorylated tau precedes the formation of neurofibrillary tangles in Alzheimer's disease.** *Brain Research* 1989; 477:90-99.
- Blasko I, Veerhuis R, Stampfer-Kountchev M, Saurwein-Teissl M, Eikelenboom P, and Grubeck-Loebenstein B. **Costimulatory Effects of Interferon- γ and Interleukin-1 β or Tumor Necrosis Factor α on the Synthesis of A β ₁₋₄₀ and A β ₁₋₄₂ by Human Astrocytes.** *Neurobiology of Disease* 2000; 7:682-689.
- Boda E, Hoxha E, Pini A, Montarolo F, Tempia F. **Brain expression of Kv3 subunits during development, adulthood and aging and in a murine model of Alzheimer's disease.** *J Mol Neurosci.* 2012; 3:606-15.
- Braak H, Braak E. **Neuropathological staging of Alzheimer-related changes.** *Acta Neuropathologica* 1991; 82(4):239-59.
- Braak H, Braak E. **Staging of Alzheimer's disease related Neurofibrillary changes.** *Neurobiology of Aging* 1994; 16(3):271-8.

- Braak H, Braak E. **Frequency of Stages of Alzheimer-Related Lesions in Different Age Categories.** *Neurobiology of Aging* 1997; 18:351-357.
- Bomfim TR, Forny-Germano L, Sathler LB, Brito-Moreira J, Houzel JC, Decker H, Silverman MA, Kazi H, Melo HM, McClean PL, Holscher C, Arnold SE, Talbot K, Klein WL, Munoz DP, Ferreira ST, De Felice FG. **An anti-diabetes agent protects the mouse brain from defective insulin signaling caused by Alzheimer's disease-associated A β oligomers.** *J Clin Invest.* 2012; 122:1339-53.
- Brion JP, Tremp G, Octave JN. **Transgenic expression of the shortest human tau affects its compartmentalization and its phosphorylation as in the pretangle stage of Alzheimer's disease.** *American Journal of Pathology* 1999; 154:255-270.
- Buee L, Bussiere T, Buee-Scherrer V, Delacourte A, Hof PR. **Tau protein isoforms, phosphorylation and role in neurodegenerative disorders.** *Brain Research Reviews* 2000; 33:95-130.
- Bukar-Maina M, Al-Hilaly YK and Serpell LC. **Nuclear Tau and Its Potential Role in Alzheimer's Disease.** *Biomolecules* 2016; 6(1).
- Cain K, Langlais C, Sun XM, Brown DG and Cohen GM. **Physiological Concentrations of K⁺ Inhibit Cytochrome c-dependent formation of the Apoptosome.** *Journal of Biological Chemistry* 2001; 45:41985-41990.
- Caspersen C, Wang N, Yao J, Sosunov A, Chen X, Lustbader JW, Xu HW, Stern D, McKhann G, Yan SD. **Mitochondrial Abeta: a potential focal point for neuronal metabolic dysfunction in Alzheimer's disease.** *FASEB Journal* 2005; 14:2040-1.
- Chanda B, Asamoah OK, Blunck R, Roux B, Bezanilla F. **Gating charge displacement in voltage-gated ion channels involves limited transmembrane movement.** *Nature* 2005; 7052:852-6.
- Chung S, Lee J, Joe EH and Uhm DY. **Beta-amyloid peptide induces the expression of voltage dependent outward rectifying K⁺ channels in rat microglia.** *Neuroscience Letters* 2001; 300:67-70.
- Combs CK, Johnson DE, Karlo JC, Cannady SB & Landreth GE. **Inflammatory mechanisms in Alzheimer's disease: Inhibition of beta-amyloid-stimulated proinflammatory responses and neurotoxicity by PPARgamma agonists.** *Journal of Neuroscience* 2000; 20:558-567.
- Corder EH, Saunders AM, Strittmatter WJ, Schmechel DE, Gaskell PC, Small GW, Roses AD, Haines JL, Pericak-Vance MA. **Gene Dose of Apolipoprotein E Type 4 Allele and the Risk of Alzheimer's Disease in Late Onset Families.** *Science* 1993; 5123:921-3.
- Davies P, Maloney AJR. **Selective loss of centralcholinergic neurons in Alzheimer's disease.** *Lancet* 1976; 2:1403.

- Coyle JT, Price DL, DeLong M. **Alzheimer's disease: a disorder of cortical cholinergic innervation.** *Science* 1983; 219:1184-1190.
- D'Amelio M, Cavallucci V and Cecconi F. **Neuronal caspase-3 signaling: not only cell death.** *Cell Death and Differentiation* 2010; 17:1104-1114.
- D'Amelio M, Cavallucci V, Middei S, Marchetti C, Pacioni S, Ferri A, Diamantini A, De Zio D, Carrara P, Battistini L, Moreno S, Bacci A, Ammassari-Teule M, Marie H, Cecconi F. **Caspase-3 triggers early synaptic dysfunction in a mouse model of Alzheimer's disease.** *Nat Neurosci.* 2011; 14:69-76.
- Das KP, Freudenrich TM, Mundy WR. **Assessment of PC12 cell differentiation and neurite growth: a comparison of morphological and neurochemical measures.** *Neurotoxicol Teratol.* 2004; 26(3):397-406.
- Davies P. **The neurochemistry of Alzheimer's disease and senile dementia.** *Medicinal Research Reviews* 1983; 3:221-36.
- De Felice FG, Velasco PT, Lambert MP, Viola K, Fernandez SJ, Ferreira ST and Klein WL. **A β oligomers induce neuronal oxidative stress through an n-methyl-D-aspartate receptor-dependent mechanism that is blocked by the Alzheimer drug memantine.** *The Journal Of Biological Chemistry* 2007; 15:11590-11601.
- Deacon RMJ and Rawlins JNP. **T-maze alternation in the rodent.** *Nat Protoc.* 2006; 1(1):7-12.
- Decker H, Jürgensen S, Adrover MF, Brito-Moreira J, Bomfim TR, Klein WL, Epstein AL, De Felice FG, Jerusalinsky D, Ferreira ST. **N-methyl-D-aspartate receptors are required for synaptic targeting of Alzheimer's toxic amyloid- β peptide oligomers.** *J Neurochem.* 2010; 115:1520-9.
- DeKosky ST, Scheff SW. **Synapse loss in frontal cortex biopsies in Alzheimer's disease: correlation with cognitive severity.** *Annals of Neurology* 1990; 5:457-64.
- De-Paula VJ1, Radanovic M, Diniz BS, Forlenza OV. **Alzheimer's disease.** *Subcellular Biochemistry* 2012; 65:329-52.
- Desai R, Kronengold J, Mei J, Forman SA, Kaczmarek LK. **Protein kinase C modulates inactivation of K v 3.3 channels.** *Journal of Biological Chemistry* 2008; 283:22283-22294.
- Diochot S, Schweitz H, Beress L and Lazdunski M. **Sea Anemone Peptides with a Specific Blocking Activity against the Fast Inactivating Potassium Channel Kv3.4.** *Journal Of Biological Chemistry* 1998; 12:6744-6749.
- Dodson PD, Forsythe ID. **Presynaptic K $^{+}$ channels: electrifying regulators of synaptic terminal excitability.** *Trends in Neurosciences* 2004; 27:210-217.

- Doyle DA, Morais Cabral J, Pfuetzner RA, Kuo A, Gulbis JM, Cohen SL, Chait BT, MacKinnon R. **The structure of the potassium channel: molecular basis of K⁺ conduction and selectivity.** *Science* 1998; 280:69-77.
- Du J, Haak LL, Phillips-Tansey E, Russell JT and McBain CJ. **Frequency-dependent regulation of rat hippocampal somato-dendritic excitability by the K⁺ channel subunit K_v2.1.** *J. Physiol.*, 2000; 522:19–31.
- Dubois JM, Rouzaille-Dubois B. **Role of potassium channels in mitogenesis.** *Progress in Biophysics and Molecular Biology* 1993; 59:1-21.
- Durell SR, Hao Y, Guy HR. **Structural Models of the Transmembrane Region of Voltage-Gated and Other K⁺ Channels in Open, Closed, and Inactivated Conformations.** *Journal of Structural Biology* 1998; 121:263-284.
- Elder GA, Gama Sosa MA, De Gasperi R, Hof PR. **Presenilin transgenic mice as models of Alzheimer's disease.** *Brain Structure and Function* 2010; 214:127-143.
- Etienne P, Robitaille Y, Wood P, Gauthier S, Nair NPV, Quirion R. **Nucleus basalis neuronal loss, neuritic plaques and choline acetyltransferase activity in advanced Alzheimer's disease.** *Neuroscience* 1986; 19:1279-1291.
- Ferri CP, Prince M, Brayne C, Brodaty H, Fratiglioni L, Ganguli M, Hall K, Hasegawa K, Hendrie H, Huang Y, Jorm A, Mathers C, Menezes PR, Rimmer E, Sczuzfca M; **Alzheimer's Disease International. Global prevalence of dementia: a Delphi consensus study.** *Lancet* 2005; 366:2112–7.
- Fischer U, Janicke RU, Schulze-Osthoff K. **Many cuts to ruin: a comprehensive update of caspase substrates.** *Cell Death and Differentiation* 2003; 10:76–100.
- Francis PT, Palmer AM, Snape M, Wilcock GK. **The cholinergic hypothesis of Alzheimer's disease: a review of progress.** *Journal of Neurology, Neurosurgery & Psychiatry* 1999; 66:137–147.
- Frick A., Magee J, Johnston D. **LTP is accompanied by an enhanced local excitability of pyramidal neuron dendrites.** *Nat. Neurosci.* 2004; 7:126–35.
- Games D, Adams D, Alessandrini R, Barbour R, Berthelette P, Blackwell C, Carr T, Clemens J, Donaldson T, Gillespie F, Guido T, Hagopian S, Johnson-Wood K, Khan K, Lee M, Leibowitz P, Lieberburg I, Little S, Masliah E, McConlogue L, Montoya-Zavala M, Mucke L, Paganini L, Penniman E, Power M, Schenk D, Seubert P, Snyder B, Soriano F, Tan H, Vitale J, Wadsworth S, Wolozin B and Zhao J. **Alzheimer-type neuropathology in transgenic mice overexpressing V717F beta-amyloid precursor protein.** *Nature* 1995; 373:523-7.
- Gervais FG, Xu D, Robertson GS, Vaillancourt JP, Zhu Y, Huang J, LeBlanc A, Smith D, Rigby M, Shearman MS, Clarke EE, Zheng H, Van Der Ploeg LH, Ruffolo SC,

- Thornberry NA, Xanthoudakis S, Zamboni RJ, Roy S, Nicholson DW. **Involvement of caspases in proteolytic cleavage of Alzheimer's Amyloid- β Precursor Protein and amyloidogenic A β peptide formation.** *Cell* 1999; 97:395–406.
- Ghelardini C, Galeotti N, Bartolini A. **Influence of potassium channel modulators on cognitive processes in mice.** *Br. J. Pharmacol.* 1998; 123:1079–84.
 - Goate A, Chartier-Harlin MC, Mullan M, Brown J, Crawford F, Fidani L, Giuffra L, Haynes A, Irving N, James L, Mant R, Newton P, Rooke K, Roques P, Talbot C, Pericak-Vance M, Roses A, Williamson R, Rossor M, Owen M and Hardy J. **Segregation of a missense mutation in the amyloid precursor protein gene with familial Alzheimer's disease.** *Nature* 1991; 349:704-6.
 - Götz J, Probst A, Spillantini MG, Schäfer T, Jakes R, Bürki K, Goedert M. **Somatodendritic localization and hyperphosphorylation of tau protein in transgenic mice expressing the longest human brain tau isoform.** *EMBO Journal* 1995; 14:1304-1313.
 - Gotz J, Chen F, Barmettler R, Nitsch RM. **Tau filament formation in transgenic mice expressing P301L tau.** *Journal of Biological Chemistry* 2001; 276:529-534.
 - Gouras GK, Olsson TT, Hansson O. **β -amyloid Peptides and Amyloid Plaques in Alzheimer's Disease.** *Neurotherapeutics* 2015; 12:3-11.
 - Graham SF, Nasarauddin MB, Carey M, McGuinness B, Holscher C, Kehoe PG, Love S, Passmore AP, Elliott CT, Meharg A, Green BD. **Quantitative measurement of [Na⁺] and [K⁺] in postmortem human brain tissue indicates disturbances in subjects with Alzheimer's disease and dementia with Lewy bodies.** *J Alzheimers Dis.* 2015; 3:851-7.
 - Greene LA, Tischler AS. **Establishment of a noradrenergic clonal line of rat adrenal pheochromocytoma cells which respond to nerve growth factor.** *Proc Natl Acad Sci USA* 1976; 73(7):2424-8.
 - Greenwald BS, Mohs RC, Davis KL.J. **Neurotransmitter deficits in Alzheimer's disease: criteria for significance.** *Journal of the American Geriatrics Society* 1983; 31:310-6.
 - Grissmer S, Nguyen AN, Aiyar J, Hanson DC, Mather RJ, Gutman GA, Karmilowicz MJ, Auperin DD, Chandy KG. **Pharmacological characterization of five cloned voltage-gated K⁺ channels, types Kv1.1, 1.2, 1.3, 1.5, and 3.1, stably expressed in mammalian cell lines.** *Molecular Pharmacology* 1994; 45:1227-34.
 - Grundke-Iqbal I, Iqbal K, George L, Tung YC, Kim KS, Wisniewski HM. **Amyloid protein and neurofibrillary tangles coexist in the same neuron in Alzheimer disease.** *Proceedings of the National Academy of Sciences USA* 1989.

- Gutman GA, Chandy KG, Adelman JP, Aiyar J, Bayliss DA, Clapham DE, Covarrubias M, Desir GV, Furuichi K, Ganetzky B, Garcia ML, Grissmer S, Jan LY, Karschin A, Kim D, Kuperschmidt S, Kurachi Y, Lazdunski M, Lesage F, Lester HA, Mckinnon D, Nichols CG, O'Kelly I, Robbins J, Robertson GA, Rudy B, Sanguinetti M, Seino S, Stuehmer W, Tamkun MM, Vandenberg CA, Wei A, Wulff H, Wymore RS. **International Union of Pharmacology. XLI. Compendium of Voltage-Gated Ion Channels: Potassium Channels.** *Pharmacology* 2003; 55(4):583-586.
- Haass C and Selkoe DJ. **Soluble protein oligomers in neurodegeneration: lessons from the Alzheimer's amyloid β -peptide.** *Nat Rev Mol Cell Biol.* 2007; 8(2):101-12.
- Haass C, Kaether C, Thinakaran G, and Sisodia S. **Trafficking and Proteolytic Processing of APP.** *Cold Spring Harb Perspect Med.* 2012; 2(5).
- Halassa MM. and Haydon PG. **Integrated Brain Circuits: Astrocytic Networks Modulate Neuronal Activity and Behavior.** *Annu Rev Physiol.* 2010; 72:335–355.
- Hauptmann S, Keil U, Scherping I, Bonert A, Eckert A and Müller WE. **Mitochondrial dysfunction in sporadic and genetic Alzheimer's disease.** *Experimental Gerontology* 2006; 41:668-673.
- He P, Zhong Z, Lindholm K, Berning L, Lee W, Lemere C, Staufenbiel M, Li R, Shen Y. **Deletion of tumor necrosis factor death receptor inhibits amyloid beta generation and prevents learning and memory deficits in Alzheimer's mice.** *Journal of Cell Biology* 2007; 178:829-41.
- Heginbotham L, Lu Z, Abramson T, MacKinnon R **Mutations in the K⁺ channel signature sequence.** *Biophysical Journal* 1994; 66(4):1061-7.
- Heneka MT, Rodríguez JJ, Verkhratsky A. **Neuroglia in neurodegeneration.** *Brain Research Reviews* 2010; 63(1-2):189-211.
- Hepler PK. **The cytoskeleton and its regulation by calcium and protons.** *Plant Physiol.* 2016; 170(1):3-22.
- Hsiao K, Chapman P, Nilsen S, Eckman C, Harigaya Y, Younkin S, Yang F, Cole G. **Correlative memory deficits, A β elevation, and amyloid plaques in transgenic mice.** *Science* 1996; 274(5284):99-102.
- Hughes FM Jr, Bortner CD, Purdy GD and Cidlowski JA. **Intracellular K⁺ Suppresses the Activation of Apoptosis in Lymphocytes.** *The Journal of Biological Chemistry* 1997; 272(48):30567-30576.
- Hung LW, Ciccotosto GD, Giannakis E, Tew DJ, Perez K, Masters CL, Cappai R, Wade JD, Barnham KJ. **Amyloid- β peptide (A β) neurotoxicity is modulated by the rate of peptide aggregation: A β dimers and trimers correlate with neurotoxicity.** *The Journal of Neuroscience* 2008; 28:11950–11958.

- Iqbal K, del C. Alonso A, Chen S, Chohan MO, El-Akkad E, Gong C-X, Khatoon S, Li B, Liu F, Rahman A, Tanimukai H, Grundke-Iqbal I. **Tau pathology in Alzheimer disease and other tauopathies.** *Biochimica et Biophysica Acta* 2005; 1739:198-210.
- Ishihara T, Zhang B, Higuchi M, Yoshiyama Y, Trojanowski JQ, Lee VMY. **Age-dependent induction of congophilic neurofibrillary tau inclusions in tau transgenic mice.** *American Journal of Pathology* 2001; 158:555-562.
- Jack CR Jr, Albert M, Knopman DS, McKhann GM, Sperling RA, Carillo M, Thies W and Phelps CH. **Introduction to Revised Criteria for the Diagnosis of Alzheimer's Disease: National Institute on Aging and the Alzheimer Association Workgroups.** *Alzheimer's & Dementia* 2011; 7(3):257–262.
- Jacobsen JS, Wu CC, Redwine JM, Comery TA, Arias R, Bowlby M, Martone R, Morrison JH, Pangalos MN, Reinhart PH, Bloom FE. **Early-onset behavioral and synaptic deficits in a mouse model of Alzheimer's disease.** *Proceeding of the National Academy of Sciences USA* 2006; 103(13):5161-6.
- Jalonen TO, Charniga CJ and Wielt DB. **Beta-Amyloid peptide-induced morphological changes coincide with increased K⁺ and Cl⁻ channel activity in rat cortical astrocytes.** *Brain Research* 1997; 746:85-97.
- Janus C, Chishti MA, Westaway D. **Transgenic mouse models of Alzheimer's disease.** *Biochimica and Biophysica Acta* 2000; 1502(1):63-75.
- Jenkinson DH. **Potassium channels-multiplicity and challenges.** *British Journal of Pharmacology* 2006; 147:S63-71.
- Kammesheidt A, Boyce FM, Spanoyannis AF, Cummings BJ, Ortegon M, Cotman C, Vaught JL, Neve RL. **Deposition of beta/A4 immunoreactivity and neuronal pathology in transgenic mice expressing the carboxylterminal fragment of the Alzheimer amyloid precursor in the brain.** *Proceeding of the National Academy of Sciences USA* 1992; 89(22):10857-61.
- Karran E, Mercken M and De Strooper B. **The amyloid cascade hypothesis for Alzheimer's disease: an appraisal for the development of therapeutics.** *Nat Rev Drug Discov.* 2011; 10(9):698-712.
- Kass RS. **The channelopathies: novel insights into molecular and genetic mechanisms of human disease.** *Journal of Clinical Investigation* 2005; 115:1986-1989.
- Kawarabayashi T, Shoji M, Younkin LH, Wen-Lang L, Dickson DW, Murakami T, Matsubara E, Abe K, Ashe KH, Younkin SG. **Dimeric amyloid beta protein rapidly accumulates in lipid rafts followed by apolipoprotein E and phosphorylated tau accumulation in the Tg2576 mouse model of Alzheimer's disease.** *J Neurosci.* 2004; 24:3801-9.

- Kim D. **Physiology and pharmacology of two-pore domain potassium channels.** *Current Pharmaceutical Design* 2005; 11(21):2717-36.
- Lacor PN, Buniel MC, Furlow PW, Sanz Clemente A, Velasco PT, Wood M, Viola KL and Klein WL. **A β Oligomer-Induced Aberrations in Synapse Composition, Shape, and Density Provide a Molecular Basis for Loss of Connectivity in Alzheimer's Disease.** *The Journal of Neuroscience* 2007; 27(4):796-807.
- LaFerla F. **Calcium dyshomeostasis and Intracellular signalling in Alzheimer's disease.** *Nat Rev Neurosci.* 2002 Nov; 3(11):862-72.
- LaFerla FM, Green KN and Oddo S. **Intracellular amyloid- β in Alzheimer's disease.** *Nat Rev Neurosci.* 2007; 8(7):499-509.
- Lamb BT, Sisodia SS, Lawler AM, Slunt HH, Kitt CA, Kearns WG, Pearson PL, Price DL, Gearhart J. **Introduction and expression of the 400 kilobase amyloid precursor protein gene in transgenic mice.** *Nature Genetics* 1993; 5(1):22-30.
- Ledo JH, Azevedo EP, Clarke JR, Ribeiro FC, Figueiredo CP, Foguel D, De Felice FG, Ferreira ST. **Amyloid- β oligomers link depressive-like behavior and cognitive deficits in mice.** *Mol Psychiatry.* 2013; 18:1053-4.
- Lewis J, McGowan E, Rockwood J, Melrose H, Nacharaju P, Van Slegtenhorst M, Gwinn-Hardy K, Murphy PM, Baker M, Yu X, Duff K, Hardy J, Corral A, Lin WL, Yen SH, Dickson DW, Davies P, Hutton M. **Neurofibrillary tangles, amyotrophy and progressive motor disturbance in mice expressing mutant (P301L) tau protein.** *Nature Genetics* 2000; 25:402-405.
- Lewis J, Dickson DW, Lin WL, Chisholm L, Corral A, Jones G, Yen SH, Sahara N, Skipper L, Yager D, Eckman C, Hardy J, Hutton M, McGowan E. **Enhanced neurofibrillary degeneration in transgenic mice expressing mutant tau and APP.** *Science* 2001; 293(5534):1487-91.
- Li Y, Um SY, McDonald TV. **Voltage-gated potassium channels: regulation by accessory subunits.** *Neuroscientist* 2006; 12(3):199-210.
- Li Y, Tan MS, Jiang T, and Tan L. **Microglia in Alzheimer's Disease.** *BioMed Research International* 2014; 2014:437-483.
- Lilliehook C, Bozdagi, O, Yao J, Gomez-Ramirez M, Zaidi NF, Wasco W, Gandy S, Santucci AC, Haroutunian V, Huntley GW, Buxbaum JD. **Altered Abeta formation and long-term potentiation in a calsenilin knock-out.** *J. Neurosci.* 2003; 23:9097-106.
- Long SB, Campbell EB, Mackinnon R. **Crystal structure of a mammalian voltage-dependent Shaker family K⁺ channel.** *Science* 2005; 309(5736):897-903.

- Long SB, Tao X, Campbell EB, MacKinnon R. **Atomic structure of a voltage-dependent K⁺ channel in a lipid membrane-like environment.** *Nature* 2007; 450(7168):376-82.
- Lu DC, Soriano S, Bredesen DE, Koo EH. **Caspase cleavage of the amyloid precursor protein modulates amyloid b-protein toxicity.** *Journal of Neurochemistry* 2003; 8:733–741.
- Macica CM, von Hehn CA, Wang LY, Ho CS, Yokoyama S, Joho RH, Kaczmarek LK. **Modulation of the kv3.1b potassium channel isoform adjusts the fidelity of the firing pattern of auditory neurons.** *Journal of Neuroscience* 2003; 23:1133-1141.
- Martin L, Latypova X, Terro F. **Post-translational modifications of tau protein: Implications for Alzheimer's disease.** *Neurochemistry International* 2011; 58:458-471.
- Maruszak A and Żekanowski C. **Mitochondrial dysfunction and Alzheimer's disease.** *Progress in Neuro-psychopharmacology and Biological Psychiatry* 2011; 35:320-330.
- Mattson MP, Partin J, Begley JG. **Amyloid β-peptide induces apoptosis-related events in synapses and dendrites.** *Brain Research* 1998; 167-176.
- Mattson MP and Chan SL. **Dysregulation of Cellular Calcium Homeostasis in Alzheimer's Disease.** *Journal of Molecular Neuroscience* 2001; 17:205-224.
- McDowell I. **Alzheimer's disease: Insights from epidemiology.** *Aging* 2001; 13(3):143-62.
- McCrossan ZA, Lewis A, Panaghie G, Jordan PN, Christini DJ, Lerner DJ, Abbott GW. **MinK-related peptide 2 modulates Kv2.1 and Kv3.1 potassium channels in mammalian brain.** *Journal of Neuroscience* 2003; 23:8077-8091.
- McCrossan ZA, Abbott GW. **The MinK-related peptides.** *Neuropharmacology* 2004; 47:787-821.
- McKhann G, Drachman D, Folstein M, Katzman R, Price D, Stadlan EM. **Clinical diagnosis of Alzheimer's disease: report of the NINCDS-ADRDA Work Group under the auspices of Department of Health and Human Services Task Force on Alzheimer's Disease.** *Neurology* 1984; 34(7):939-44.
- Minkeviciene R, Rheims S, Dobszay MB, Zilberter M, Hartikainen J, Fülöp L, Penke B, Zilberter Y, Harkany T, Pitkänen A, Tanila H. **Amyloid beta-induced neuronal hyperexcitability triggers progressive epilepsy.** *J Neurosci.* 2009; 29(11):3453-62.
- Misonou H, Mohapatra DP, Park EW, Leung V, Zhen D, Misonou K, Anderson AE and Trimmer JS. **Regulation of ion channel localization and phosphorylation by neuronal activity.** *Nat. Neurosci.* 2004; 7:711–8.

- Moreno H, Kentros C, Bueno E, Weiser M, Hernandez A, Vega-Saenz De Miera E, Ponce A, Thornhill W and Rudy B. **Thalamocortical projections have a K⁺ channel that is phosphorylated and modulated by cAMP-dependent protein kinase.** *Journal of Neuroscience* 1995; 15:5486.
- Moechars D, Dewachter I, Lorent K, Reverse D, Baekelandt V, Naidu A, Tesseur I, Spittaels K, Haute CV, Checler F, Godaux E, Cordell B, Van Leuven F. **Early phenotypic changes in transgenic mice that overexpress different mutants of amyloid precursor protein in brain.** *Journal of Biological Chemistry* 1999; 274(10):6483-92.
- Mori C, Spooner ET, Wisniewsk KE, Wisniewski TM, Yamaguch H, Saido TC, Tolan DR, Selkoe DJ, Lemere CA. **Intraneuronal Abeta42 accumulation in Down syndrome brain.** *Amyloid* 2002; 9:88-102.
- Mucke L, Masliah E, Yu GQ, Mallory M, Rockenstein EM, Tatsuno G, Hu K, Kholodenko D, Johnson-Wood K, McConlogue L. **High-level neuronal expression of abeta 1-42 in wild-type human amyloid protein precursor transgenic mice: synaptotoxicity without plaque formation.** *Journal of Neuroscience* 2000; 20(11):4050-8.
- Murakoshi H, Shi G, Scannevin RH and Trimmer JS. **Phosphorylation of the K_v2.1 K⁺ channel alters voltage-dependent activation.** *Mol. Pharmacol.* 1997; 52:821–8.
- Murakoshi H. and Trimmer JS. **Identification of the K_v2.1 K⁺ channel as a major component of the delayed rectifier K⁺ current in rat hippocampal neurons.** *J. Neurosci.* 1999; 19:1728–35.
- Murphy GG, Fedorov NB, Giese KP, Ohno M, Friedman E, Chen R, Silva AJ. **Increased Neuronal Excitability, Synaptic Plasticity, and Learning in Aged K_vβ1.1 Knockout Mice.** *Current Biology* 2004; 14:1907–1915.
- Nagele RG, Wegiel J, Venkataraman V, Imaki H, Wang KC. **Contribution of glial cells to the development of amyloid plaques in Alzheimer's disease.** *Neurobiol Aging.* 2004; 25(5):663-74.
- Nestor PJ, Scheltens P & Hodges JR. **Advances in the early detection of Alzheimer's disease.** *Nature Reviews* 2004; 5:S34–S41.
- Neve RL, Harris P, Kosik KS, Kurnit DM, Donlon TA. **Identification of cDNA clones for the human microtubule-associated protein tau and chromosomal localization of the genes for tau and microtubule-associated protein 2.** *Molecular Brain Research* 1986; 1:271-280.
- Nordberg A. **In vivo detection of neurotransmitter changes in Alzheimer's disease.** *Annals of the New York Academy of Sciences* 1993; 695:27-33.

- Oddo S, Caccamo A, Shepherd JD, Murphy MP, Golde TE, Kaye R, Metherate R, Mattson M, Akbari Y, LaFerla F. **Triple-Transgenic Model of Alzheimer's Disease with Plaques and Tangles: Intracellular A β and Synaptic Dysfunction.** *Neuron* 2003; 39:409-421.
- Oddo S, Caccamo A, Smith IF, Green KN & LaFerla FM. **A dynamic relationship between intracellular and extracellular pools of A β .** *The American Journal of Pathology* 2006;168:184-194.
- O'Grady SM & Lee SY **Molecular diversity and function of voltage-gated (Kv) potassium channels in epithelial cells.** *International Journal of Biochemistry and Cell Biology* 2005; 37, 1578-1594.
- Orkand RK, Nicholls JG, Kuffler SW. **Effect of nerve impulses on the membrane potential of glial cells in the central nervous system of amphibia.** *J Neurophysiol.* 1966; 29:788-806.
- Overk CR and Masliah E. **Pathogenesis Of Synaptic Degeneration In Alzheimer's Disease And Lewy Body Disease.** *Biochem Pharmacol.* 2014; 88(4):508-16.
- Pal S, Hartnett KA, Nerbonne JM, Levitan ES and Aizenman E. **Mediation of neuronal apoptosis by K v 2.1-encoded potassium channels.** *J. Neurosci.* 2003; 23:4798–802.
- Palop JJ, Chin J, Roberson ED, Wang J, Thwin MT, Bien-Ly N, Yoo J, Ho KO, Yu GQ, Kreitzer A, Finkbeiner S, Noebels JL, Mucke L. **Aberrant excitatory neuronal activity and compensatory remodeling of inhibitory hippocampal circuits in mouse models of Alzheimer's disease.** *Neuron* 2007; 55(5):697-711.
- Pannaccione A, Secondo A, Scorziello A, Cali G, Tagliatela M and Annunziato L. **Nuclear factor- κ B activation by reactive oxygen species mediates voltage-gated K $^+$ current enhancement by neurotoxic β -amyloid peptides in nerve growth factor-differentiated PC-12 cells and hippocampal neurons.** *Journal of Neurochemistry* 2005; 94, 572-586.
- Pannaccione A., Boscia F., Scorziello A, Adornetto A, Castaldo P, Sirabella R, Tagliatela M, Di Renzo GF and Annunziato L. **Up-regulation and increased activity of Kv3.4 channels and their accessory subunit mink-related peptide 2 induced by amyloid peptide are involved in apoptotic neuronal death.** *Molecular Pharmacology* 2007; 72:665-673.
- Paula-Lima AC, Adasme T, SanMartín C, Sebollela A, Hetz C, Carrasco MA, Ferreira ST, Hidalgo C. **Amyloid β -peptide oligomers stimulate RyR-mediated Ca $^{2+}$ release inducing mitochondrial fragmentation in hippocampal neurons and prevent RyR-mediated dendritic spine remodeling produced by BDNF.** *Antioxid Redox Signal.* 2011; 14:1209-23.

- Paula-Lima AC, Brito-Moreira J, Ferreira ST. **Deregulation of excitatory neurotransmission underlying synapse failure in Alzheimer's disease.** *J Neurochem.* 2013; 126(2):191-202.
- Pearson BE, Choi TK. **Expression of the human beta-amyloid precursor protein gene from a yeast artificial chromosome in transgenic mice.** *Proceeding of the National Academy of Sciences USA* 1993; 90(22):10578-82.
- Perea G.,Navarrete M.,and Araque A.**Tripartite synapses: astrocytes process and control synaptic information.** *TrendsNeurosci.* 2009; 32:421–431.
- Perea G, Sur M and Araque A. **Neuron-glia networks: integral gear of brain function.** *Frontiers in Cellular Neuroscience* 2014; 8:1-8.
- Perry EK. **The cholinergic hypothesis: ten years on.** *British Medical Bulletin* 1986; 42:63-69.
- Perry EK, Perry RH, Blessed G, Tomlinson BE. **Neurotransmitter enzyme abnormalities in senile dementia: Choline acetyltransferase and glutamic acid decarboxylase activities in necropsy brain tissue.** *Journal of the Neurological Sciences* 1977; 34:247-265.
- Petkov GV. **Role of potassium ion channels in detrusor smooth muscle function and dysfunction.** *Nat Rev Urol.* 2011; 9(1):30-40.
- Pham E, Crews L, Ubhi K, Hansen L, Adame A, Cartier A, Salmon D, Galasko D, Michael S, Savas J, Yates R, Glabe C, and Masliah E. **Progressive accumulation of amyloid-beta oligomers in Alzheimer's disease and in amyloid precursor protein transgenic mice is accompanied by selective alterations in synaptic scaffold proteins.** *FEBS Journal* 2010; 277:3051-67.
- Pignataro G, Esposito E, Cuomo O, Sirabella R, Boscia F, Guida N, Di Renzo G, Annunziato L. **The NCX3 isoform of the Na⁺/Ca²⁺ exchanger contributes to neuroprotection elicited by ischemic postconditioning.** *J Cereb Blood Flow Metab.* 2011; 31(1):362-70.
- Pignataro G, Boscia F, Esposito E, Sirabella R, Cuomo O, Vinciguerra A, Di Renzo G, Annunziato L. **NCX1 and NCX3: two new effectors of delayed preconditioning in brain ischemia.** *Neurobiol Dis.* 2012; 45(1):616-23.
- Pooler AM, Noble W, Hanger DP. **A role for tau at the synapse in Alzheimer's disease pathogenesis.** *Neuropharmacology* 2014; 76:1-8.
- Pourrier M, Schram G, Nattel S. **Properties, Expression and Potential Roles of Cardiac K⁺ Channel Accessory Subunits: MinK, MiRPs, KChIP, and KChAP.** *Journal of Membrane Biology* 2003; 194:141-152.

- Quirion R. **Cholinergic Markers in Alzheimer Disease and the Autoregulation of Acetylcholine Release.** *J Psychiatry Neurosci.* 1993; 18(5):226-34.
- Ramsden M, Plant LD, Webster NJ, Vaughan PF, Henderson Z and Pearson HA. **Differential effects of un-aggregated and aggregated amyloid beta protein (1-40) on K⁺ channel currents in primary cultures of rat cerebellar granule and cortical neurons.** *Journal of Neurochemistry* 2001; 79:699-712.
- Ransohoff RM and Brown MA. **Innate immunity in the central nervous system.** *Journal of Clinical Investigation* 2012; 122:1164-1171.
- Reike F, Warland R, de Ruyter van Steveninck R, Bialek W. **Spikes: Exploring the Neural Code.** *Bradford Book - MIT Press, Cambridge* 1997, MA: MIT Press.
- Reitz C, Mayeux R. **Alzheimer disease: Epidemiology, Diagnostic Criteria, Risk Factors and Biomarkers.** *Biochemical Pharmacology* 2014; 88(4):640-51.
- Rogaev EI, Sherrington R, Rogaeva EA, Levesque G, Ikeda M, Liang Y, Chi H, Lin C, Holman K, Tsuda T, Mar L, Sorbi S, Nacmias B, Piacentini S, Amaducci L, Chumakov I, Cohen D, Lannfelt L, Fraser PE, Rommens JM and St George-Hyslop PH. **Familial Alzheimer's disease in kindreds with missense mutations in a gene on chromosome 1 related to the Alzheimer's disease type 3 gene.** *Nature* 2002; 376(6543):775-778.
- Rossi G, Dalpra L, Crosti F, Lissoni S, Sciacca FL, Catania M, di Fede G, Mangieri M, Giaccone G, Croci D, Tagliavini F. **A new function of microtubule-associated protein tau: Involvement in chromosome stability.** *Cell Cycle* 2008; 7:1788-1794.
- Roy S, Zhang B, Lee VM, Trojanowski JQ **Axonal transport defects: a common theme in neurodegenerative diseases.** *Acta Neuropathologica* 2005; 109:5-13.
- Rudy B, Kentros C, Weiser M, Fruhling D, Serodio P, Vega-Saenz de Miera E, Ellisman MH, Pollock JA, Baker H **Region-specific expression of a K⁺ channel gene in brain.** *Proceedings of the National Academy of Sciences USA* 1992; 89:4603-4607.
- Rudy B, Chow A, Lau D, Amarillo Y, Ozaita A, Saganich M, Moreno H, Nadal MS, Hernandez-Pineda R, Hernandez-Cruz A, Erisir A, Leonard C, Vega-Saenz de Miera E. **Contributions of Kv3 channels to neuronal excitability.** *Annals of the New York Academy of Sciences* 1999; 868:304-343.
- Ruta V, Chen J, MacKinnon R. **Calibrated Measurement of Gating-Charge Arginine Displacement in the KvAP Voltage-Dependent K⁺ Channel.** *Cell* 2005, 123:463-475.
- Saijo K & Glass CK. **Microglial cell origin and phenotypes in health and disease.** *Nature Reviews* 2011; *Immunology* 11:775-787.

- Santa-cruz K, Lewis J, Spires T, Paulson J, Kotilinek L, Ingelsson M, Guimaraes A, DeTure M, Ramsden M, McGowan E, Forster C, Yue M, Orne J, Janus C, Mariash A, Kuskowski M, Hyman B, Hutton M, Ashe KH. **Tau suppression in a neurodegenerative mouse model improves memory function.** *Science* 2005; 309(5733):476-81.
- Saraiva LM, Seixas da Silva GS, Galina A, da-Silva WS, Klein WL, Ferreira ST, De Felice FG. **Amyloid- β triggers the release of neuronal hexokinase 1 from mitochondria.** *PLoS One* 2010; 16:5-12.
- Selkoe DJ. **Alzheimer's Disease: Genes, Proteins, and Therapy.** *Physiological Reviews* 2001; 81(2):741-66.
- Serrano-Pozo A, Frosch MP, Masliah E and Hyman BT. **Neuropathological Alterations in Alzheimer Disease.** *Cold Spring Harbor Perspectives in Medicine* 2011; 1(1).
- Sherrington R, Rogaev EI, Liang Y, Rogaeva EA, Levesque G, Ikeda M, Chi H, Lin C, Li G, Holman K, Tsuda T, Mar L, Foncin JF, Bruni AC, Montesi MP, Sorbi S, Rainero I, Pinessi L, Nee L, Chumakov I, Pollen D, Brookes A, Sanseau P, Polinsky RJ, Wasco W, Da Silva HA, Haines JL, Pericak-Vance MA, Tanzi RE, Roses AD, Fraser PE, Rommens JM, St George-Hyslop PH. **Cloning of a gene bearing missense mutations in early-onset familial Alzheimer's disease.** *Nature* 1995; 375(6534):754-60
- Siegel GJ **Basic Neurochemistry** 2005
- Stocker M. **Ca⁽²⁺⁾-activated K⁺ channels: molecular determinants and function of the SK family.** *Nature Reviews* 2004; *Neuroscience* 5(10):758-70.
- Stine WB, Dahlgren KN, Krafft GA, LaDu MJ. **In Vitro Characterization of Conditions for Amyloid- β Peptide Oligomerization and Fibrillogenesis.** *The Journal of Biological Chemistry* 2003; 13:11612–11622.
- Strittmatter WJ, Weisgraber KH, Huang DY, Dong LM, Salvesen GS, Pericak-Vance M, Schmechel D, Saunders AM, Goldgaber D, Roses AD. **Binding of human apolipoprotein E to synthetic amyloid beta peptide: isoform specific effects and implications for late-onset Alzheimer disease.** *Proceedings of the National Academy of Sciences USA* 1993; 90(17):8098-102.
- Strop P, Bankovich AJ, Hansen KC, Garcia KC and Brunger AT. **Structure of a Human A-type Potassium Channel Interacting Protein DPPX, a Member of the Dipeptidyl Aminopeptidase Family.** *Journal of Molecular Biology* 2004; 343:1055-1065.
- Swerdlow RH, Khan SM. **A “mitochondrial cascade hypothesis” for sporadic Alzheimer's disease.** *Medical Hypotheses* 2004; 63:8-20.

- Swerdlow RH, Burns JM and Khan SM. **The Alzheimer's disease mitochondrial cascade hypothesis.** *Journal of Alzheimer's Disease* 2010; 20:265-279.
- Swerdlow RH, Burns JM, Khan SM. **The Alzheimer's disease mitochondrial cascade hypothesis: progress and perspectives.** *Biochimica and Biophysica Acta* 2014; 1842(8):1219-31.
- Takahashi RH, Almeida CG, Kearney PF, Yu F, Lin MT, Milner TA, Gouras GK. **Oligomerization of Alzheimer's β -Amyloid within Processes and Synapses of Cultured Neurons and Brain.** *J Neurosci.* 2004; 24(14):3592-9.
- Takumi T, Ohkubo H, Nakanishi S. **Cloning of a membrane protein that induces a slow voltage-gated potassium current.** *Science* 1988; 242:1042-1045.
- Tesco G, Ho Koh Y, Tanzi RE. **Caspase activation increases β -Amyloid generation independently of caspase cleavage of the β -Amyloid precursor protein (APP).** *The journal of biological chemistry* 2003; 46:46074–46080.
- Thal DR, Rüb U, Schultz C, Sassin I, Ghebremedhin E, Del Tredici K, Braak E and Braak H. **Sequence of A β -Protein Deposition in the Human Medial Temporal Lobe.** *Journal of Neuropathology and Experimental Neurology* 2000; 59:733-748.
- Verkhratsky A, Olabarria M, Noristani HN, Yeh CY and Rodriguez JJ. **Astrocytes in Alzheimer's Disease.** *Neurotherapeutics: The Journal of the American Society for Experimental* 2010; 7:399-412.
- Verkhratsky A, Rodríguez JJ, Steardo L. **Astroglipathology: a central element of neuropsychiatric diseases.** *Neuroscientist* 2014; 20(6):576-88.
- Vitvitsky VM, Garg SK, Keep RF, Albin RL, Banerjee R. **Na⁺ and K⁺ ion imbalances in Alzheimer's disease.** *Biochim Biophys Acta.* 2012; 11:1671-81.
- Walker JM, Fowler SW, Miller DK, Sun AY, Weisman GA, Wood WG, Sun GY, Simonyi A, Schachtman TR. **Spatial learning and memory impairment and increased locomotion in a transgenic amyloid precursor protein mouse model of Alzheimer's disease.** *Behav Brain Res.* 2011; 222:169-75.
- Walsh DM, Klyubin I, Fadeeva JV, Cullen WK, Anwyl R, Wolfe MS, Rowan MJ, Selkoe DJ. **Naturally secreted oligomers of amyloid β protein potently inhibit hippocampal long-term potentiation in vivo.** *Nature* 2002; 416(6880):535-9.
- Weingarten MD, Lockwood AH, Hwo SY, Kirschner MW. **A Protein Factor Essential for Microtubule Assembly.** *Proceedings of the National Academy of Sciences USA* 1975; 72:1858-1862.
- Wyss-Coray T, Loike JD, Brionne TC, Lu E, Anankov R, Yan F, Silverstein SC, Husemann J. **Adult mouse astrocytes degrade amyloid-beta in vitro and in situ.** *Nature Medicine* 2003; 9:453-457.

- Xu J, Yu W, Jan YN, Jan LY, Li M. **Assembly of voltage-gated potassium channels. conserved hydrophilic motifs determine subfamily-specific interactions between the alpha-subunits.** *Journal of Biological Chemistry* 1995; 270:24761-24768
- Yan R and Vassar R. **Targeting the β secretase BACE1 for Alzheimer's disease therapy.** *Lancet Neurology* 2014; 13(3):319–329
- Yang J, Jan YN, Jan LY. **Determination of the subunit stoichiometry of an inwardly rectifying potassium channel.** *Neuron* 1995; 15(6):1441-7
- Yellen G. **The voltage-gated potassium channels and their relatives.** *Nature* 2002; 419(6902):35-42.
- Yu SP, Yeh CH, Sensi SL, Gwag BJ, Canzoniero LM, Farhangrazi ZS, Ying HS, Tian M, Dugan LL, Choi DW. **Mediation of neuronal apoptosis by enhancement of outward potassium current.** *Science* 1997; 278:114-117.
- Yu SP, Farhangrazi ZS, Ying HS, Yeh CH, Choi DW. **Enhancement of outward potassium current may participate in β -amyloid peptide-induced cortical neuronal death.** *Neurobiology of Disease* 1998; 5:81-88.
- Zhao J, O'Connor T and Vassar R. **The contribution of activated astrocytes to A β production: implications for Alzheimer's disease pathogenesis.** *Journal of Neuroinflammation* 2011; 8:150.
- Zheng H and Koo EH. **The amyloid precursor protein: beyond amyloid.** *Molecular Neurodegeneration* 2006; 3:1-5.